PERFORMANCE, COMBUSTION AND EMISSION STUDIES OF A SINGLE CYLINDER DIESEL ENGINE BY DUAL FUEL MODE PROPELLED WITH BIOGAS DERIVED FROM FOOD WASTE

Thesis

Submitted in partial fulfillment of the requirement for the degree of

DOCTOR OF PHILOSOPHY

by

JAGADISH C

Reg. No. 165068ME16F04

DEPARTMENT OF MECHANICAL ENGINEERING

NATIONAL INSTITUTE OF TECHNOLOGY KARNATAKA

SURATHKAL, MANGALORE – 575025

JUNE 2022

PERFORMANCE, COMBUSTION AND EMISSION STUDIES OF A SINGLE CYLINDER DIESEL ENGINE BY DUAL FUEL MODE PROPELLED WITH BIOGAS DERIVED FROM FOOD WASTE

Thesis

Submitted in partial fulfillment of the requirement for the degree of

DOCTOR OF PHILOSOPHY

by

JAGADISH C

Under the Guidance of

Dr. VEERSHETTY GUMTAPURE

Associate professor

DEPARTMENT OF MECHANICAL ENGINEERING

NATIONAL INSTITUTE OF TECHNOLOGY KARNATAKA

SURATHKAL, MANGALORE – 575025

JUNE 2022

DECLARATION

I hereby *declare* that the Research Thesis entitled "**PERFORMANCE, COMBUSTION AND EMISSION STUDIES OF A SINGLE CYLINDER DIESEL ENGINE BY DUAL FUEL MODE PROPELLED WITH BIOGAS DERIVED FROM FOOD WASTE**" which is being submitted to the **National Institute of Technology Karnataka, Surathkal** in partial fulfillment of the requirements for the award of the Degree of **Doctor of Philosophy** in **Mechanical Engineering** is a *bonafide report of the research work carried out by me.* The material contained in this Research Thesis has not been submitted to any University or Institution for the award of any degree.

Register Number: **165068ME16F04**

Name of the Research Scholar: **JAGADISH C**

Signature of the Research Scholar:

Department of Mechanical Engineering

Place: NITK, Surathkal

Date: 16|6|2022

CERTIFICATE

This is to *certify* that the Research Thesis entitled **"PERFORMANCE, COMBUSTION AND EMISSION STUDIES OF A SINGLE CYLINDER DIESEL ENGINE BY DUAL FUEL MODE PROPELLED WITH BIOGAS DERIVED FROM FOOD WASTE"** submitted by **JAGADISH C (Register Number: 165068ME16F04)** as the record of the research work carried out by him, is *accepted as the Research Thesis submission* in partial fulfillment of the requirements for the award of degree of Doctor of Philosophy.

Research Guide

Dr. VEERSHETTY GUMTAPURE

Associate professor

Department of Mechanical Engineering

National Institute of Technology Karnataka, Surathkal

Chairman-DRPC

Department of Mechanical Engineering

National Institute of Technology Karnataka, Surathkal

Date: 16.6.2022

ACKNOWLEDGEMENT

ABSTRACT

Reduction in petroleum products, ever increasing rate of fossil fuels consumption, environment concern and strict emission norms have directed researchers, policy makers to focus on alternative energies to meet the energy demand for various applications. Present research work emphasizes on the application of biogas derived from food waste on the diesel engine operated by dual mode to enhance the performance and mitigate the emissions. Generalized studies on the diesel engine characteristics using biogas (BG) by dual fuel mode with the different ratios ranging from 20% to 60% with a step of 10% are explored. To understand the nature of combustion, the concept of cycle by cycle variation and return map in terms of maximum cylinder pressure (P_{max}) is studied for diesel and dual mode for 100 cycles. The nature of stability and instability in the combustion is measured by coefficient of variation (COV), such that BG20 showed lower COV of P_{max} by 2.3% and BG30 showed slightly higher COV of P_{max} by 1.89% than diesel. Return map, indicated that BG20 and BG30 showed greater combustion stability compared to other biogas proportions. Next objective was to study the effect of injection timing (25.5° bTDC - 29.5° bTDC) on the diesel engine for dual mode of operation. Overall, 27.5° bTDC injection timing showed optimum results compared to other injection timings as well BG50 is optimized compared to other biogas with respect to better engine performance and less emissions. To enhance the engine performance, oxygen enrichment (21% to 27% v/v) is implemented to the engine along with BG50. The thermal efficiency for BG50 with 27% oxygen concentration was improved by 18.37% compared to BG50 without oxygen induction. But NO_x emission increased drastically compared to diesel, which is the foremost disadvantage of the oxygen enrichment process and hence the oxygen level is optimized to 25%. The work is extended to study the effect of vaporized water-methanol (MVI) induction to bring down the NO_x emission intensity for BG50 with 25% O_2 as well to enhance the performance of the dual engine. Using the shell and tube heat exchanger, the water-methanol is vaporized using the heat from the waste exhaust gas and it is inducted into the intake manifold. Engine efficiency improved for BG50 at 25% O_2 with 20% MVI compared to BG50 at 25% O_2 without vapor induction by 9% and NO_x emission improved significantly for BG50 at 25% O_2 with 30% MVI compared to BG50 at 25% O_2 without vapor induction by 86.82% at full load. The final outcome of the current research work is, use of BG50 operated at 27.5° bTDC injection timing with 25% oxygen enrichment and 20% vaporized water-methanol induction rate is superior

alternative for modified single-cylinder CI engine for enhanced engine performance and emission characteristics. To conclude, the aim of the present research work was to examine the potential of using the higher proportions of biogas in the dual fuel diesel engine. Also, to replace the diminishing fossil fuels to meet the energy demand and for various applications. Moreover, to work towards the efficient conversion of heat into energy without compromising the performance and emissions of the engine. The investigation was also well planned by focusing on the new techniques to improve the performance and implement on the engine to stabilize the operation practically. The study also deals with the emission reduction techniques to reduce the exhaust emissions and to implement the methods practically on the automobiles ranging from small to heavy vehicles. Overall agenda of the research was to provide an affirmative solution to the complex issues faced by the transportation sectors with reasonable expenditure.

Keywords: *Biogas, cyclic by cycle variations, dual mode, emissions, food waste, ignition delay, ignition timing, oxygen enrichment, vaporized water-methanol induction.*

TABLE OF CONTENTS

LIST OF TABLES

LIST OF FIGURES

NOMENCLATURE

AD	Anaerobic digestion	FLW	Food loss and waste
BDC	Bottom dead center	GHG	Greenhouse gas
BEC	Biogas energy contribution	HCCI	Homogeneous charge compression ignition
BG	Biogas	HRT	Hydraulic retention time
BGES	Biogas energy share	IC	Internal combustion
BTE	Brake thermal efficiency	IT	Injection timing
bTDC	before top dead centre	LED	Light-emitting diodes
BP	Brake power	LFR	Liquid fuel replacement
BSEC	Brake specific energy consumption	LHV	Lower heating value
CHP	Combined heat and power	LMTD	Logarithmic mean temperature difference
CO	Carbon monoxide	MSW	Municipal solid waste
CN	Cetane number	MSP	Methanol substitution percentage
COV	Coefficient of variation	MVI	Methanol vapor Induction
CR	Compression ratio	NHRR	Net heat release rate
CV	Calorific value	NO_x	Nitrogen oxide
DAQ	Data Acquisition System	POD	Proper orthogonal decomposition
DI	Direct injection	SM	Smoke meter
DM	Dual mode	SO	Smoke opacity
DP	Differential pressure	SCR	Selective catalyst reduction
EGA	Exhaust gas analyzer	TDC	Top dead center
EGR	Exhaust gas recirculation	UBHC	Unburnt hydrocarbon
EGT	Exhaust gas temperature	VFA	Volatile fatty acids

SYMBOLS

m_f — Mass flow rate of the biogas in kg/h

$\sigma_{P_{max}}$ — Standard deviation of P_{max}

$\overline{P}_{max}$ — Mean value of maximum cylinder pressure

ρ^*_a — Density of air inlet

γ^* — specific heat ratio

$\overline{m}_f$ — Mass fraction of the fuel mixture

$P^{'}$ — Instant cylinder pressure

P_{max} — Maximum cylinder pressure

σ^* — Quality of intake mixture to the engine

E^*_A — Activation energy in kJ/kg

$O^{|}_f$ — Mole fraction of dual mode

$\sigma^{'}$ — Standard deviation

W_i — Uncertainty

$X^{'}$ — Mean value

R_t — Retention time

CHAPTER 1

INTRODUCTION

Increasing urbanization and industrialization have resulted in phenomenal growth for transportation demand worldwide for every type of locomotives. The need for increased power in industries and prime movers has resulted in a steep rise in the demand for petroleum-based fuels. From the survey, it is found that fossil fuels take nearly 80% of the primary energy consumed in the world, of which, up to 58% alone is consumed by the transportation sector at present (Salvi et al. 2013). Over the last two decades, the global primary energy consumption has grown at an average rate of about 2% a year, which is expected to continue in the future, mainly because of the estimated increase in the world's population and the anticipated economic growth of developing countries. To achieve the progress and growth of human beings, the availability and environmental impact of energy resources will contribute a major role in the physical future of our planet. Moreover, the dependence on fossil fuels cannot be continued on the current outline of energy consumption, because of two major constraints: the impact of fossil fuel usage on the environment and the reduction of their reserves. The majority of the energy requirements for industrial as well as domestic purposes are directly interrelated to greenhouse gas (GHG) emissions.

The majority of the various energy resources represented in Figure 1.1 contribute to achieve the energy demand worldwide and the maximum energy distribution is from crude oil with 31%. The current oil reserves worldwide are around 196.8 trillion cubic meters, natural gases around 244.1 thousand million tonnes, and coal reserves nearby 1,054,782 tonnes. The consumption of fossil fuel worldwide from 1990 to 2018 is given in Figure 1.2. Due to the population and economy, year-over-year demand, it is evident that fossil fuel energy reserves are gradually decreasing. The energy consumption is increasing at a higher rate which is caused by the usage of air conditioning systems and people spending 90% of their time indoors to attain more comfortness. The combustion of petroleum fuels generates GHG namely CH_4, SO_2, NO_x, and other toxic gases which

are responsible for the generation of acid rains and global warming. Global warming is a by-product of the rapid increase of global use of energy and it drives climate change. Scientific data depicts that human beings are affected by the ever-increasing average global temperature which is increased by more than 2°C. Also, millions of flora and fauna are at risk of destruction. From the national submissions received by the United Nations Framework Convention on Climate Change (UNFCCC) on the emissions of GHG in 2020 from 75 parties, it was calculated that the total amount was about 80% and most of the worldwide emissions were from energy consumption.
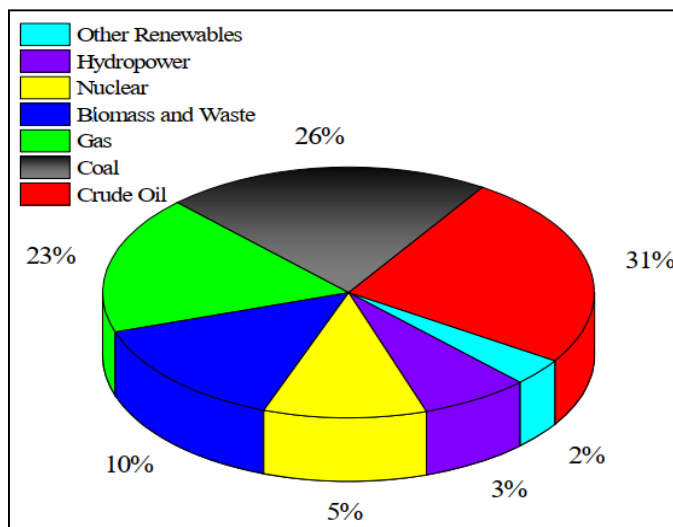
Figure 1.1: Global energy demand distribution (Yaqoob et al. 2021)

To overcome these global issues, renewable energy is the key to replace conventional fossil fuels which are at the diminishing stage. Instead of the usage of fossil fuels, alternative biomass energy can be achieved from the production of gases. Moreover, to reduce global emissions and to bring them under control the ever-diminishing fossil fuels can be replaced by growing renewable fuels (Teh et al. 2021). At the same time, India is experiencing a fuel crisis as a result of its reliance on Gulf countries to provide its ever-increasing energy consumption to maintain its growth rate (Prabakar et al. 2018). Developing countries such as India, produce a significant amount of waste each year, approximately 62 million tonnes, with a 4% annual growth rate.
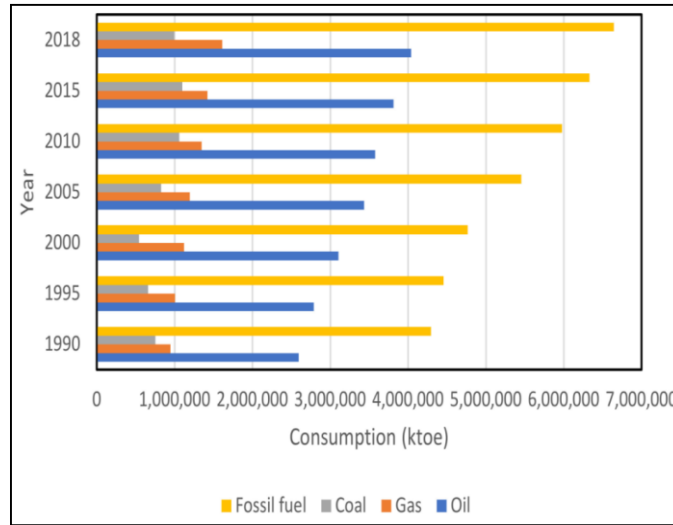
Figure 1.2: The fossil fuel consumption worldwide from 1990 to 2018 (Teh et al. 2021)

To reduce India's dependence on fossil fuels, efficient waste management systems are required to convert the abundantly available waste into energy, particularly biogas (Bhatia et al. 2017, Xu et al. 2018). Because, the use of fossil fuels emits greenhouse gases and has several negative environmental effects, converting waste biomass to biogas has emerged as one of the most important alternatives, not just for developing nations but for the entire world (Fermoso et al. 2018). Conversely, there are currently a variety of procedures for converting waste into different fuels, such as bioethanol, biodiesel, producer gas, and syngas, although all of these processes require additional waste processing, such as pre-treatment, hydrolysis, transesterification, and gasification (Solarte-Toro et al. 2016). Furthermore, all of these processes are highly energy-intensive and less environmentally friendly when compared to anaerobic digestion (AD), which does not require such typical processing or high energy inputs and, more importantly, it is simple to start using ruminant dung as it is readily available in the rural regions (Surendra et al. 2014).

1.1 Waste Generation and Characterization Statistics in India

Fundamental waste management planning has to be implemented in estimating the magnitude and characteristics of MSW in India and predicting future waste

generation. Several factors such as type of commercial activity, the standard of living, type of season, eating habits contribute to the amount of MSW generation. Around 133760 tonnes of MSW per day is generated all over India out of which 91152 tonnes are collected and 25884 tonnes approximately are treated. In terms of per capita, the MSW generation in India accounts for the 0.17 kg per person per day in small towns and 0.62 kg per person per day in urban areas. The rate of waste generation relies upon the elements such as population, financial status, and level of business movement, culture, and city/region. Overall data on MSW generation across the various states of India is shown in Figure 1.3. Maximum generation of waste is observed in the states such as Maharashtra (115364–19 204 tonnes per day), Uttar Pradesh, Tamil Nadu, West Bengal (11523–15363 tonnes per day), Andhra Pradesh, Kerala (7683–11522 tonnes per day) and Madhya Pradesh, Rajasthan, Gujarat, Karnataka, and Mizoram (3842–7662 tonnes per day). However, lower generation of waste is observed in the states such as Jammu and Kashmir, Bihar, Jharkhand, Chhattisgarh, Orissa, Goa, Assam, Arunachal Pradesh, Meghalaya, Tripura, Nagaland, and Manipur (less than 3841 tonnes per day) (Kumar et al. 2017).
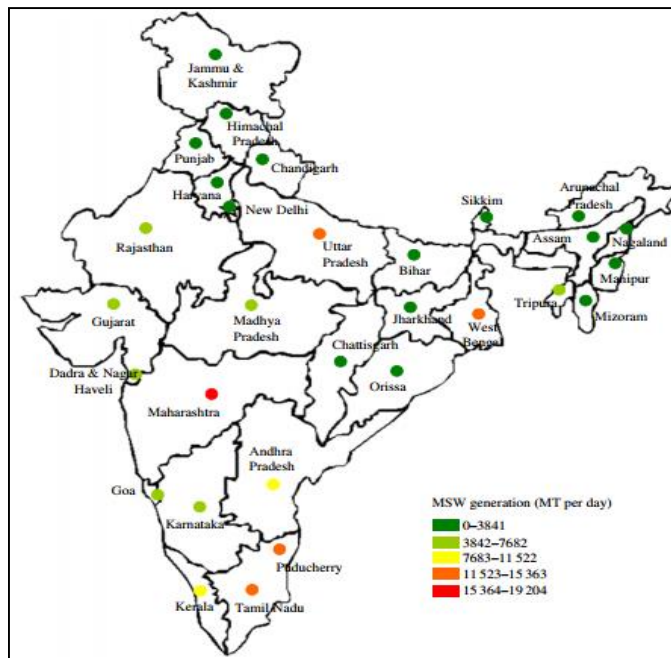
Figure 1.3: MSW generation over entire India (2009–2012) (Kumar et al. 2017)

4

1.1.1 Food Waste as a Global Challenge

Any food and inedible pieces of food removed from the food supply chain to be recovered or disposed of is referred to as food waste. Even though it is universally agreed that any definition should include food that is lost during the primary manufacturing phase (including farming, fishing, and aquaculture). This comprises food crops that are not harvested and plowed in, harvested and exported to a market other than food (for example, composting, digesting, or ethanol generation), harvested and then disposed of (e.g. incinerated, landfilled, sent to sewer, or disposed of to sea). Likewise, food waste incorporates all the material that enters the food store network yet isn't consumed, for example, both edible and inedible materials which might be produced in food handling, promoting, and arrangement, and post-readiness food that isn't eaten. These classifications are presently reflected in the definition for food loss and waste (FLW) prescribed by the European parliament to the Commission and the Member States defined as: 'food waste implies food expected for human utilization, either inedible, eliminated from the creation or inventory network to be disposed of, including at essential creation, preparing, fabricating, transportation, stockpiling, retail and customer levels, except for essential production losses (Achinas et al. 2017).

1.1.2 Energy from Food Waste

Food waste is the second most common type of MSW delivered to landfills in the United States, accounting for around 18% of total garbage. Every year, almost 30 million tonnes of food waste are disposed of in landfills. The majority of the less than 3% of food waste that is currently diverted from landfills is composted to make fertilizer. Various waste characterizations depicting the different materials discharged across the landfills are shown in Figure 1.4. Food waste is highly biodegradable and has a substantially higher rate of volatile solids degradation (86-90%) than biosolids. This means that even if more material is added to the digesters, the final residue will only be slightly higher. The most essential purpose for anaerobically digesting food waste is to capture the energy content, which is arguably the most important factor.
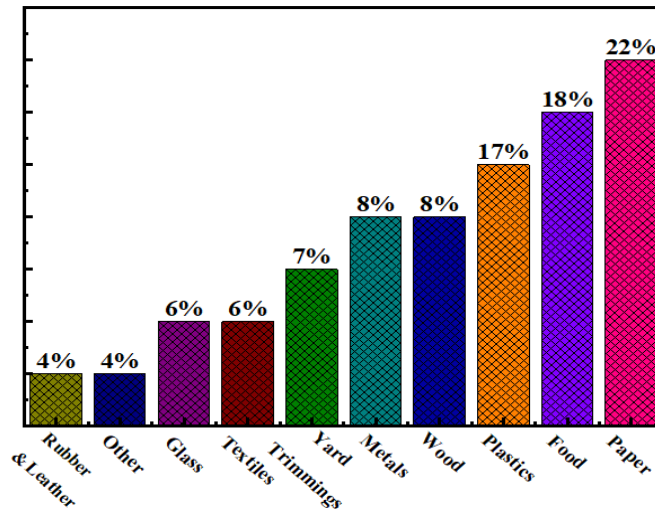
Figure 1.4: Various waste materials disposed in landfills worldwide (Gao et al. 2017)

Post-consumer food scraps, unlike biosolids and animal manures, have no prior energy collection. Food waste contains up to three times the energy potential of biosolids, according to a study conducted by the East Bay Municipal Utility District. Capturing energy from food waste is becoming more essential as energy prices rise and the focus shifts to renewable energy generation and energy independence. When facilities begin digesting the food waste, the increased energy generation allows them to offset their energy consumption and sell extra energy back to the grid (Gao et al. 2017).

Food waste has THREE TIMES the methane production potential as bio-solids!

- Cattle manure= 25 m^3 gas/ton
- Biosolids= 120 m^3 gas/ton
- **Food waste= 376 m^3 gas/ton**

1.2 Anaerobic Digestion Process

Anaerobic digestion is a series of biological processes that use a diverse population of bacteria to break down organic materials into biogas, primarily methane and a combination of solid and liquid effluents occurring in the absence of oxygen.

6

Organic materials are composed of organic compounds resulting from the remains or decomposition of previously living organisms such as plants and animals and their waste products. Sources of organic material for anaerobic digestion include dairy manure, food processing waste, plant residues, and other organic wastes such as municipal waste water, food waste, fats, oils, and grease. Anaerobic digestion can be divided into four steps.

Step 1. Hydrolysis: The first step, hydrolysis occurs as extracellular enzymes produced by hydrolytic microorganisms decompose complex organic polymers into simple, soluble monomers. Proteins are broken down into amino acids, lipids into long- and short-chain fatty acids, starch into glucose, and carbohydrates into sugars.

Step 2. Acidogenesis: The small molecules from hydrolysis are converted by acidogens to a mixture of volatile fatty acids (VFAs) such as acetic, propionic, and butyric acids and other minor products such as hydrogen, carbon dioxide, and acetic acid. Acidogenesis is usually the fastest step in the anaerobic conversion of complex organic matter in liquid-phase digestion.

Step 3. Acetogenesis: In the third step, acetogenic bacteria further convert the volatile fatty acids to acetate, CO_2, and hydrogen.

Step 4. Methanogenesis: step 3 provides substrates for methanogenesis, the last step in the anaerobic process for methane production.

A stable anaerobic digestion process requires maintaining a balance between several microbial populations. The hydrolysis and acidogenesis steps have the most robust microbes which thrive in the broadest environmental range. The pH range is maintained under normal circumstances by the buffering action of the system provided by CO_2 in the form of bicarbonate alkalinity (Baig et al. 2017). Figure 1.5 shows the steps involved in the anaerobic digestion process.
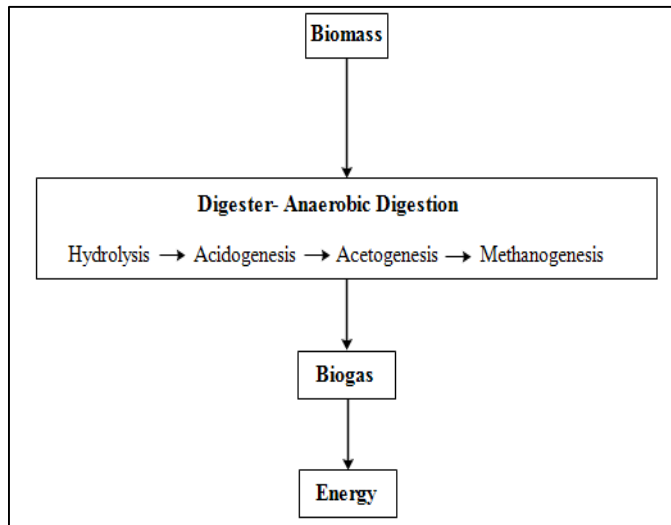
Figure 1.5: Four steps of anaerobic digestion process (Baig et al. 2017)

1.2.1 Biogas: Sources and Composition

Anaerobic fermentation, by which biogas is produced from organic wastes, depends on various operating parameters such as temperature, pH, hydraulic retention time (HRT), carbon to nitrogen ratio (C/N), nutrients addition, the particle size of the substrate, etc. The primary sources of biogas include agricultural residues and wastes and human and animal wastes, industrial wastewater treatment systems, stabilization of sewage sludge, landfill management, biomass slurries arising in the food and drink industries which are shown in Figure 1.6.

There are now over 800 farm-based digesters operating in Europe and North America. More than 1000 high-rate anaerobic digesters are operated worldwide to treat organic polluted industrial wastewater including processors of beverages, food, meat, pulp and paper, and milk. Biogas is primarily composed of methane (CH_4) and carbon dioxide (CO_2) with smaller amounts of hydrogen sulfide (H_2S). Trace amounts of hydrogen (H_2), nitrogen (N_2), carbon monoxide (CO), saturated or halogenated carbohydrates, and oxygen (O_2) are occasionally present in the biogas. The composition varies according to the types of feed biomass materials, the method of digestion, and digester retention time. A hydraulic retention period for biogas production normally

ranges from 30-50 days from an anaerobic digester, except the landfill sources. Biogas is typically composed of 60-65 mol% CH_4, 35-40 mol% CO_2, 0.1-0.5 mol% H_2S, and traces of other gases and vapors of various organic compounds (e.g., aromatics, chlorinated hydrocarbons, alcohols, etc.). When conditions are best, organic wastes in a digester can generate a gas containing up to 80% by volume of methane. But more general properties are typically 60% CH_4 and 40% CO_2. The energy value of biogas ranges from about 18.6 to 30.2 MJ/m^3, compared to pure CH_4 (35.7 MJ/m^3) and pipeline NG (35.7 MJ/m^3, in the US) (Nirendra et al. 2006).
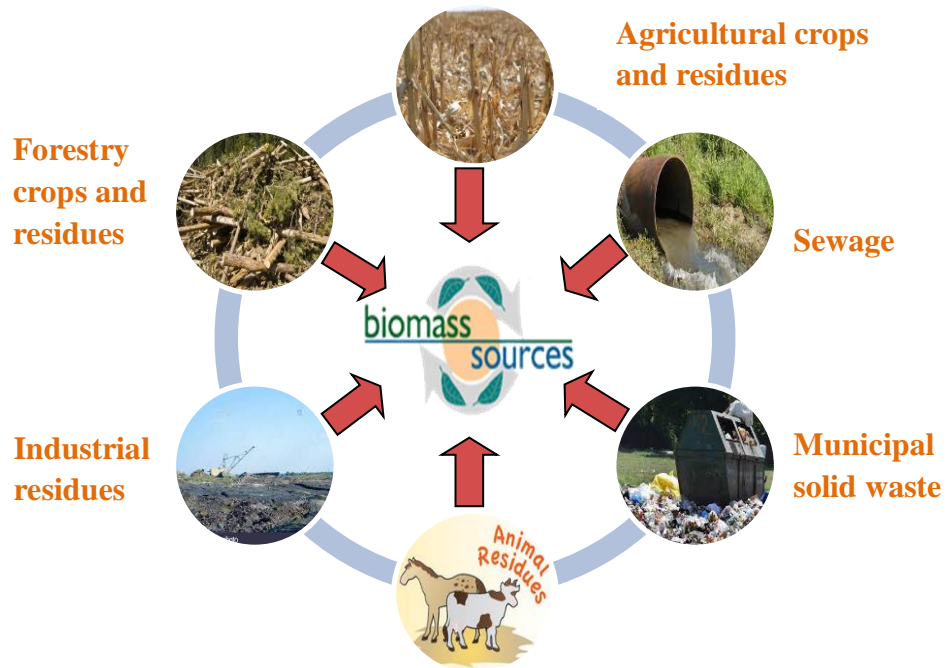
Figure 1.6: Resources of biogas (Baig et al. 2017)

1.2.2 Applications of Biogas

Biogas has the potential to completely replace the fossil fuels in India for a variety of applications, including domestic, commercial, industrial, and transportation, as indicated in Figure 1.7. Biogas has been used in rural India to power light-emitting diodes (LED) lamps and for cooking, where it can replace the conventional LPG because it is 3 times safer and 20 times less expensive than CNG or LPG. Biogas can also be utilized as

a fuel in a dual-fuel engine for co-generation of heat and electricity in a combined heat and power (CHP) plant, which can reduce the fossil fuel use by 80% while also lowering energy production costs by 4.7 to 83%. Biogas can be converted to compressed biogas (CBG) after CO_2, H_2S, and water vapors are removed. CBG can then be used in prime movers. With so many wastes available, India's biogas generation potential is so great that it might replace 15 to 20% of the country's natural gas usage. The energy content of biogas is 6.5 kWh with a methane content of 65%, and it will be 9.7 kWh with a methane content of 97%, which is nearly equal to 1 L of petrol or diesel, i.e. 9.1 and 9.8, respectively. The use of biogas as a clean transportation fuel addresses contemporary concerns about fossil fuel economics, ecology, and energy (Bhatia et al. 2020).
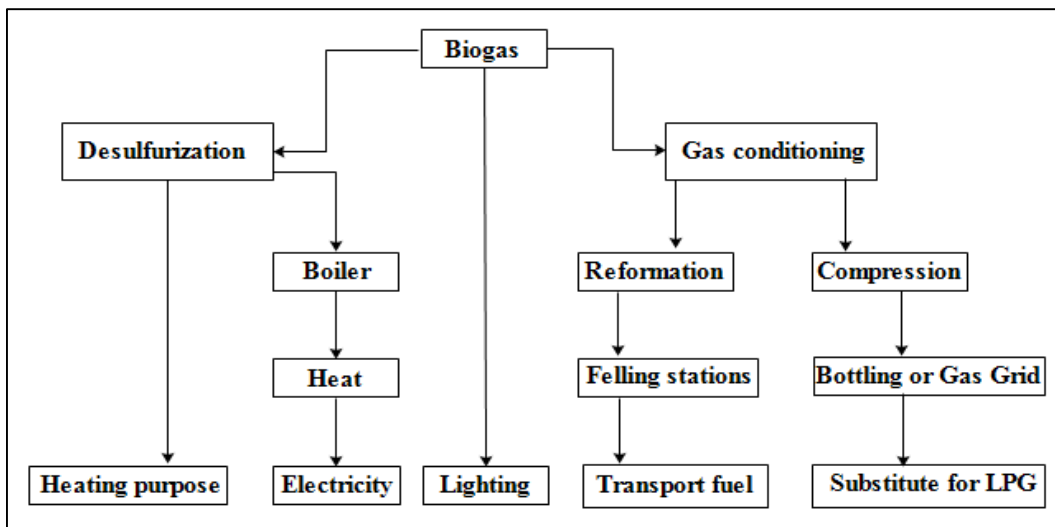
Figure 1.7: Various applications of biogas (Bhatia et al. 2020)

1.2.3 Biogas: A Potential Energy for IC Engines

The utilization of biogas in IC engines is a long-established and reliable technology. Thousands of engines are used on sewage works, landfill sites, and other biogas installations. The engine sizes range from 45 kW on small farms up to larger MW on large-scale landfill sites. Power generation from landfill gas using spark-ignition engines, dual-fuel engines, and gas turbines has been successfully demonstrated in the UK for engine sizes ranging from about 0.5 to over 4 MW. For an engine/generator set,

assuming the engine efficiency is 30% and the generator efficiency is about 70%, the gas production rate required to produce 1 kW of electricity is 0.56 m^3/hr. The relatively high self-ignition temperature of methane is 640 °C, which limits the use of this fuel as a power feed source for diesel engines (Heywood 2018). Application of a dual-fuel supply system, thanks to which gas fuel is supplied to an intake manifold, in which an air-gas mixture is formed and is then delivered into the engine combustion chamber. During the compression stroke, a little amount of liquid fuel is injected into the combustion chamber initiating the self-ignition of gas fuel. In such a system, gas is supplied under small overpressure to the suction manifold, which does not require the application of complex gas installations. Such an engine supply method is a solution that is relatively simple in design, does not require significant interference in a standard installation, and allows simultaneous engine operation in both single and dual-fuel systems (Sahoo et al. 2014).

1.3 Working Principle of Diesel Engine

The diesel engine also called as CI or Compression Ignition engine runs on a variety of fuels which was invented by Dr. Rudolf Diesel (1890). Right from the evolution of the industrial era, the diesel engine has been revolutionized worldwide in several applications, such as in industries, marine, and railway installations in isolated locations. The CI engine generally operates on two or four-stroke cycles, normally diesel engines provide higher thermal efficiency compared to petrol engines. The basic working principle of a four-stroke diesel engine is shown in Figure 1.8 and briefly explained as follows. During the suction stroke, the air is inducted into the combustion chamber through the intake manifold, and during this stroke, the exhaust valve remains closed. The quantity of air that is inducted inside the combustion chamber is dependent on the swept volume of the cylinder and the engine speed. At the compression stroke, the piston compresses the air, and both the intake and exhaust valves remain closed such that the compressed air gets hotter because of the friction and the inter-molecular collision. At the end of the compression stroke, the fuel is injected with the help of a fuel injector actuated by a high-pressure fuel pump.

Though the injector has a very small nozzle hole, the fuel passes with a high velocity and gets atomized. The high pressure and high temperature of the compressed air now mix with the atomized fuel and makes its vapor. The vaporized fuel mixes with the air and when the air-fuel mixture temperature is higher than the fuel's self-ignition temperature, a series of spontaneous chemical reactions occur leading to rapid combustion. Moreover, after combustion, the piston reaches the bottom dead center (BDC), and the burnt gases are swept out of the cylinder through the exhaust manifold, by the upward movement of the piston towards the top dead center (TDC) (Cengel 2013).
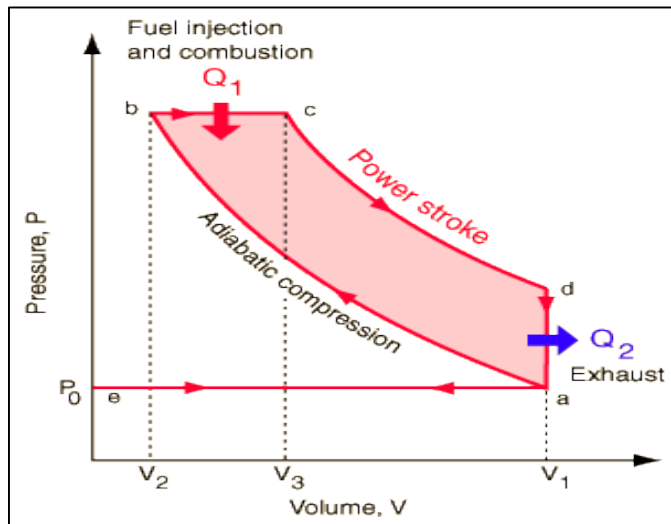
Figure 1.8: Pressure v/s volume diagram of diesel cycle (Cengel 2013)

1.4 Dual-Fuel Mode

As discussed about the diesel engine operation in the previous section, the diesel fuel is injected into the combustion chamber through the fuel injector with high pressure (about 200 bar). Only the air is inducted into the cylinder during the suction stroke and is compressed during the compression stroke. Because of the high self-ignition temperature, the gaseous fuel does not auto-ignite. Hence, it is fired by a small diesel fuel which ignites spontaneously as it comes into contact with the hot compressed air at the end of the compression phase. The advantage of this type of engine is that it uses the difference of flammability of two used fuels. Again, in case of lack of gaseous fuel, this engine runs

according to the diesel cycle by switching from the dual-fuel mode. The disadvantage is the necessity to have liquid diesel fuel available for dual-fuel engine operation (Barik et al. 2015). Figure 1.9 shows the dual fuel mode operation. Dual-fuel engines are seldom equipped with throttles to control power output. Because dual-fuel engines rely on the compression-ignition of the diesel pilot, they share some characteristics with diesel engines in addition to some unique advantages and drawbacks of their own. However, dual-fuel engines resemble diesel engines more than spark-ignition engines (Kumar et al. 2018).
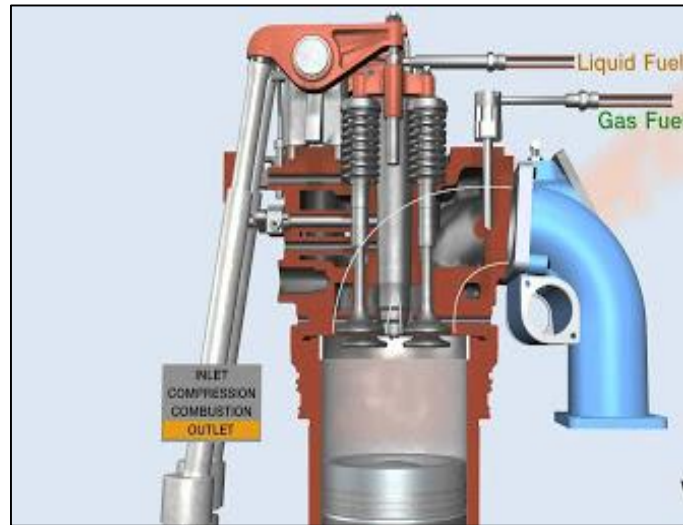
Figure 1.9: Dual fuel mode method (Kumar et al. 2018)

1.5 Cycle by Cycle Variation

The basic difficulty with the engines since their inception is the cycle-to-cycle variation. This reduces the engine performance and generates higher emissions. In a diesel engine, the combustion process does not repeat itself from one cycle to the next. If the pressure trace in the cylinder is measured, this is immediately visible (Johansson 1996). The cylinder pressure has traditionally been employed to measure the fluctuations. As a result, pressure-related measures are now used to quantify the fluctuation intensity (Heywood 2018). The maximum pressure and associated crank angle position are widely utilized characteristics. In a well-functioning engine, the peak pressure obtained can vary

13

by 30% from cycle to cycle. The cylinder pressure has traditionally been employed to measure the fluctuations. As a result, pressure-related measures are now used to quantify the fluctuation intensity. A commonly utilized parameter is the variation in indicated mean effective pressure (IMEP) produced per engine cycle. The coefficient of variation, or COV of IMEP, is calculated by normalizing the standard deviation with the average value. In general, the combustion process in a diesel engine will fluctuate throughout the flame propagation phase.

Because the fuel and residual gases are not well mixed with the air, the laminar flame speed varies with location and time. This same turbulence level is unlikely to be uniform, and the mean flow state will shift from cycle to cycle and change in location. Although huge flames are likely to fluctuate, these flames will have the advantage of integrating out in homogeneity of the fuel, residual, and flow fields. As a result, cycle to cycle variance is predicted to be the most problematic in this stage of the combustion (Kyrtatos et al. 2018).

1.6 Emission Reduction Methods

When the load is increased, the peak cycle temperature rises and with the presence of oxygen causes the generation of NO_x. Several methods have been tried to reduce NO_x production. Use of EGR (Exhaust gas recirculation), turbocharging with intercooling, the addition of diluents or water injection with the intake charge, and so on are some of them. Injection of water into the intake manifold has been shown to lower NO_x emissions in SI, CI, HCCI, and LPG engines. Increasing the intake charge humidity was also mentioned as a good way to reduce NO_x emissions. Water addition as a supplement to an internal combustion engine is a notion that has been around for over 50 years. Even though water does not burn, it is good at absorbing heat due to its higher specific heat capacity and latent heat of evaporation. Under standard atmospheric pressure and temperature, the latent heat of evaporation of water is 2256 kJ/kg. Because it is a good heat absorber, the cylinder's peak temperature will drop, lowering the NO_x emissions dramatically. The fuel/air equivalence ratio, maximum cycle temperature, and burning rate influence NO_x production (Ganesan 2003). Peak NO_x emissions occur under

slightly lean conditions when the combustion temperature is high and there is an abundance of oxygen to react with the nitrogen due to dissociation. The water injection lowers NO_x emissions in the lean zone, which has a local maximum between 0.9 and 1.0 equivalence ratios. The main causes for the reduction in NO_x are a drop in temperature and a fall in combustion rate due to the injection of water. For a stoichiometric fuel/air mixture, adding 0.5 g of water/g of fuel results in a lower adiabatic flame temperature of around 150 K. As a result, using the induction approach, water is introduced to the fuel-air charge at the intake manifold, which is presumably the simplest and most successful method (Salve et al. 2016).

1.7 Organization of Thesis

In the current research work, every detail of the experimental studies related to the diesel engine characteristics operated with diesel mode and different ratios of biogas derived from food waste operated in dual mode is executed. The study is extended to investigate the influence of cyclic variations and injection timing for both diesel and dual-mode. To enhance the engine performance oxygen enrichment is implemented and to mitigate the emissions vaporized methanol induction system is adopted. Overall description of the entire work is summarized in this section.

Chapter 1 Introduction

This chapter describes the overview of the generation and utilization of fossil fuels in several applications, shows the alternative replacement to the diminishing non-renewable sources. Present energy demand across the globe, details about fossil fuel consumption from history until present, wastes and types of waste, as well as waste generation scenario in India are illustrated. Introduction to biogas sources, composition, energy extraction, and application of biogas in the internal combustion (IC) engines. This chapter also discusses the working principle of the diesel engine, dual fuel concept, and includes a small description of the present work.

Chapter 2 Literature review

This chapter deals with the literature survey on biogas application in internal combustion engines, comparative studies of biogas with other gaseous fuels. Also, literature that deals with the utilization of gaseous fuels in diesel engine on dual fuel mode are explored along with the details of the biogas combustion. Especially focusing on the water injection, steam injection methods for emission reduction are surveyed. The review work is extended by exploring the concepts such as cyclic variations, the effect of injection timing, and the oxygen enrichment method incorporated to enhance the performance of the engine and the objectives of the research work are framed.

Chapter 3 Extraction of the biogas

In this chapter, the extraction of biogas from an anaerobic digester plant and the process of filling the biogas into the tyre tube, transporting the filled biogas from the plant to the research laboratory, and lastly transferred into the cylinder is executed. Details about the determination of extracted biogas composition using gas chromatography are presented.

Chapter 4 Experimental setup and methodologies

The details of the experimental engine setup, modification to the engine components for the dual-fuel operation, step-by-step method of experiment, and the data acquisition technique for the combustion, performance, and emission analysis are described in this chapter. A detailed discussion on the usage of the instruments is specified and uncertainty analysis for the instruments is also presented.

Chapter 5 Results and discussion

In this chapter, the results of the combustion, performance, and emissions obtained from operating a single-cylinder, four-stroke, air-cooled, DI diesel engine on the dual fuel mode using biogas with necessary engine modifications. The concept of cyclic variations, the influence of injection timing upon the engine performances are explored with the addition of oxygen enrichment and vaporized methanol induction system are discussed and the obtained experimental results are analyzed.

Chapter 6 Conclusions and scope for future research

This chapter presents a module-wise conclusion of the findings from the experimental investigation accomplished in this study with major outcomes and it also mentions the scope for future work.

1.8 Closure

In this chapter, the background of the energy crisis and the energy demand are highlighted. In addition, the need of renewable energy for different applications and motive to replace the conventional fossil fuels are briefly described. The motivation behind the present research work are discussed by providing the broad outlines of the organization of thesis with the significant features of the individual chapters are illustrated.

CHAPTER 2

LITERATURE REVIEW

Conventional fossil fuels provide most of the energy for various applications such as in industries, agricultural sector, transportation activities, power generation etc., and **is** used across the globe. This demand for the energy is increasing very rapidly at the faster consumption rate causing depletion of fossil fuels. Concern over the environmental issues and strict emission norms formulated has created a driving force to focus on renewable energies to reach the energy demand and to mitigate the emissions. On this prospect a detailed literature review on the usage of various renewable fuels such as biogas for prime movers along with various methods to enhance the performance of the engine and different techniques to eradicate emissions is reported in this chapter.

2.1 Biogas as an Alternative Fuel for IC Engine

Raj et al. (2009) highlighted the potential role of biogas obtained from textile cotton waste as an alternative fuel. A batch type digester was used to conduct experiments such that the methane gas was generated from the waste cotton with a different proposition of water with or without the addition of seeding material. The biogas was produced by using different seeding materials such as pig dung, cow dung, and goat waste. Experiments were conducted for various proportions such as 2.5, 5, and 7.5, 10 and 15% of seeding material at various temperatures. Two types of links were used at air inlet for proper mixings such as venturi meter attachment and T-joint. From the experimental study, it is concluded that the use of venturimeter at the inlet port of the engine is an effective method to supply the biogas as it indicated less diesel was consumed than T-joint. Also from the result, it is observed that the use of biogas as dual fuel in a single-cylinder diesel engine had the tendency to save 60% of diesel.

Bedoya et al. (2009) investigated the effects of mixing system and pilot fuel quality on CI engine running on dual fuel mode at fixed engine speed and four loads. The experiments were carried out on a power generation diesel engine with simulated biogas (60% CH_4– 40% CO_2) as the primary fuel, and diesel and palm oil biodiesel as pilot fuels. In the first

experimental phase, the maximum substitution level that allowed stable engine operation at part load was determined. In the second experimental phase, the mixing system for dual fuel operation was modified using a supercharger, a special mixer (Kenics mixer), and a large mixing length (250 mm) from the mixer to the engine inlet manifold. Whereas, in the last phase of the experiment, Dual fuel engine was evaluated at the same engine loads as the previous phase using palm oil biodiesel as pilot fuel. The experimental result disclosed that the full diesel substitution is attainable using palm oil biodiesel as pilot fuel on biogas dual-fuel engine. The combination of a supercharger and Kenics mixer in the inlet system of bio-gas dual-fuel engines can be applied as a strategy to increase thermal efficiency and substitution level of pilot fuel as well as to reduce methane emissions at part load.

Rossetto et al. (2013) examined the availability of biogas from the waste in rural areas, urban waste in landfills and sewage treatment systems in Brazil processed in an anaerobic digester as a result methane gas is generated. The generated biogas is used on Otto cycle engine to generate the required torque and power, whereas, natural gas was used as a reference parameter. The experiment was performed first by using the systems commercially available for these fuels, so they could serve as a comparative for the other tests. Next tests were made for the several combinations of ignition point, gas mixer, and compression rate. From the experimental results it was concluded that the best power result for biogas was obtained when the compression rate was maintained at 12.5:1, long gas mixer at spark advance 45°.

Awogbemi et al. (2015) explored the development and testing of a spark-ignition engine fuelled with biogas-petrol blend with a ratio of 20:80. The biogas was produced using cow dung seeded with rice husk and banana peels as feedstock in a plastic digester such that in order to find out the composition of the different constituent gases a gas chromatography was used. A 5 HP single-cylinder four-stroke spark-ignition Honda GX 140 engine AC dynamometer was used to determine the performance and emission characteristics. The results showed that biogas–petrol blend generated a higher torque,

brake power, indicated power, brake thermal efficiency, and brake mean effective pressure but lower fuel consumption and exhaust temperature than petrol.

Bhaskor and Ujjwal (2015) explored the potential of three different types of biodiesel i.e. Rice bran oil methyl ester (RBME), Pongamia oil methyl ester (PME) and Palm oil methyl ester (POME) as pilot fuels for biogas run dual fuel diesel engine. Also, a comparative study among the three biodiesels under dual fuel mode is carried out on the basis of performance, combustion and emission analysis. The diesel engine is converted into biogas run dual fuel diesel engine by connecting a venturi-gas mixer at the inlet manifold. Experiments were conducted at injection timing (IT) of 23°bTDC and CR of 17.5 for different loading conditions. The results indicated that under dual fuel mode, RBME-biogas produced a maximum brake thermal efficiency of 19.97% in comparison to 18.4% and 17.4% respectively for PME-biogas and POME-biogas at 100% load. The emission study revealed that under dual fuel mode, on an average, there was an increase of CO emission by 25.74% and 32.58% for PME-biogas and POME-biogas, respectively in comparison to RBME-biogas. Furthermore, on average, the HC emissions for PME-biogas and POME-biogas increased by 11.73% and 16.27%, respectively in comparison to RBME-biogas. On the other hand, on average, there was a decrease in NO_x emission by 5.8% and 14%, respectively for PME-biogas and POME-biogas respectively in comparison to RBME-biogas.

Senthilkumar and Vivekanandan (2016) studied the performance characteristics of CI engine using biogas and diesel as dual fuel mode. The experimental test results show that when the engine operated with 60% biogas+40% diesel indicated better brake thermal efficiency with minimum fuel consumption when compared to diesel. The results also showed when the engine operated with biogas-air rich mixture achieved better thermal efficiency compared to the engine operated with diesel-air mixture under the same operating condition. Because of the low energy content of the biogas mixture, the Brake thermal efficiency decreases in all the biogas-diesel mixtures compared to diesel fuel, whereas, exhaust gas temperature (EGT) decreased in case of the biogas-diesel

combination compared to a diesel engine. From the experimental results, it is concluded that biogas-diesel of ratio 20% biogas+80% diesel performed better than other ratios.

Salve et al. (2016) attempted to disclose the effect of compression ratio on the performance, combustion and emission characteristics of a dual fuel diesel engine run on synthesized biogas. Experiments were carried out for variations in compression ratio, pilot diesel fuel quantity and loads, at a constant speed for diesel and dual-fuel operation. Brake thermal efficiency increases as pilot fuel quantity increase at all loads conditions. The peak cylinder pressure in dual fuel mode is lower than that of diesel mode and net heat release rate is lower in dual fuel mode than diesel mode. NO_x emissions found lower in dual-fuel operation as that of diesel. The brake thermal efficiency in the dual fuel mode improves with an increase in load and compression ratio. Brake specific fuel consumption decreases with an increase in load and compression ratio. The peak cylinder pressure in dual fuel mode is lower than that of diesel mode for all CRs. The net heat release is higher in diesel mode in comparison to dual fuel mode, whereas, the NO_x emission decreased in dual fuel mode as compared to diesel mode.

Debabrata and Murugan (2016) investigated the combustion, performance and emission characteristics of a direct injection (DI) diesel engine, modified to operate with raw biogas diesel dual fuel. The key objective of this experimental investigation was to characterize the biogas obtained from the seed cake of Karanja (SCK) produced by the aerobic digestion. With a step of 1.5°CA, the injection timing of diesel was varied from 23°CA bTDC to 27.5°CA bTDC in the dual-fuel operation. The results indicated that dual-fuel operation with the injection timing of 26°CA bTDC gave an overall better result than other injection timings. The brake specific carbon monoxide (BSCO) and brake specific hydrocarbon (BSHC) emissions were higher by about 2% and 10% respectively than diesel operation, at full load. At full load, the smoke emission was lower by about 39% than that of diesel. The cylinder peak pressure was higher by about 14 bar and the brake specific fuel consumption (BSFC) was higher by about 25% than those of diesel operation, at full load.

Bora and Saha (2016) examined the effect of compression ratio on performance, combustion and emission characteristics of a rice bran biodiesel-biogas run a dual fuel diesel engine. Experiments were conducted at three different compression ratios (CRs) of 18, 17.5 and 17, and at a standard injection timing of 23° bTDC at different loading conditions. Under dual fuel mode (DFM), the maximum brake thermal efficiencies (BTEs) are found to be 20.27, 19.97 and 18.39% for CRs of 18, 17.5 and 17, respectively for a full load. For the same loading condition, the maximum liquid fuel replacement (LFR) is found to be 80, 79 and 78.2% for CRs of 18, 17.5 and 17, respectively. On average, there is a reduction in carbon monoxide and hydrocarbon emissions by 17.67% and 17.18% when CR is increased from 17 to 18. However, for the same set of CRs, there is an increase of oxides of nitrogen as well as carbon dioxide emissions by 42.85% and 14.13%, respectively.

Debabrata et al. (2017) explored the possibility of using Karanja Methyl Ester (KME) as a pilot fuel in biogas run direct injection (DI) diesel engine of the compression ratio of 17.5:1. Here the biogas is primary fuel and is inducted with the intake air, whereas, KME is pilot fuel and was injected directly into the combustion chamber. The injection timing of the pilot fuel, in the biodiesel dual fuel mode (BDFM), was varied from 21.5°CA bTDC to 27.5°CA bTDC in steps of 1.5°CA. The BDFM with injection timing was denoted as BDFMX, where X indicates the injection timing. BDFM 24.5 (biodiesel dual fuel mode of 24.5°CA) gave better performance and lower emissions than those of other injection timings. The results disclosed that the brake specific fuel consumption (BSFC) for BDFM 24.5 was found to be higher by about 23.9% than that of KME, at full load. About 6.6% increase in the brake thermal efficiency was observed for BDFM 24.5 in comparison with BDFM 23.0, at full load. BDFM 24.5 gave a reduction in the CO, HC and smoke emissions of 17.1, 18.2, and 2.1%, in comparison with the BDFM 23.0, at full load, respectively. But, the Nitrogen oxide emission for BDFM 24.5 was higher by about 5.5 % than that of BDFM 23.0, at full load.

Gnanamoorthi and Navin (2019) came out with possible ways to reduce the emission generated as well as to improve the performance and combustion of the direct injection diesel engine operated with dual fuel mode using biogas for different mass flow rate. Using the seeds of tamarind and rice bran, biogas is generated by anaerobic digestion process using a batch type digester. Tamarind seed as well as rice bran weighing 85 kg each is mixed with water maintaining the proportion ratio of 1:9 by volume basis and an overall volume of 23.008 m^3 of biogas are generated in the batch type digester by allowing it to kept for 30 days hydraulic retention time. The biogas composition was determined by using gas chromatography, which indicates 63% CH_4 and 37% CO_2. The engine is operated by dual-fuel mode for the various mass flow rate of biogas such as 0.25, 0.5, 0.75 and 1 kg/hr in such a way that biogas is introduced to the engine at intake manifold through venturi-meter. From the results, authors concluded that NO_x and sootness were decreased by 23.27% and 7.1% compared to diesel at full load but on the other hand brake thermal efficiency decreased and brake specific energy consumption increased than diesel mode.

2.2 Comparative Studies of Biogas with other Gases

Porpatham et al. (2007) investigated the effect of hydrogen addition on the performance of a biogas fuelled spark ignition engine. Hydrogen was added in small amounts (5, 10 and 15% on the energy basis) to biogas and tested in an SI engine at a constant speed at different equivalence ratios to study the effects on performance, emissions and combustion. The engine was initially tested on biogas and then hydrogen was added with appropriate proportion. Hydrogen significantly enhances the combustion rate and extends the lean limit of the combustion of biogas. From the experimental result, it is found that improvement in brake thermal efficiency and brake power. However, beyond 15% hydrogen, the need to retard the ignition timing to control knock does not lead to improvements in high equivalence ratios. Significant reductions in hydrocarbon levels were seen. There was no increase in nitric oxide emissions due to the use of retarded ignition timing and the presence of carbon dioxide. Peak pressures and heat release rates are lower with hydrogen addition as the ignition timing is to be retarded to avoid knock.

There is a reduction in cycle-by-cycle variations in combustion with lean mixtures. On the whole 10%, hydrogen addition was found to be the most appropriate.

Park et al. (2011) studied the performance of an SI engine fueled by biogas operated with two major parts namely N_2 dilution test and H_2 addition experiments. In the N_2 dilution test, simulated biogas fuels with varying methane concentrations were used to run the engine by keeping the ratio of natural gas and N_2 to 20:80 by volume fraction from 100% natural gas with an increment of 20% in N_2. In case of hydrogen addition test, experiments were conducted with the biogas of 80% N_2 dilution keeping the H_2 concentrations to 5, 10, 20, and 30%, with these conditions the engine was operated at a constant speed of 1800 rpm under a 60 kW power output condition. From the N_2 dilution test, the result revealed that the thermal efficiency improved because of the addition of inert gas in biogas and significantly NO_x emission was reduced. Whereas, in the case of H_2 addition test, the engine test results showed improvement in in-cylinder combustion characteristics, reducing THC emissions while enriching NO_x generation as well as maximizing engine efficiency at 5-10% H_2 concentration.

Chandra et al. (2011) investigated the performance of diesel engine which was converted into spark ignition mode and run on compressed natural gas (CNG), methane-enriched biogas (Bio-CNG) and biogas produced from bio-methanation of jatropha and Pongamia oil seed cakes. In order to convert from CI to SI mode a magneto ignition system was mounted on the crankshaft of the engine for the supply of spark current to the spark plug installed at the place of diesel fuel injector. The engine was operated at 30°, 35° and 40° ignition advance of TDC with 12.65 compression ratios. The experimental result was compared with diesel as original fuel, the power deteriorations of the engine were observed to be 31.8, 35.6 and 46.3% on compressed natural gas, methane-enriched biogas, and raw biogas, respectively, due to its conversion from CI to SI mode. At 35° TDC of advance injection timing maximum brake power was produced for all tested fuels. From the result obtained it was concluded that the methane-enriched biogas

showed almost similar engine performance as compared to CNG in terms of brake power output, specific gas consumption and thermal efficiency.

Karen et al. (2012) studied the effect of oxygen-enriched air on a diesel-biogas dual-fuel engine. The experiment was carried out with three levels of oxygen (22, 25, 27% volume basis) injected in the air intake at 40, 50, and 70% of full load with stationary compression ignition (CI) engine in dual-mode using a typical biogas composition of 60 vol. % CH_4 and 40% vol. % CO_2. While operating at every engine load the oxygen concentration in the intake air engine was varied from 21% to 27% O_2 v/v. The experimental results revealed that small additions of O_2 to intake combustion air improve combustion stability in a biogas-diesel engine. Whereas, the ignition delay (ID) time and methane emissions were decreased when using oxygen-enriched air with respect to normal air (21% O_2) and the thermal efficiency was increased.

Subramanian et al. (2013) studied the performance and emission characteristics of a self-propelled spark-ignition vehicle powered with the methane-enriched biogas (93% CH_4) and base CNG (89.14%) under modified Indian driving cycle (MIDC). Here the feedstock for biogas production is pinnata seed cake which is a waste byproduct obtained during biodiesel production and fed into the digester with a proportion of 25% oil and 75% seed. Experimental tests were conducted by two parts first part comprises of four successive cycles with a maximum speed of 50 km/h, whereas, the second part comprises of one extra-urban driving cycle with a maximum speed of 90 km/h. The experimental results indicated that the vehicle's emission with the enriched biogas fuel meets the BS-IV Emission Norms such that CO, HC, and NO_x emissions are slightly higher than the base CNG. There is no significant change in fuel economy of the vehicle powered with the enriched biogas (24.11 km/kg) as compared to base CNG (24.38 km/kg). For both the fuels the transient emission characteristics such as CO, HC, and NO_x of the engine with respect to time is very higher when compared with urban cycle (low speed) than an extra-urban cycle (high speed).

2.3 Combustion Studies on Biogas

Seung and Chang (2011) studied the influence of dual-fuel combustion characteristics on the exhaust emissions and combustion performance in a diesel engine fueled with biogas–biodiesel dual-fuel. The experimental investigation was conducted in two combustion modes under a steady-state condition with different engine loads 20, 40, 60, 80 and 100%. In the single-fuel combustion mode, neat biodiesel and a diesel pilot fuel were fueled without any additives, and then the combustion and exhaust emission characteristics of each fuel were compared at various test conditions. The experimental results of this study showed that the combustion characteristics of single-fuel combustion for biodiesel and diesel indicated similar patterns at various engine loads. In the dual-fuel mode, the peak pressure and heat release for biogas–biodiesel were slightly lower compared to biogas–diesel at low load. At 60% load, biogas–biodiesel combustion exhibited the slightly higher peak pressure, the rate of heat release (ROHR) and indicated mean effective pressure (IMEP) than those of diesel. Also, the ID for biogas–biodiesel indicated shortened trends compared to ULSD dual-fueling due to the higher cetane number (CN) of biodiesel. Significantly lower NO_x emissions were emitted under dual-fuel operation for both cases of pilot fuels compared to single-fuel mode at all engine load conditions.

Debabrata and Murugan (2014) investigated the combustion performance and emission characteristics of a DI diesel engine fueled with biogas-diesel in dual fuel mode. Whereas, the biogas was produced by the anaerobic digestion of non-edible de-oiled cakes obtained from oil crushing units and the obtained biogas was used as an alternative gaseous fuel in a DI diesel engine, in the dual-fuel mode. Diesel was used as pilot fuel and biogas was inducted through the intake manifold, at four different flow rates, viz., 0.3, 0.6, 0.9 and 1.2 kg/h, along with the air. The results specified that the biogas inducted at a flow rate of 0.9 kg/h showed better performance and lower emission than that of the other flow rates. The cylinder peak pressure in the dual fuel operation is found to be overall higher by about 11 bar than that of diesel operation. About 36% increase in the BSFC and 6.2% drop in BTE is noticed in dual-fuel operation with a biogas flow rate

of 0.9 kg/h in comparison with diesel, at full load. The NO_x and smoke emissions in the dual fuel operation found to be lower by about 39% and 49% respectively, compared to that of diesel operation.

Bhaskor and Ujjwal (2016) attempted to eliminate the negative impact of the dual-fuel combustion on the engine efficiency and environment by optimizing the effects of injection timing and a compression ratio of raw biogas powered dual fuel diesel engine at standard diesel injection timing i.e. 23° bTDC. The test was conducted on VCR diesel engine, which is converted into biogas run dual fuel diesel engine by connecting a venturi gas mixer at the inlet manifold. Experiments were conducted at different loading conditions for a set of combinations comprising of three IT such as 26°, 29°, and 32° bTDCs, and four CR 18, 17.5, 17 and 16. The results specified that a combination of pilot fuel IT of 29° BTDC and CR of 18 produced a maximum brake thermal efficiency of 25.44% and liquid fuel replacement of 82.67% at BMEP of 4.24 bar. For the same situation, the HC and CO emissions are found to be least, whereas, the NO_x, as well as CO_2 emissions, found to be the highest. From the study, it's concluded that the optimization of IT of pilot fuel along with the use of high CR is a must for effective practical utilization of raw biogas run dual fuel diesel engines.

Sunmeet and Subramanian (2017) investigated the effects of simulated biogas on a single-cylinder diesel engine under dual fuel mode (biodiesel-simulated biogas). Experimental tests were conducted at two loads (part and full load) to measure performance, combustion and emission characteristics. The Pongamia pinaata biodiesel (B100) was used as pilot fuel, whereas, biogas composition was simulated by blending of CO_2 (30, 40 and 50% by weight) in natural gas and was used as the main fuel. Natural gas and CO_2 were injected into the engine's intake manifold using two gas injectors with the individual control mechanism. The brake thermal efficiency (BTE) of the engine decreases with an increase in CO_2 content in natural gas. NO_x and smoke emissions decreased significantly with the biogas-fueled engine, whereas, HC and CO emissions increased slightly. The combustion characteristics including heat release rate and

cumulative heat release decreased with biogas. A notable point emerged from this study is the effect of CO_2 in natural gas on the performance, combustion and emissions characteristics of the engine are less as compared to the effect of its energy share and load. It is well established through this study that the raw biogas could be used in a biodiesel-fueled diesel engine under dual fuel mode.

Saket et al. (2017) studied the effects of varying composition of biogas on performance and emission characteristics of compression ignition engine using exergy analysis. The author focused on experimental evaluation and quantification of these variations of the engine performance. The experiment was conducted on a small compression ignition engine in dual fuel mode using three compositions of biogas: BG93, BG84, and BG75 (containing 93, 84 and 75% of CH_4 by volume respectively). Second-law of thermodynamics is implemented to evaluate individual process inefficiencies, exergy analysis for different compositions of biogas. Based on second-law analysis it was found that BG93 dual fuel operation at full load showed most comparable performance with diesel operation. Biogas dual fuel operation showed 80–90% diesel substitution at lower engine loads, whereas, at higher loads, total irreversibility of the engine was increased from 59.56% for diesel operation to 61.44, 64.18 and 64.64% for BG93, BG84, and BG75 biogas compositions respectively. Furthermore, combustion irreversibility was found to be decreasing with higher CO_2 concentrations in biogas. Based on second-law analysis it was found that BG93 showed comparable results to that of diesel operation with 26.9% and 27.4% respectively.

2.4 Studies on cyclic variations

Rakesh and Avinash (2011) examined the impacts of the cyclic variations incase of double cylinder homogeneous charged compression ignition (HCCI) engines using ethanol through port injection. Authors observed that by controlling the mixing of fuel, air as well as residual gases the combustion in HCCI engine can be effectively attained. But at lower and higher loads the combustion found to be unstable rather than smooth operation. By studying the combustion for 100 consecutive cycles, tests were conducted

at different intake air temperatures as well as various air-fuel ratios. For various operating conditions of the engine, coefficient of variations (COV) were obtained, such that the authors observed, as the P_{max} increases COV increases for varying rich mixture, on the other hand as the temperature of intake air is increased the COV also increases.

Panagiotis et al. (2016) investigated the cyclic variations of cylinder pressure in the direct injection diesel engines. Cyclic variations were determined by employing single injection, for lower temperature, at the end of compression as well as varying oxygen concentration. From the results, authors observed that greater deviations of maximum cylinder pressure for different cycles were developed indicating larger cyclic variations. On the other hand, few cycles showed zero pressure variations even though there is an increase in average intensity of variations under increased premixed conditions. Whereas, at when the charge was maintained at the lower temperature the peak pressure dissimilarity in between the average cycle as well as cycle having lower variations was found to be greater than 3% of peak pressure.

Wang et al. (2016) studied the cyclic variations existence in a diesel engine using methanol operated through dual fuel condition by determining the parameters such as methanol substitution percentage (MSP), impact of engine load, intake temperature and injection timing for In-cylinder pressure of 100 consecutive combustion cycles. Authors concluded the results as per the experimental observation saying that the magnitude of the cyclic variations involved in dual fuel mode combustion at lower load increases and is very vulnerable to the quantity of methanol. Significant improvement was observed in case of coefficient of variation (COV) of maximum in-cylinder pressure ($COVP_{max}$) and maximum averaged temperature ($COVT_{max}$) which scatters more as the MSP goes higher. However, authors found that combustion stability is very sensitive to intake temperature and COVs of every combustion parameter reduced as the intake temperature increased at lower loads. On the other hand, the intake temperature showed less effect upon the COV at full load.

Qiang et al. (2019) evaluated the cycle-to-cycle variations (CCVs) using 2D visualisation and cylinder pressure (pilot fuel in an optical heavy duty engine driven with methane and diesel. The combustion behaviour is measured using a high-speed colour camera based on natural luminosity (NL). Authors reconstructed and analysed the image using proper orthogonal decomposition (POD). The POD-based coefficient of variation (COV), as well as the pressure-based and global intensity-based COV, are used to assess cyclic variability. The fluctuations in the luminosity field, which can offer information on chemical kinetics, are presented by the POD-based and global intensity-based COVs. Finally, the impact of methane lambda, pilot fuel rate, and charge air temperature on CCVs was thoroughly investigated. The findings demonstrated that CCVs are inhibited by higher methane concentrations. The igniting parameters of the pilot fuel determined the appearance of the CCVs. When the charge air temperature is below the critical point, increasing the charge air temperature has a primitive influence on CCVs, thereafter, it has an inhibitive effect on CCVs.

2.5 Relative Studies on Injection Timing Effects

Kannan and Anand (2011) investigated the effects of injection timing as well as pressure on the characteristics of the conventional diesel engine fuelled with diestrol consisting of 30% waste cooking palm oil (WCO) methyl ester, 60% diesel and 10% ethanol blend. Authors found major improvement in performance with 31.3% engine efficiency at injection timing of 25.5° bTDC and injection pressure of 240 bar. Significant improvement in emissions was also observed with 33% decrease in CO, 27.3% decrease in Sootness and 6.3% decrease in CO_2 emissions NO_x emission decreased by 4.3% as compared to diesel fuel. However, UBHC emission increased with minor variation. In addition to this, for similar operating condition higher peak cylinder pressure as well as heat release rate and lowest ID of 12.7° CA was attained for diestrol fuel with respect to diesel fuel.

Donghui et al. (2011) studied the effect of injection timing and EGR rate on the combustion and emissions of a Ford Lion V6 using neat biodiesel produced from soybean oil. Authors observed from the results that, with the increasing of EGR rate, the BSFC

and soot emission were slightly increased, and NOₓ emission was evidently decreased. Under the higher EGR rate, the peak pressure was slightly lower, and the peak heat release rate kept almost identical at lower engine load, and was higher at higher engine load. With the main injection timing retarded, the BSFC was slightly increased, NO_x emission was evidently decreased, and soot emission hardly varied. The second peak pressure was evidently decreased and the heat release rate was slightly increased.

Harun Kumar et al. (2018) illustrated the behaviour of the diesel engine when it is subjected to advance (27° bTDC), actual (23° bTDC) and retard (19° bTDC) injection timings using 20% biodiesel such that spill method is employed to achieve different injection timings. Authors found maximum BTE was enhanced by 3.18% with reduction in CO by 17.3%, NO_x by 31.34%, UBHC emission by 57.3% and smoke opacity by 8.1% for full load at retard injection timing as compared to the actual injection timing of the engine. Better combustion properties were achieved with in-cylinder pressure of 69.29 bar and heat release rate of 69.12 J/°CA for 190° bTDC as compared to other injection timings.

Abdul and Ramesh (2019) investigated the effect of post and pilot diesel injection to see the energy conversion efficiency and emissions of a common rail dual fuel engine. They observed that the higher than normal methane concentrations (normal: 51–53%) increased the NO levels while having minimal effect on efficiency. When low quantities of methane were utilized, NO levels could be efficiently reduced, especially at low biogas energy shares (BGES). According to the simulation studies, the decrease in NO is attributed to the lower in-cylinder temperature rather than a lower oxygen content as a result of higher CO_2. To compensate for the increase in ID and reduction in the combustion rate when the proportion of methane was reduced from 68% to 24%, the start of diesel injection had to be advanced by 3 °CA (at a BGES of 60 percent). Because of the split injection procedure, there was a reduction in smoke emission with pilot injection due to increased charge uniformity. However, because of the diffusion combustion the post-injected fuel undergoes in the biogas diesel dual fuel (BDDF) mode.

2.6 Effects of Oxygen Enrichment Method

Cacua et al. (2012) examined the effect of oxygen-enriched air from 21 to 27% O_2 by volume in a dual diesel-biogas engine. Thermal efficiency, pollutant emissions, and combustion parameters were determined as a part of the operation. Experiments have been carried out with a dual-mode stationary compression ignition (CI) engine linked coupled to a generator. Authors have used the biogas consisting of 60% CH_4 and 40% CO_2 (by volume) into the engine operation. The oxygen content in the intake air engine was tested and ranged from 21% to 27% O_2 v/v. While compared to the normal air (21% O_2), the ID time and methane emissions were reduced as oxygen levels are increased, however the thermal efficiency increased.

Li et al. (2013) investigated the enrichment of engine characteristics in a 6-cylinder diesel engine by oxygen enrichment inducted at intake manifold using rapeseed oil (RSO) to minimize the deterioration occurring due to the particulate matter by enriching the oxygen concentrations. Authors, observed that by increasing oxygen content measured in terms of volume basis from 21 to 24% the ID reduced, combustion and emission characteristics such as CO, UBHC and sootness was reduced evidently but on the other hand NO_x emission increased at higher rate. However, major improvement was achieved in heat release rate such that due to small ID, the peak heat release rate decreased at premixed combustion stage but at the diffusion combustion stage decrement in peak heat release rate was observed. Conversely, maximum in-cylinder pressure improved by 6% and cylinder temperature by 9% as the oxygen enrichment is enhanced. Overall, the oxygen enrichment was optimized to 22% with optimum NO_x emission and improvement in the performance.

Baskar et al. (2016) analyzed the effect of oxygen concentration ranging from 21 to 27% by volume basis with increment of 2% operated in a single cylinder diesel engine at constant speed of 1500 rpm. By analyzing the results, authors came out with the conclusion stating that engine efficiency improved by 4 to 8% as well as improvement in power. Emissions profile such as unburnt hydrocarbon, carbon monoxide and sootness

reduced by 40%, 55% and 60%, correspondingly. However, NO_x emission increased drastically as the oxygen concentration increased to 27% significantly. On the other hand, significant improvement was observed in case of sootness as it exhibited better combustion indicating less particulate matter.

Madhankumar et al. (2019) studied the effect of oxygen enrichment in a CI engine on performance, emission, and combustion characteristics with mahua oil (MO). Authors motive of the work was to reduce the smoke emissions from MO operation and to reduce CO_2 emissions and to be economical. Authors observed that MO's poor physical qualities, such as its high viscosity and density, generate atomization issues, which result in increased smoke, HC, and CO emissions. The difficulty in forming a mixture with straight vegetable oil in a CI engine is improved by raising the oxygen content, an oxygen cylinder separate from the engine is used to induct the oxygen. The engine used in this experiment is a twin-cylinder tractor engine that runs at 1500 rpm. Performance, emission, and combustion parameters were measured under various loading circumstances (25, 50, 75, and 100% of rated power) with different intake-oxygen concentrations ranging from 21 % (by volume) to 24 % (by volume) with MO and compared to diesel. At maximum load, a 24 % increase in the oxygen reduced smoke, HC, and CO emissions by 36, 34, and 50 %, respectively. When compared to diesel, BTE was reduced by around 5% when using MO at maximum load. In comparison to plain MO, BTE was improved by 10% with a 24% (by volume) increase with MO at maximum load.

2.7 Techniques for Emission Reduction

Gonca (2014) studied the effects of steam injection on performance and NO_x emissions of a diesel engine running with ethanol-diesel blend applied into a single-cylinder, four-stroke, direct injection, naturally aspirated diesel engine by using two-zone combustion model for 15% ethanol addition and 20% steam ratios at full load condition. In addition to this, a combustion simulation has been performed using the two-zone combustion model so as to examine the influences of steam injection on the performance and NO_x

emissions of the engine. The combustion models have been performed for the optimum steam rate (20% of injected fuel by mass) with the 15% ethanol rate of injected fuel by volume and the results of two experimental and four theoretical engine modes have been explored. The results obtained are compared with a conventional diesel engine (D), steam injected diesel engine (D + S20), diesel engine fueled with an ethanol-diesel blend (E15) and steam injected diesel engine fueled with the ethanol-diesel blend (E15 + S20) in terms of performance and NO_x emissions. The results showed that as NO_x emissions considerably decrease the performance significantly increases with the steam injection method.

Patnaik et al. (2016) investigated the combined effects of diesel, diesel-ferric chloride ($FeCl_3$), diesel-steam injection, and diesel-$FeCl_3$-steam injection upon the performance and emission characteristics of the diesel engine. The experiment is executed by generating the saturated steam by means of shell and tube heat exchanger along with the waste energy from the engine exhaust gas such that the heat exchanger is designed by limiting the steam flow rate to 3% and 5% operated for 60% and 80% engine load. Promising outcomes were achieved by the authors in terms of improvement in brake thermal efficiency using the combination of diesel-ferric chloride ($FeCl_3$), diesel-steam injection, and diesel-$FeCl_3$-steam injection by 8%, 4%, and 3% as compared to diesel mode. However, as compared to diesel mode the combination of diesel-$FeCl_3$-steam injection the maximum cylinder pressure as well peak combustion gas temperature showed decrement by 4%. Whereas, emissions were improved with reduction in NO, CO_2, O_2 and UBHC, moreover, CO, UBHC and sootness decreased for the combination of diesel-$FeCl_3$ compared to only the diesel mode.

Hadia et al. (2017) investigated the combined effects of compression ratios and steam injection on performance, combustion and emission characteristics of an HCCI engine numerically. The work is performed in two parts, in the first part of the work, the cylinder temperatures obtained with different intake values (480, 485, 492.5, 497.5, and 510 K) are simulated and compared to published results obtained in the same conditions in order to validate the numerical tool. Whereas, in the second part, the numerical tool is used to

analyze the combined effects of compression ratio and steam injection on HCCI engine, such that the analysis achieved in term of scalar quantities such as temperature, pressure and ignition timing using the Internal Combustion Engine (ICE) model. For model assessment, computed results are compared to the published data available in the literature obtained with the same boundary conditions. Results show that the performance of the HCCI engine is very low if the steam injection exceeds 20%. So he concluded that a compression ratio of 18 with a steam injection of 10% is recommended as it leads to CO reduction of 40% and keeps 10% the consumption of the fuel.

Horng et al. (2017) explored the effects of injecting methanol for different injection timings as well as inlet air temperature at the intake port of the diesel engine. In order to determine the optimal ratio for methanol energy share optimization technique such as Taguchi methodology was incorporated. Authors implemented the electronic control unit for varying injection timing through electronic injector as well as to control the quantity of the methanol. By using an electric heater air inlet temperature is varied as per the requirement. The experimental results obtained are compared with the Taguchi methodology for confirmation tests. Around 95% confidence level is achieved with predicting with the experimental results. Factors which are considered for optimization showed the largest reduction in smoke emission of 41.5%, NO_x around 61.7%, UBHC of 8.6% and carbon monoxide emissions of 32.4%.

Table 2.1: Summary of biogas as an alternative fuel for IC engine operated in dual fuel mode

Sl No	Author	Type of fuel used	Objective	Type of engine and its specifications	Experimental major outcomes
1)	Raj et al. (2009)	- Biogas from textile cotton waste (batch type digester)	- To generate biogas as an additional source of energy.	- Four-stroke, single-cylinder, water-cooled, 5.2 kW @ 1500 rpm.	- 5 to 7.5% of cow or pig dung with cotton waste by weight generates around 77% of methane. - Around 60% of diesel is saved by using biogas as dual fuel.
2)	Bedoya (2009)	- Simulated biogas (60% CH_4–40% CO_2) as the primary fuel. - Diesel and palm oil biodiesel as pilot fuels.	- To study the varying mixing system and pilot fuel quality. - Study of the supercharged mixing system.	- Lister Petter TR2, DI, four-stroke, two cylinders, naturally aspirated, air-cooled, 20 kW @ 3000 rpm.	- The combination of a supercharger and Kenics mixer in the inlet system of the dual-fuel engine increases thermal efficiency. - Methane and carbon monoxide emissions were reduced.
3)	Rossetto et al. (2013)	- Biogas from anaerobic digestion of waste in rural areas of Brazil.	- Performance of an Otto cycle engine fed with biogas.	- National Volkswagen, model Ap 1.8 L, 45kW@5000 rpm.	- Best power result for biogas was obtained at a compression rate of 12.5:1, long gas mixer and spark advance 45°.

4)	Bhaskora nd Ujjwal (2015)	- Rice bran oil methyl ester (RBME), Pongamia oil methyl ester (PME) and Palm oil methyl ester (POME) as pilot fuels --Biogas as primary fuels.	- A comparative study among the three biodiesels under dual fuel mode.	- Research engine test setup, Code 240 Single cylinder, four-stroke, DI diesel engine, 3.5 kW @ 1500, Water-cooled.	- RBME-biogas produced a maximum brake thermal efficiency of 19.97% at 100% load. - HC emissions for PME-biogas and POME-biogas increased by 11.73% and 16.27%, in comparison to RBME-biogas. - Decrease in NO_x emission by 5.8% and 14%, for PME-biogas and POME-biogas.
5)	Bora and Saha (2016)	- Rice bran biodiesel-biogas.	- To study the effect of compression ratio (18, 17.5 and 17)	- Single cylinder, DI, water-cooled, variable compression ratio, 3.5 kW diesel engine.	- At full load, max BTEs under dual fuel mode are found to be 20.27%, 19.97% and 18.39% for CRs of 18, 17.5 and 17. - Reduction in CO and HC emissions by 17.67% and 17.18% when CR is increased from 17 to 18. - Increase in NO_x as well as CO_2 emissions by 42.85% and 14.13%.
6)	Debabrata and Murugan (2016)	- Raw biogas-diesel.	- To characterize the biogas obtained from the seed cake of Karanja (SCK).	- Kirloskar TAF 1, Single cylinder, 4stroke, CI, air-cooled, direct injection, 4.4 kW	- Dual fuel operation with the injection timing of 26°CA bTDC gave an overall better result than other injection timings. - NO_x emission was higher with advanced pilot

				@1500 rpm.	injections than that of original injection timing.
7)	Awogbemi et al. (2016)	- 20% biogas+80% petrol blend.	- To develop and test the biogas-petrol blend to run a spark-ignition engine.	- Honda GX 140, four-stroke, single-cylinder, spark-ignition engine, 5hp @ 4000 rpm.	- Biogas–petrol blend generated higher torque, brake power; indicated power, brake thermal efficiency, and brake mean effective pressure. - Lower fuel consumption and exhaust temperature than petrol.
8)	Salve et al. (2016)	- Synthesized biogas (65% CH_4 and 35% CO_2).	- To unfold the effect of compression ratio (15 to 18).	- Kirloskar made 3.5 kW single cylinder, direct injection, water-cooled, and variable compression ratio diesel engine.	- BSFC decreases as pilot fuel quantity increases. - Brake thermal efficiency increases as pilot fuel quantity increase at all loads conditions. - NO_x emissions found lower in dual-fuel operation.
9)	Senthilkumar and Vivekanandan(2016)	- 80% biogas+20% diesel, 60% biogas+40% diesel, 40%biogas+60% diesel, 20%biogas+80% diesel.	- To generate biogas from a $1m^3$ capacity floating drum type biogas plant. - To Develop a CI engine that can run using biogas as secondary fuel.	- Diesel engine, single-cylinder, water-cooled, 5 kW with the rated speed of 1500 rpm.	- BTE decreases in all the biogas-diesel mixtures. - EGT decreases in case of the biogas-diesel fuelled engine. - Engine brake power reported lower in case of a biogas-diesel mixture.

| 10) | Debabrata et al. (2017) | - Karanja methyl ester (KME) as a pilot fuel
 - Biogas derived from Karanja seed cake. | - To Study, the behavior of diesel engine fueled with Karanja methyl ester-biogas at different injection timings.
 -Injection timing of 21.5° CA bTDC to 27.5° CA bTDC in steps of 1.5° CA. | - Kirloskar TAF 1, Single cylinder, 4 stroke, CI, NA,
 4.4 kW @ 1500 rpm. | - BDFM24.5 gave an optimum result for combustion, performance and emission characteristics than other injection timings.
 - The BSFC for BDFM24.5 is higher by 23.9% than that of KME, but it is 5.1% lower than that of BDFM23.0, at full load.
 - About 6.6% increase in BTE was observed for BDFM24.5 in comparison with the BDFM23.0, at full load.
 - The NO_x emission for BDFM24.5 was higher by about 5.5% than that of BDFM23.0, at full load. |

Table 2.2: Summary of comparative studies on biogas with other gases

Sl No	Author	Type of fuel used	Objective	Type of engine and its specifications	Experimental major outcomes
1)	Porpatham et al. (2007)	- Biogas and hydrogen.	- To study the effect of hydrogen in the petrol engine. (5%, 10%, &15%)	- A single-cylinder, four-stroke, air-cooled direct injection diesel engine 4.4 kW @ 1500 rpm.	- Hydrogen significantly enhances the combustion rate. - Significant reductions in hydrocarbon levels were seen. - There was no increase in nitric oxide emissions. - Peak pressures and heat release rates are lower with

				hydrogen addition.
2)	Park et al. (2011)	- Biogas with various methane concentrations	- N$_2$ dilution test - H$_2$ addition test.	- Naturally aspirated (NA), 8-L spark ignition engine, 60 kW @1800 rpm.	- Increase engine efficiency at 5-10% H$_2$ concentration. - Addition of hydrogen improved in-cylinder combustion characteristics.
3)	Chandra et al. (2011)	- CNG, methane-enriched biogas and biogas from biomethanation of jatropha and Pongamia oil seed cakes	- To determine the suitability of utilization of biogas and methane enriched biogas in a diesel engine.	- 5.9 kW single-cylinder, an air-cooled diesel engine having 1500 rated rpm.	- Maximum brake power produced by the engine was found at ignition advance of 35° TDC for all the tested fuels. - The power deteriorations of the engine were observed to be 31.8%, 35.6% and 46.3% on all fuels.
4)	Karen et al. (2012)	- Biogas(60% CH$_4$ and 40% CO$_2$)- diesel and	- To test the effect of oxygen-enriched air(from 21 to	- Lister Petter TR2, DI, four-stroke, two cylinders, naturally aspirated, air-cooled 20 kW @ 3000 rpm.	- Small additions of O$_2$ to intake combustion air improve combustion stability. - The additional O$_2$ helps to attenuate the negative effects of CO$_2$ in the combustion. - Thermal efficiency was observe to be increased.

Sl No	Author	Type of fuel used	Objective	Type of engine and its specifications	Experimental major outcomes
		oxygen	27%v/v)		
5)	Subramanian et al. (2013)	- Methane enriched biogas (93% CH$_4$) and base CNG (89.14%)	- Comparative evaluation of mass emission and fuel economy.	- 3-Cylinder in-line, SI engine, 4-valves per cylinder with i-GPI bi-fuel technology, 44.2 kW (CNG) @ 6200 rpm.	- No significant difference in fuel economy between enriched biogas (24.11 km/kg) and base CNG (24.38 km/kg) - Mass emissions such as CO, HC, and NO$_x$ are slightly higher with the enriched biogas than base CNG.

Table 2.3: Summary of combustion studies on biogas

Sl No	Author	Type of fuel used	Objective	Type of engine and its specifications	Experimental major outcomes
1)	Seung and Chang (2011)	- Biogas (organic waste biomass)– Biodiesel (100% methyl ester of soybean oil)	- Combustion characteristics on the reduction of exhaust emissions. - To evaluate combustion pressure and the rate of heat release.	- Four-cylinder, turbo-Charged, Water-cooled, Indirect injection (IDI), prechamber compression ignition (CI) engine. The rated maximum power is 15.21 kW @ 4000 rpm.	- The peak pressure and heat release for biogas–biodiesel was slightly lower compared to biogas–diesel at low load. - At 60% load, biogas–biodiesel combustion exhibited the slightly higher peak pressure, the rate of heat release than those of diesel. - The ID for biogas–biodiesel indicated shortened trends compared to diesel. -Lower NO$_x$ emissions were emitted under dual-fuel operation for both cases.

2)	Debabrata and Murugan (2014)	- Biogas from anaerobic digestion of Pongamia pinnata de-oiled cakes.	- Produce, and characterize the biogas obtained from P. pinnata de-oiled cake, through the anaerobic digestion. -Combustion, performance and emission characteristics.	- Single cylinder, four-stroke, air-cooled, direct injection diesel engine, with a rated power output of 4.4 kW @1500 rpm.	- The biogas at the flow rate of 0.9 kg/h showed better performance. - The ID in the dual fuel operation is longer. - Overall the cylinder peak pressure in the dual fuel operation is higher by about 11 bar. - The NO_x and smoke emissions in the dual fuel operation showed lower by 39% and 49%.
3)	Bhaskor and Ujjwal (2016)	- Raw biogas (60% CH_4 +40% CO_2)	- To optimize the operating parameters like IT of pilot fuel and CR. -ITs of 26°, 29°, and 32°bTDC -CRs of 18, 17.5, 17 and 16	- 3.5 kW single cylinder, direct injection, water-cooled, variable compression ratio diesel engine.	- Pilot fuel IT at 29° BTDC and CR of 18 was found to be optimum of maximum brake thermal efficiency of 25.44%. - The emissions of CO and HC are found to be least. - NO_x as well as CO_2 emissions are found to be the highest.
4)	Sunmeet and	- Pongamia	- To assess the	- Kirloskar oil engines	- The BTE reduced as the CO_2 level in natural

| | Subramanian (2017) | pinaata biodiesel (B100)
- Biogas and Natural gas | feasibility of using raw biogas in a biodiesel. | (EA10), 5 KVA, 19.5:1 CR, 947.38 CC Diesel engine. | gas rises.
- NO_x and smoke emissions decreased dramatically.
- HC and CO emissions increased slightly.
- The heat release rate and cumulative heat release decreased with increase in biogas. |

Table 2.4: Summary of studies on cyclic variations

Sl No	Author	Type of fuel used	Objective	Type of engine and its specifications	Experimental major outcomes
1)	Panagiotis et al. (2016)	- Diesel	- To investigate the cyclic variations of cylinder pressure in the diesel engine. - To study cyclic variations with varying oxygen concentration.	- MTU 396 series diesel engine, single-cylinder @ 2100 rpm.	- Greater deviations of P_{max} for different cycles was developed indicating larger cyclic variations. - Few cycles showed zero pressure variations even though there is an increase in the average intensity of variations under increased premixed conditions.
2)	Rakesh and Avinash (2011)	- Ethanol	- To study the impacts of the cyclic variations using ethanol through	- Double cylinder, HCCI engine, 4.85 kW @1500 rpm, 1318	- At lower and higher loads the combustion found to be unstable. - As the P_{max} increases COV increases for

			port injection. - To study the cyclic variations for various intake air temperatures from 120, 140, and 160 °C at different air-fuel ratios.	CC HCCI engine.	varying rich mixture. - The temperature of intake air is increased the COV also increases.
3)	Wang et al. (2016)	-Methanol	- To study the cyclic variations in a diesel engine for different methanol concentration. - To determine the COV in terms of maximum cylinder pressure and temperature.	- 4.21 L, Inline 4 cylinder diesel engine, 103 kW @ 1600 rpm.	- COV increased as the methanol quantity increased at lower loads. - $COVP_{max}$ and $COVT_{max}$ scattered as the methanol percentage increased. - Combustion stability is sensitive to intake temperature.
4)	Cheng et al. (2019)	- Methane	- To analyze the cycle to cycle variations in an optically accessible dual fuel engine with a high-speed color camera.	- 4-Stroke diesel single-cylinder, 1400 rpm, optical engine, 17.9:1 CR.	- The inclusion of CH_4 significantly reduces the ID, resulting in the appearance of COVs at a later time. - The drop in the pressure-based COV becomes noticeable as the t_{pilot} is increased more.

Table 2.5: Summary of relative studies on injection timing effects

Sl No	Author	Type of Fuel used	Objective	Type of Engine and its specifications	Experimental major outcomes
1)	Kannan and Anand (2011)	- Diestrol (30% waste cooking palm oil (WCO) methyl ester, 60% diesel and 10% ethanol blend)	- To study the influence of injection Pressure. - To study the influence of timing on diesel engine combustion, performance and emission behaviors with diestrol fuel.	- TV1 kirloskar, 5.2 kW @1500 rpm, water cooled, diesel engine.	- At 240 bar injection pressure & 25.5° bTDC injection timing, maximum BTE of 31.3% was achieved. - CO, CO_2, SO & NO_x emissions reduced by 33%, 6.3%, 27.3%& 4.3% compared to diesel. - Diestrol exhibited lesser ID of 12.7° CA at same operating condition.
2)	Harun Kumar et al. (2018)	- Biodiesel blend (20% Tamarind seed methyl ester)	- To study the influence of injection timing upon diesel engine parameters.	- Kirloskar TAF1, 4.4 kW @ 1500 rpm, single cylinder diesel engine.	- Engine efficiency improved by 3.18%. - Emissions decreased by 17.3%, 57.3%, 31.34% and 8.1% for CO, UBHC, NO_x, & sootness at retard injection timing.
3)	Rahman, K. A., and Ramesh, A. (2019)	- Biogas (CH_4 – 57%, CO_2 – 41%)	- To evaluate the influence of variations in composition on the energy conversion efficiency and emissions under the effects of post and pilot injection of	- Mahindra Maxximo (CRDi) naturally aspirated twin cylinder water cooled engine, 454.5 cc per cylinder, 19.2	- Increasing the biogas and decreasing the proportion of CH_4 in biogas reduced NO_x emission significantly. - Smoke decreased with increase in BGES. No significant change in smoke emission with change in biogas composition.

| 4) | Donghui et al. (2011) | - Soyabean biodiesel | - To study the effect of injection timing and EGR rate on the combustion and emissions. | - Ford Lion 6-cylinder 4-stroke direct injection, Variable geometry turbocharger, Common rail (up to 1.65 MPa) Fuel | - Increasing of EGR rate, BSFC and soot emission were slightly increased.
 - NO_x emission evidently decreased.
 - Under higher EGR rate, the peak pressure was slightly lower, and the peak heat release rate kept almost identical at lower engine load.
 - With injection timing retarded, BSFC slightly increased, NO_x emission decreased, and soot emission barely varied. |

(First row continued from previous page: "diesel." | "kW @ 3600 rpm.")

Table 2.6: Summary of effects of oxygen enrichment process

Sl No	Author	Type of Fuel used	Objective	Type of engine and its specifications	Experimental major outcomes
1)	Li et al. (2013)	- Rape seed oil (RSO)	- To study the effect of intake air (from 21% to 24%). - To minimize the	- Perkins Phaser 180Ti, 6 cylinders, 134 kW @ 272 rad s⁻¹, Turbo-charged and	- ID reduced and emission characteristics such as CO, UBHC and sootness was reduced evidently - NO_x emission increased at higher rate.

					- Maximum in-cylinder pressure improved by 6% and cylinder temperature by 9%.
			deterioration of particulate matter of RSO.	inter-cooled, diesel engine.	- The oxygen enrichment was optimized to 22%.
2)	Baskar et al. (2016)	- Diesel	- To analyze the effect of oxygen levels from 21 to 27% by volume basis upon engine characteristics.	- Kirloskar TAF1, 4.33 kW @ 1500 rpm, single cylinder diesel engine.	- Engine efficiency improved by 4 to 8%. - UBHC, CO and sootness reduced by 40%, 55% and 60%. - NO_x emission increased drastically.
3)	Madhankumar et al. (2019)	- Mahua oil (MO)	- To study the effect of oxygen enrichment in a CI engine on performance, emission and combustion characteristics with mahua oil (MO) as base fuel	- Simpsons S 217 tractor engine, 12.4 kW @ 1500 rpm, Vertical in-line diesel engine.	- Oxygen enrichment of 24% reduced smoke, HC and CO emissions by 36, 34 and 50%. - The direct combustion of MO improved with reduced smoke, HC and CO emissions. - BTE was improved by 10% with 24% (by volume) with MO compared to neat MO.
4)	Cacua et al. (2012)	- Biogas (CH_4 – 60%, CO_2 – 40%)	- To investigate the influence of oxygen levels (21 to 27% O_2) on a diesel engine.	- Lister Petter TR2, DI, four stroke, two cylinders, naturally aspirated, air cooled, 20 kW @	- ID time and methane emissions were decreased. - Thermal efficiency increased.

				3000 rpm.	

Table 2.7: Summary of studies related to techniques for emission reduction

Sl No	Author	Type of Fuel used	Objective	Type of engine and its specifications	Experimental major outcomes
1)	Gonca (2014)	- Ethanol–diesel blend - (D + S20) - Ethanol–diesel blend (E15) - Ethanol–diesel blend (E15 + S20)	- Investigation On the effects of ethanol-diesel blends on the performance and emissions.	- Single cylinder, four-stroke, direct injection, naturally aspirated diesel, 13 kW @ 2400 rpm.	- The effective efficiency and effective power of the engine fueled mixture is increased up to 12.5% and 4.1%. - NO_x emissions reduced up to 34% with steam injection.
2)	Hadia et al. (2017)	- Diesel	- Combine effects of compression ratio and steam injection. - Combustion is performed by using the ICE mode	- HCCI Engine	- By increasing the compression ratio, the ignition duration decreases and the CO_2 concentration is also decreased. - At any compression ratio, the CO reduction is almost constant if the steam injection is still constant. - 10% the consumption of the fuel is reduced.
3)	Horng et	- Methanol	- Effects of	- Single cylinder,	- 95% confidence level is achieved with

	al. (2017)		injecting methanol for different injection timings. - To determine the optimal ratio for methanol energy share Taguchi methodology was incorporated.	four-stroke, diesel Engine, 9.2 kW @ 2400 rpm.	predicting with the experimental results. - Factors which are considered for optimization showed the largest reduction in smoke emission of 41.5%, NO_x around 61.7%, UBHC of 8.6% and carbon monoxide emissions of 32.4%.
4)	Patnaik et al. (2016)	- Diesel - Diesel-ferric chloride ($FeCl_3$) - Diesel-steam injection -Diesel-$FeCl_3$-steam injection	- To explore the impact of different steam injections on the performance and emission parameters.	- Single cylinder, 4-stroke, water cooled, diesel Engine, 3.5 kW @ 1500 rpm.	- Brake thermal efficiency improved using the diesel-ferric chloride ($FeCl_3$), diesel-steam injection, and diesel-$FeCl_3$-steam injection by 8%, 4%, and 3% compared to diesel mode. - Maximum cylinder pressure as well peak combustion gas temperature showed decrement by 4%. - NO, CO_2, O_2 and UBHC emissions improved. - CO, UBHC and sootness decreased for the diesel-$FeCl_3$ compared to the diesel mode.

2.8 Summary of Literature Review

The literature has provided extensive study on generation of biogas from various sources and also shown the application of biogas operated in a diesel engine with various operating conditions. A wide outline from every aspects is provided, covering all the methods incorporated to enhance the diesel engine performance and mitigate the emissions using the biogas.

The following observations are formulated based on the literature review:

➢ Biogas is produced from various sources such as agricultural, industrial wastes, Jatropha and Karanja seed cake, textile cotton waste, Rice bran oil methyl ester, Pongamia oil methyl ester and other organic elements but however, studies related to the biogas obtained from food waste are scanty.

➢ Effects of various biogas mass flow rate have been explored on the different types of engines. Eventually, research related to the effect of higher mass flow rate of biogas on dual fuel engines are limited.

➢ Generally, gaseous fuels are very vulnerable to the changes and it has more tendency towards undergoing cyclic variations, when it is operated in dual mode. Literature review have revealed that, studies related to cycle by cycle variations for various gaseous and liquid fuels have been reported. Still, studies related to cyclic variations in diesel engine using biogas are not reported.

➢ Even though authors have observed that the biogas gives a higher resistance to knocking because of its higher octane number, auto-ignition temperature and makes it suitable to operate with injection timing. Yet, there is no open literature available on biogas operated with higher injection timings.

➢ Wider flammability limit and homogenous mixing nature of biogas has given provision to operate with other gaseous fuels such as CNG, hydrogen, producer gas, LPG without compromising performance and emissions. However, there are no experimental studies reported on the biogas with oxygen enrichment.

➢ Several emission reduction techniques such as EGR, water emulsion, SCR, water injection, steam injection have been incorporated and studied the effects on the engines using several renewable fuels. Most efficient and promising technique, vaporized water-methanol induction system to enhance the engine performance and reduce emissions using biogas has not been reported in the literature.

2.9 Research Gap

From the literature, it is observed that several research works have been conducted on the performance and emission characteristics of biogas operated in a dual mode. However, studies related to the engine operated under dual-mode using a higher mass flow rate of biogas obtained from food waste are less. Also, the work related to the behavior of the diesel engine under cycle by cycle variation using biogas are scanty. Although, the effects of injection timing upon the engine are studied, limited investigation are observed for higher proportions of biogas under varying injection timing. Various emissions reduction techniques even though implemented, work related to vaporized water-methanol induction method under dual fuel mode is limited and moreover studies related to biogas operated with oxygen induction is partial. Hence, based on these observations, objectives of the research work are framed in order to achieve the research gap.

2.10 Objectives

The major objectives of the research work are as follows:

➢ To study the performance, combustion and emission characteristics of diesel engine by dual-fuel mode using biogas.

➢ To study the engine behavior under cycle by cycle variations experimentally with the different operating conditions.

➢ To investigate the impact of injection timing upon the engine using different biogas proportions.

➢ To implement and study the influence of oxygen enrichment for the optimized biogas proportion along with intake air.

➢ To study the effect of the vaporized water-methanol induction system on the diesel engine characteristics for the oxygen-enriched optimized biogas.

Henceforth, the objective has been framed to investigate the effects of biogas under dual fuel mode of operation in CI engine at different engine loads corresponding to the different operating conditions for improving the performance and thereby to reduce the emissions.

2.11 Closure

A detailed review of the literature significant to the present research work is provided in this chapter. Fundamental methods to operate the engine by varying the parameters are explored. Different techniques to enhance the performance of the engine are briefly discussed and the overall summary of the literature review are highlighted. Based upon the research gap, the objective of the present investigation is formulated. The process of extracting the biogas from the anaerobic digester plant and measurement of the biogas composition are discussed in the next chapter.

CHAPTER 3

EXTRACTION OF BIOGAS

The present chapter provides details about the anaerobic digester and the process of extracting the biogas from the digester plant. A brief description about the facilities incorporated in the plant to extract the biogas from the plant and transferring into the tyre tube using an air compressor is also included. The details about the working principle, working procedure of the gas chromatography and determination of the biogas composition are also reported in the current chapter.

3.1 Biogas Plant

The biogas which is used for conducting the experimental work is taken from biogas plant situated near Urwa ground monitored by Mangalore City Corporation (MCC) as seen in Figure 3.1, is situated 14.1 km away from the NITK campus. The capacity of the digester plant is two tonnes and can process all the biodegradable waste in a day.

Figure 3.1: Biogas plant near Urwa ground, Mangalore

Biogas is generated by an anaerobic digestion process using food waste collected from different hotels in the city. The biogas plant produces 140 to 180 m^3 of gas and 120 to 150 kg of compost every day. The process of extracting the biogas was a challenging

task because the pressure coming out from the digester was at low pressure and it is difficult to fill the gas in a cylinder or tyre tubes. To overcome this issue, we came up with a plan of extracting biogas by using a compressor provided with the necessary fittings. The extraction of the biogas process using a compressor is shown in Figure 3.2 (a & b). Figure 3.2 (a) shows the gas exit from the digester connected with a hosepipe and it is interconnected to the inlet of the compressor. Further, the outlet of the compressor is connected to the inlet of a heavy vehicle tyre tube. As the compressor is switched ON, the biogas is sucked and compressed to an operating pressure of 7 bar. The compressed biogas exits out from the compressor and gets filled into the tyre tube as observed in Figure 3.2 (b). After this stage, the tyre tube containing compressed biogas is transported back to the NITK campus.
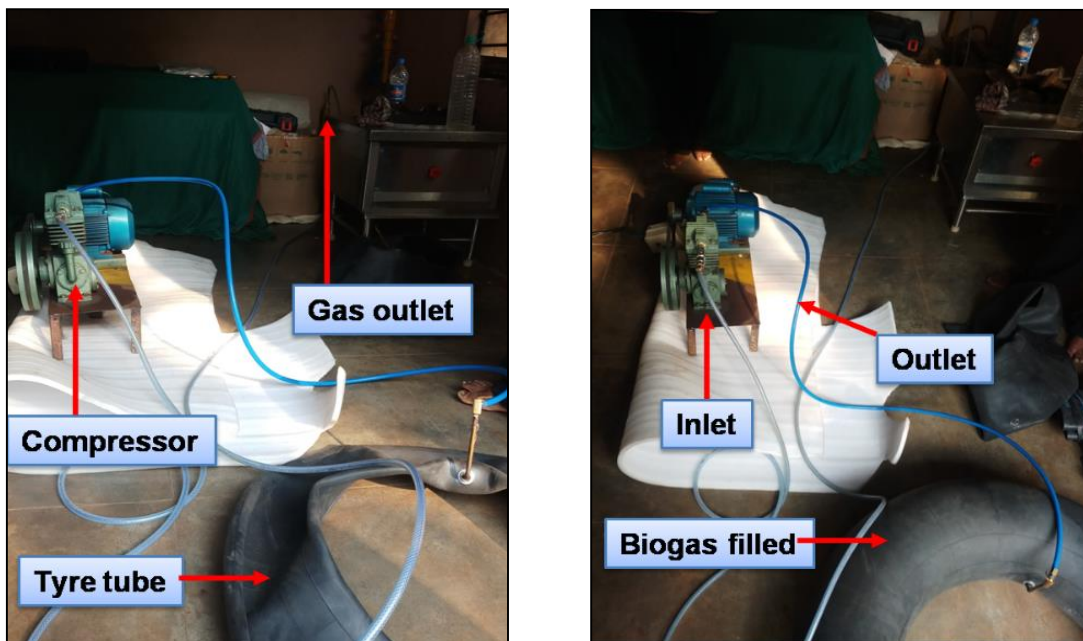
Figure 3.2: (a) Biogas before filled into the tube   (b) Biogas filled in the tube

3.2 Filling of Biogas into the Cylinder

The tube filled with biogas is kept in an Internal Combustion engine research laboratory. It is convenient to operate the biogas when it is filled in a cylinder rather than directly with the tyre tube. In the next stage, the biogas is transferred from the tube to the

cylinder as shown in Figure 3.3 (a & b). Figure 3.3 (a) shows the biogas before being filled into the cylinder and Figure 3.3 (b) shows the compressed biogas filled into the cylinder. The process of extracting biogas from the tube and filling it into the cylinder is the same as the process of extracting biogas from MCC. After filling the compressed biogas into the cylinder it is ready to operate with the diesel engine by dual fuel mode of operation. Table 3.1 represents the properties of biogas compared with diesel.
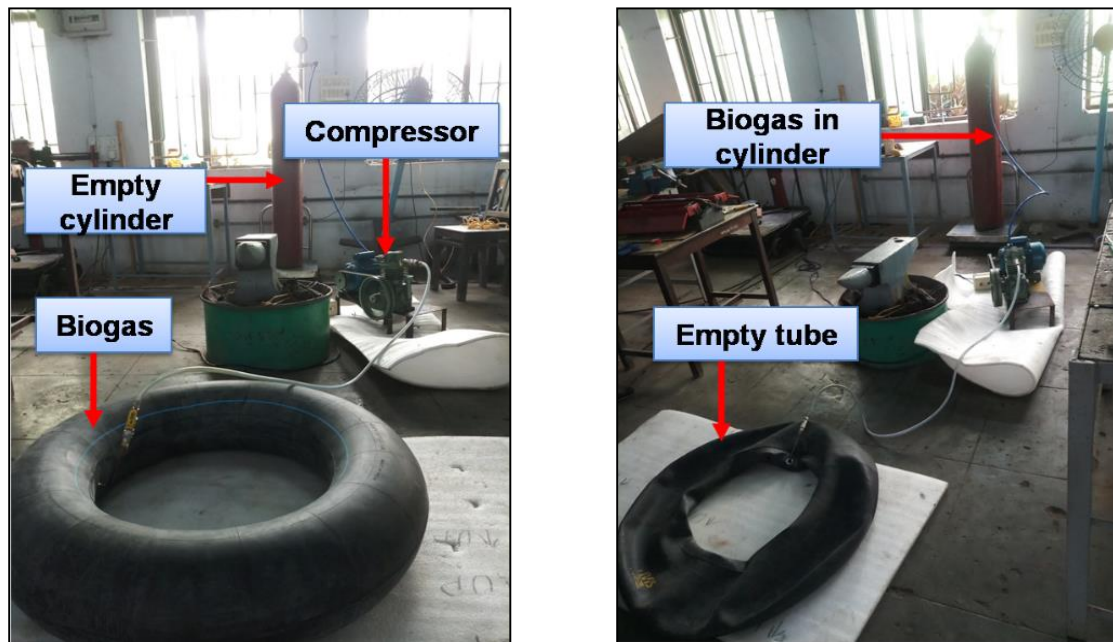
Figure 3.3: (a) Compressed Biogas in the tube   (b) Biogas filled in the cylinder

Table 3.1: Properties of fuels (Chandra et al. 2011)

Property	Diesel	Biogas	Raw Biogas
Composition (% v/v)	$C_{12}H_{26}$	CH_4-65% CO_2-32% Other gases-3%	CH_4-88.10% CO_2-11.89%*
Lower heating value (MJ/kg)	42.06	25	28.05*
Density (kg/m^3)	840	1.11	0.716*
Auto-ignition temperature (°C)	280	650	-
Octane number	-	110	-

Measured values

3.3 Working Principle of the Gas Chromatography

The vital factor for gas chromatography to attain equilibrium is the partition, and the components of the sample will partition between the stationary and mobile phases. Compounds with a stronger affinity for the stationary phase spend more time in the column, elute later, and have a longer retention time (R_t) than those with a stronger affinity for the mobile phase.

Intermolecular interactions cause affinity for the stationary phase and the polarity of the stationary phase can be selected to maximize interactions and consequently separation.

- ➢ The sample is therefore partitioned between the gas and a small layer of a nonvolatile liquid maintained on a solid support, resulting in separation.
- ➢ A sample containing the solutes is injected into a heated block, where it is quickly vaporized.
- ➢ The stationary phase adsorbed the solutes, which are then desorbed by a fresh carrier gas.
- ➢ Each solute will go through the column at its own pace.
- ➢ Depending on the partition coefficients and band spreading, their bands will disperse into discrete zones.
- ➢ Quantitative data can be obtained by measuring the appearance time, height, width, and area of these peaks.

The working principle of the gas chromatography through schematic layout is shown in Figure 3.4.

3.4 Working Procedure of the Gas Chromatography

Step 1: Injection and Vaporization of the Sample

1. A small amount of liquid sample to be examined is extracted using a syringe.

2. The syringe needle is inserted into the gas chromatograph's hot injection port, and the sample is swiftly injected.

3. The vaporized components are then mixed with the inert gas mobile phase and sent to the gas chromatography column, where they are separated.

Step 2: Separation in the Column

1. The ability of the components in the mixture to adsorb on or bind to the stationary phase is used to separate them.

2. A component that adsorbs the least strongly to the stationary phase will spend the least amount of time in the column and thus have the shortest retention period (R_t). It will be the first to emerge from the gas chromatograph.

Step 3: Detecting and Recording Results

1. The component that has been held in the column for the least duration is detected first. The component that has been kept in the column, the longest is discovered last.

2. A signal is sent from the detector to the chart recorder, resulting in a peak on the chart paper. The first component to be discovered is recorded first.
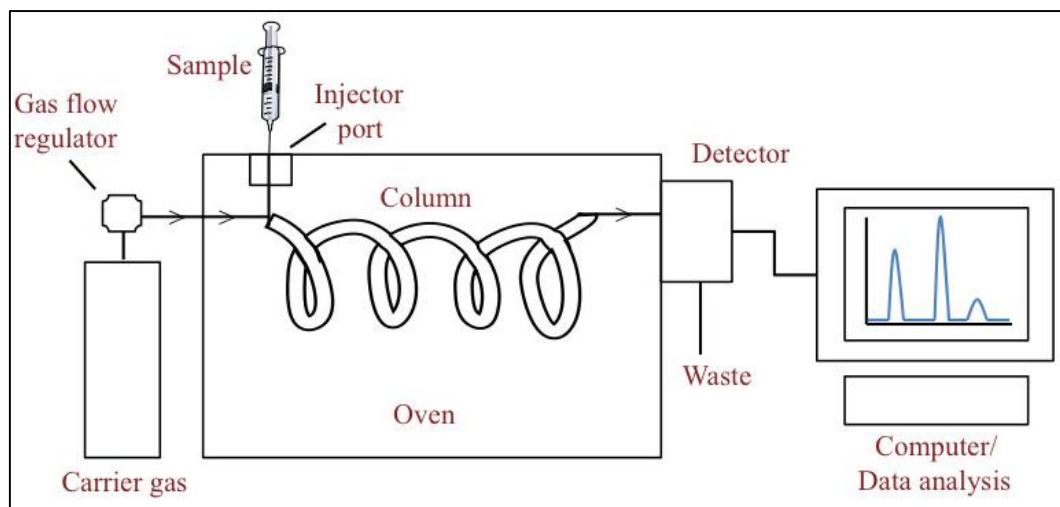
Figure 3.4: Schematic diagram of the gas chromatography operation (Sagar Aryal. 2018)

3.5 Analysis of the Biogas using Gas Chromatography

The composition of the biogas is determined by using gas chromatography in the Environmental lab, Civil department within the NITK campus as shown in Figure 3.5. Gas chromatography is a unique analytical tool, as it has the provision of separating components present in the mixture for consequent utilization. Chromatography makes a very little sample of the volatile components to separate and to determine the composition of each component present.

Figure 3.5: Biogas testing in gas chromatography

The samples are loaded by the means of injection port, such that the sample passes through the column which determines the components separated. A carrier gas generally helium, carries the sample injected throughout the instrument, detector as well as the data processor. Figure 3.5 depicts the typical gas chromatography instrument in the laboratory. The result obtained from the gas chromatography depicts that the sample collected from the biogas plant consists of methane (CH_4 -88.10%) as a chief constituent, carbon dioxide (CO_2-11.895%) and remaining other traces elements. The result of the biogas composition is shown in Figure 3.6. The report indicates that the largest peak curve having 12.24 mVolt is methane gas with a 2.0 retention time and the smallest curve of 4.158 mVolt is carbon dioxide with a 3.999 retention time. After testing the

composition of biogas from gas chromatography, the biogas is considered to be a methane-enriched gas. This indicates that biogas can be effectively utilized for various applications such as cooking and the most important application i.e. as an alternative fuel for vehicles. The vital reason for using biogas as an alternative fuel is because the biogas is renewable energy, obtained from waste, non-toxic, less pollutant, and eco-friendly.
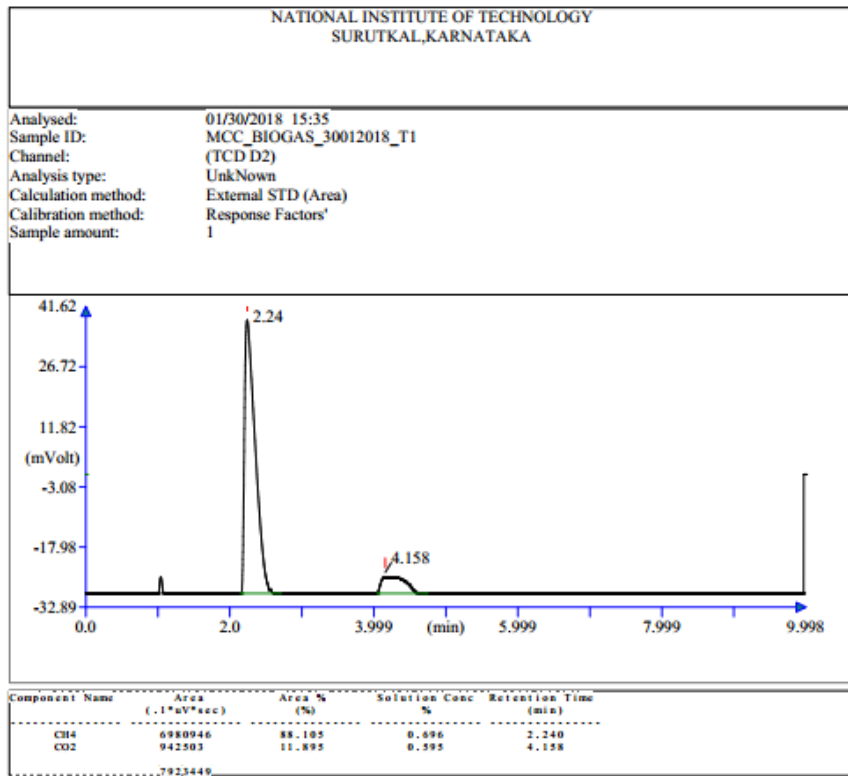
Figure 3.6: Composition of the biogas

3.6 Closure

The details of the biogas extraction from the anaerobic digestion plant and transferring the compressed biogas into the cylinder are discussed in the present chapter. Before using the biogas in the engine, the composition of biogas is determined using gas chromatography. In the next chapter, the modifications performed to achieve the dual fuel mode condition and the basic operation of the engine under diesel and dual-mode are discussed.

CHAPTER 4

EXPERIMENTAL METHODOLOGY

The present chapter provides detail about the methodology involved in the execution of the research objectives by exhibiting the complete information about the basic layout of the experimental work. Initial modification required to set up the engine to operate under dual-mode is also included. The concept of the cycle by cycle variations for diesel and dual-mode are studied. To study the effects of injection timing for diesel and dual-mode cases the method of achieving the different injection timing is explored. The experimental matrix is included to understand the method of oxygen enrichment mechanism and its effects on the engine behavior. Also, the complete details of the last objective, the study of the vaporized water-methanol induction method to enhance the engine properties along with the specifications of the heat exchanger used are provided in this chapter. The error that occurred in the instruments used for the present investigation is represented by performing the uncertainty analysis. At the end of this chapter, the description of the measuring system used to perform the present investigation is included.

4.1 Basic Experimental Operation

Before the initiation of the experiment, a few modifications have to be implemented to the existing CI (compression Ignition) engine using necessary fittings. The biogas from the cylinder is introduced to the diesel engine through the intake manifold rather than using the gas injectors such that homogeneous mixing of the air and biogas is achieved inside the intake manifold as shown in Figure 4.1. The biogas is allowed to flow through the flow line by passing through the air filter with required pressure controlled by the pressure regulator. The mass flow rate for the different biogas proportions are determined by equation 4.1. The required amount of biogas is allowed to flow through the flow meter by slowly allowing the biogas to get mixed thoroughly with air inside the inlet manifold. Further, the biogas-air mixture flows into the cylinder of the engine and gets combusted through the dual fuel mode of operation.
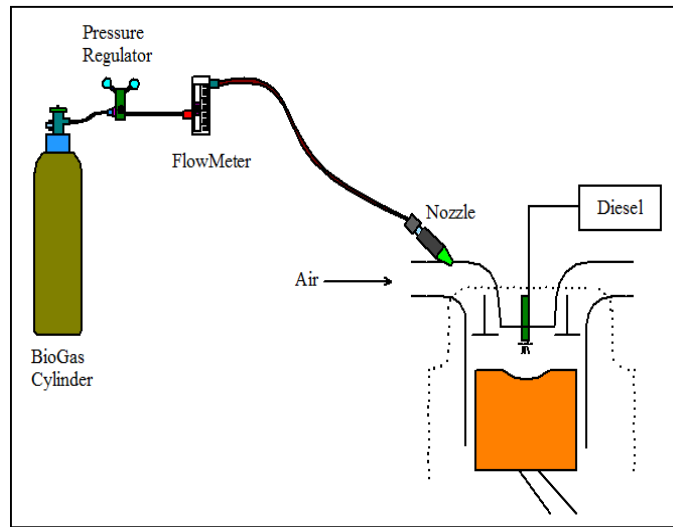
Figure 4.1: Method of inducting biogas in the engine (Madhankumar et al. 2019)
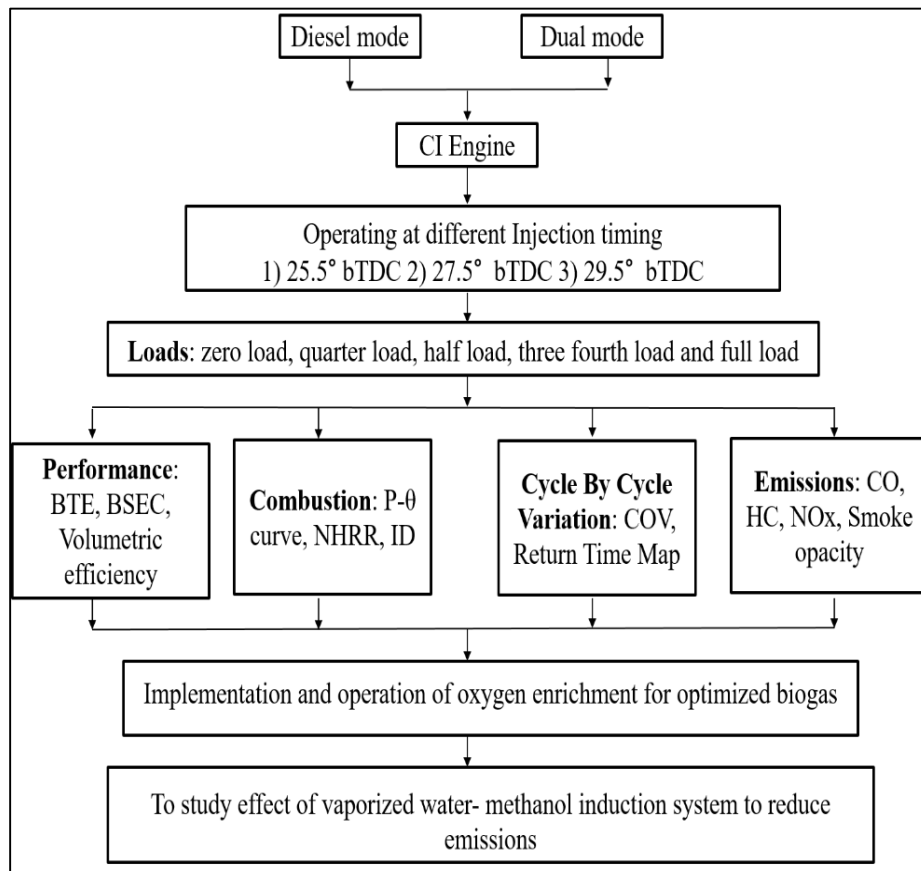
Figure 4.2: Flow chart of the experimental procedure

The methodology for executing the defined objectives of the research work is specified as follows: Initially, the experiments are conducted with baseline fuel diesel and then with different biogas ratios for different injection timing at standard injection pressure. Various parameters such as performance, emission characteristics, and combustion characteristics, as well as cycle by cycle variations, are obtained from the test. Based upon the experimental results, the biogas is optimized for the standard injection timing and in the next investigation, oxygen enrichment is incorporated for the optimized biogas proportions to study the effects. The investigation is extended to reduce the emissions by employing the emission reduction technique namely vaporized water-methanol induction. Figure 4.2 shows the flowchart of a detailed procedure to conduct the experiments.

4.2 Experimental Setup for Dual-Mode Operation

Engine tests are conducted on a computerized single-cylinder four-stroke, naturally aspirated, open chamber (Direct Injection), and water-cooled diesel engine test rig as shown in Figure 4.3. The engine is directly coupled to an eddy current dynamometer. The engine and the dynamometer are interfaced to a control panel, which is connected to a computer. The test rig is provided with the necessary equipment and instruments for combustion pressure and crank angle measurements with accuracy. These signals are interfaced to the computer through an ADC card PCI-1050 which is mounted on the motherboard of the computer.

The provision is also made for interfacing the airflow, fuel flow, temperatures, and load measurement with the computer. The setup has a stand-alone type independent panel box consisting of the air box, fuel tank, manometer, fuel measuring unit, transmitters for air-flow and fuel flow measurements, process indicator, and engine indicator. For measurement of water flow rate for engine cooling, rotameters are provided. The computer software *IC Engine Soft Version 9.0* supplied by the test rig supplier ―Apex Innovations Pvt.Ltd is used for recording the test parameters such as fuel flow rate, temperatures, air-flow rate, load, etc. and for calculating the engine performance characteristics such as brake power, indicated power, frictional power,

BMEP, IMEP, brake thermal efficiency, indicated thermal efficiency, brake specific fuel consumption, volumetric efficiency, etc. The details of the calorific value and the density of the fuel are provided in the software as an input for calculating the above-mentioned performance parameters. The experimental setup view of the modified diesel engine is depicted in Figure 4.3, such that Figure 4.3 (a) indicates modified dual diesel engine. Whereas, Figure 4.3 (b) depicts the control panel connected to the engine. Figure 4.4 shows the experimental test rig block diagram of the diesel engine with the different notations involved.
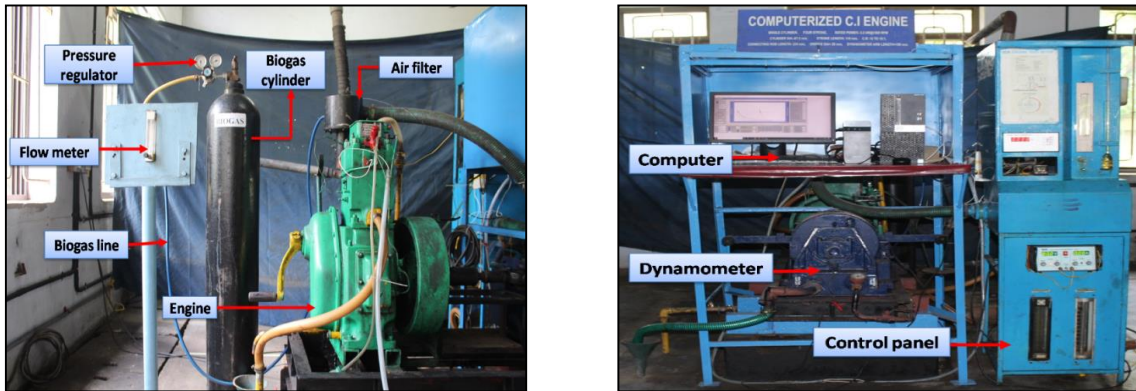
Figure 4.3: (a) Modified diesel engine   (b) Control panel interfaced to the engine
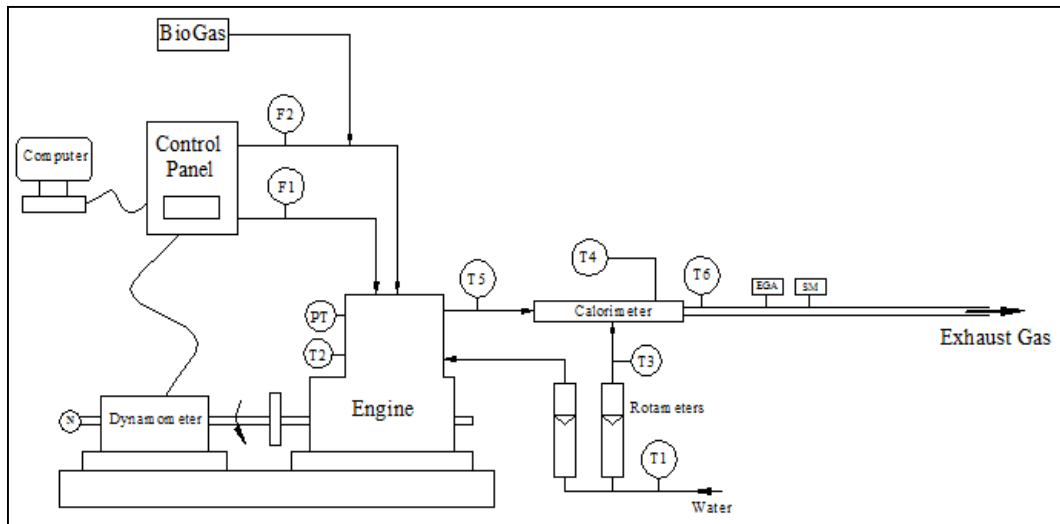
Figure: 4.4 Experimental test rig block diagram

T1- Inlet engine water temperature	PT-Pressure transducer
T2- Outlet engine jacket water temperature	N- rpm decoder
T3- Inlet temperature of calorimeter	T4-Outlet calorimeter water temperature
T5- Exhaust gas temperature before calorimeter	EGA-Exhaust gas analyzer
T6-Exhaust gas temperature after calorimeter	F1-fuel flow DP(Differential Pressure) unit
SM-Smoke meter	F2-Air intake DP unit

Initially, the baseline readings of the diesel are obtained for the injection timing of 27.5° bTDC, thereafter with biogas (BG) proportion of 20%, 30%, 40%, 50%, and 60% (i.e. BG60-60% of biogas by mass basis) respectively. Before inducting the biogas into the engine, the engine is operated with the diesel mode until a steady-state condition is reached. Biogas is inducted into the engine at the intake manifold of the engine by releasing the gas slowly through the mass flow meter.

As the biogas is released it gets mixed with air uniformly inside the intake manifold, then the biogas-air mixture gets combusted when the little quantity of diesel comes into contact with the compressed biogas-air mixture (dual fuel mode). The experiments are performed for the remaining gases at all the loads and the experimental results are analyzed and evaluated by comparing with the baseline readings of diesel. The method of inducing the biogas into the engine at the intake manifold is shown in Figure 4.1 and Figure 4.3 shows the views of the engine setup prepared in the research laboratory.

The mass flow rate for various biogases is obtained by the following equation:

$$m_f = \frac{BSEC \times BP}{CV} \tag{4.1}$$

where, BP is the brake power in kW and

CV is the calorific value of fuels in MJ/kg.

Detailed specifications of the modified diesel engine used for the research work are given in Appendix-I.

4.3 Experimental Studies of the Cycle by Cycle Variations on the Dual-Fuel Engine

In this section, the impact of cyclic variations upon the diesel engine under the diesel and dual-mode is investigated by studying the variation of maximum cylinder pressure (P_{max}). Also, the combustion behavior through return map for hundred cycles at full load and compiling the results to determine the coefficient of variation for all the fuels. During the combustion process, the engine undergoes cycle by cycle variations or cyclic variation which causes a destructive impact on the engine's performance inhibiting power loss, reduction in brake thermal efficiency, and degradation in emissions. Generally, cycle by cycle variation occurs due to the variation in combustion, in addition to these various factors such as composition mixture, cyclic cylinder charging and in-cylinder mixture motion, etc are also the reasons to cause cyclic variations.

However, in the case of petrol, diesel, and HCCI engines the reason for the cycle by cycle generation is different from each other (Wang et al. 2014). Normally, the problem of cycle variations in petrol engines is caused due to the changes in the burning rate for every cycle. Also, due to the cyclic variation in the amount of fuel, motion of gases in cylinder, presence of air and exhaust gases in the cylinder, composition of mixture variations across the spark plug which causes a difference in combustion are also the reasons (Heywood 2018). Cyclic variations are found to be higher for homogeneous charge compression ignition (HCCI) engine, because of the higher impact of minute perturbations in temperature as well as the composition of the fuel-air auto-ignition (Hyun and Sik 2011). On the other hand, cyclic variations are quite less in the case of diesel engines due to their nature of dominance in non-premixed combustion, also the initiation of fuel injection governs the air-fuel mixing and then combustion. However, the instabilities of a fuel injection system or long-lasting ID are also considered as the cause

of cyclic variations. Nowadays high-speed efficient diesel engines consist of multiple pilot injections which reduce major ID in most of the diffusion-dominated combustion (Kyrtatos et al. 2016). For hundred successive cycles, combustion, as well as cyclic variations are studied by entering the value for the required number of cycles directly in the *IC Engine software.* For every operating condition, the combustion data for diesel and dual-mode can be determined by obtaining either maximum cylinder pressure (P_{max}) or indicated mean effective pressure (IMEP). In the present investigation, the cyclic variations are analyzed by considering the P_{max} of individual fuels for 100 cycles. Cyclic variations are obtained by determining the standard deviation ($\sigma_{P_{max}}$), mean value, and coefficient of variation (COV) for both the above-mentioned parameters (Santoso et al. 2012). The P_{max} values are obtained and saved in the *IC Engine software* directly through the supporting file of the excel spreadsheet which includes the parameters such as mean value, standard deviation, and COV expressed in terms of percentage, and are determined by the following expression:

$$\overline{P}_{max} = \frac{1}{n} \sum_{i=1}^{n} P_{max,i} \tag{4.2}$$

where P_{max} is the maximum cylinder pressure

$\overline{P}_{max}$ is the mean value and

n is the number of combustion cycles = 100

Standard deviation is given by:

$$\sigma_{P_{max}} = \sqrt{\frac{\sum_{i=1}^{n} (\overline{P}_{max} - P_{max,i})^2}{n-1}} \tag{4.3}$$

Coefficient of variation (COV) is given by:

$$COV_{P_{max}} = \frac{\sigma_{Pmax}}{\overline{P}_{max}} \tag{4.4}$$

4.4 Experimental Studies on Injection Timing upon the Engine using Diesel-Biogas

In this section, the impact of three injection timings (29.5°, 27.5°, and 25.5° bTDC) on the performance, combustion, and emission characteristics of the modified diesel engine operated with diesel-biogas combination through the dual-mode operation is investigated.

4.4.1 Methodology

The influence of injection timing upon the engine is explored using the compressed biogas inducted at the inlet manifold of the engine with different fractions of biogas ranging from BG20 to BG 60 with 10% increment (i.e. BG20-20% of biogas by mass basis) and is operated under dual fuel mode. For, calculating the mass flow rate of the different biogas proportions is given in detail in the section 4.2 using the equation 4.1.

The engine is operated for three different injection timings namely Advance (29.5° bTDC), Actual (27.5° bTDC), and Retard (25.5° bTDC) respectively. The required injection timing is achieved by changing a small part called a shim which is located beneath the fuel pump such that each shim is of 2 mm thickness and 2° CA. The actual injection timing of the diesel engine is 27.5° bTDC consisting of 2 shims, if 1 shim is removed then the injection timing will be advanced to 29.5° bTDC and if the total three shims are included under the fuel pump then the injection timing will be retarded to 25.5° bTDC. The experiment is conducted for all the three injection timings with the biogas proportions ranging from BG20-BG60 which are inducted at the intake manifold of the engine operated for 25% to 100% load with 25% increment at a constant speed of 1500 rpm. The different loading is achieved from 0 to 100% load by varying the voltage and current knob simultaneously until the engine speed arrives at a constant speed of 1500 rpm. However, under dual fuel mode operation, the zero load is omitted and is directly started from 25% load until the final load. Initially, the test is conducted for diesel only at the actual timing (27.5° bTDC) for all the loads and then the process is switched over to the dual-mode by inducting the biogas which is operated for the three injection timings. Then the results of the engine parameters such as performance, combustion, and emission

with biogas at all the three injection timings are compared with diesel at actual injection timing. Figure 4.5 represents the different pictorial views of the injection timing attainment. The matrix of the experimental work is mentioned briefly in Table 4.1.

Table 4.1: Matrix of the experiment

Method	Fuel used	IT (bTDC)	Ratios	Load	Speed (rpm)
Diesel mode	Only Diesel	27.5°	100%	0%, 25%, 50%, 75%,100%	1500
Dual-mode	Biogas-Diesel	25.5° (Retard) 27.5° (Actual) 29.5° (Advance)	20% to 60% (10% rise)	25%, 50%, 75%,100%	
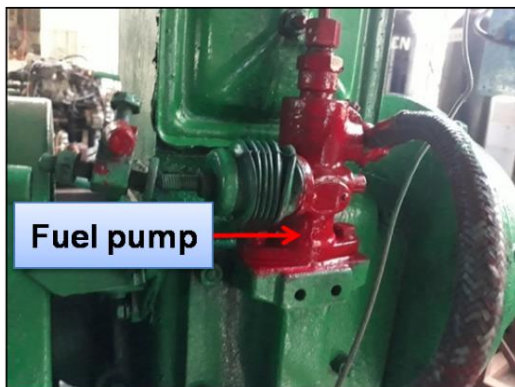
Figure 4.5: a) Fuel Pump   b) Open view of the fuel pump
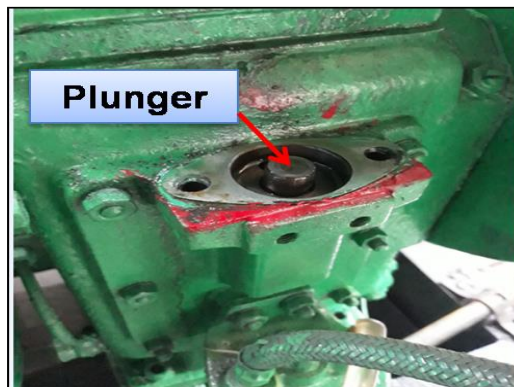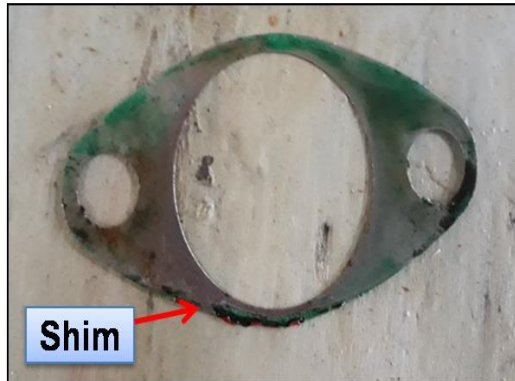
c) Shim used

4.5 Enhancement of Engine Characteristics by Oxygen Enrichment Mechanism

In the previous section, the impact of three different injection timing using different biogas proportions upon the engine is explored as well as fuel timing is optimized based upon the experimental observations. In the current section, the implementation of oxygen enrichment with different oxygen levels for selected injection timing (27.5° bTDC) and biogas proportion (BG50) is examined.

4.5.1 Experimental setup

A capacity of 47 liters oxygen cylinder is used for inducing oxygen into the engine. Two separate flow meters, as well as pressure regulators, are used to measure and release the biogas and oxygen gases from the respective cylinders (Jagadish and Gumtapure 2019, 2020) as shown in Figure 4.6. Initially, the pressure of the oxygen is regulated using a pressure regulator and thereafter flows to the flow meter, the required quantity of the oxygen is released by operating manually.

In this experiment, the oxygen concentration is selected from 21% to 27% with an increment of 2% by volume basis to enhance the engine characteristics for the optimized biogas under dual mode. A mixing device is used to create a homogeneous mixing of the biogas and oxygen gas such that the oxygen from the flow meter flows into the mixing chamber and gets mixed homogeneously with the biogas (BG50) flown from the other side through the pipe fittings and thereafter the gases flow into the intake manifold of the

engine directly through the air filter as shown in Figure 4.6. To avoid the return of the gases a non-return valve is fixed at the entry and exit of the gas pipe, a schematic block diagram of the experimental setup is represented in Figure 4.7.
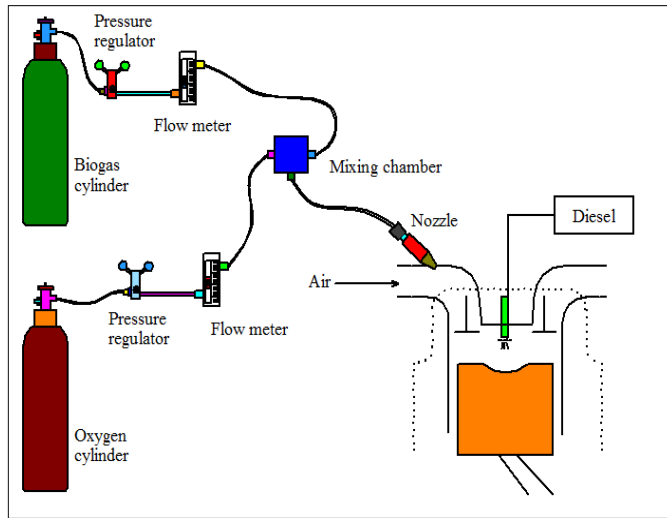
Figure 4.6: Method of oxygen enrichment for optimized biogas
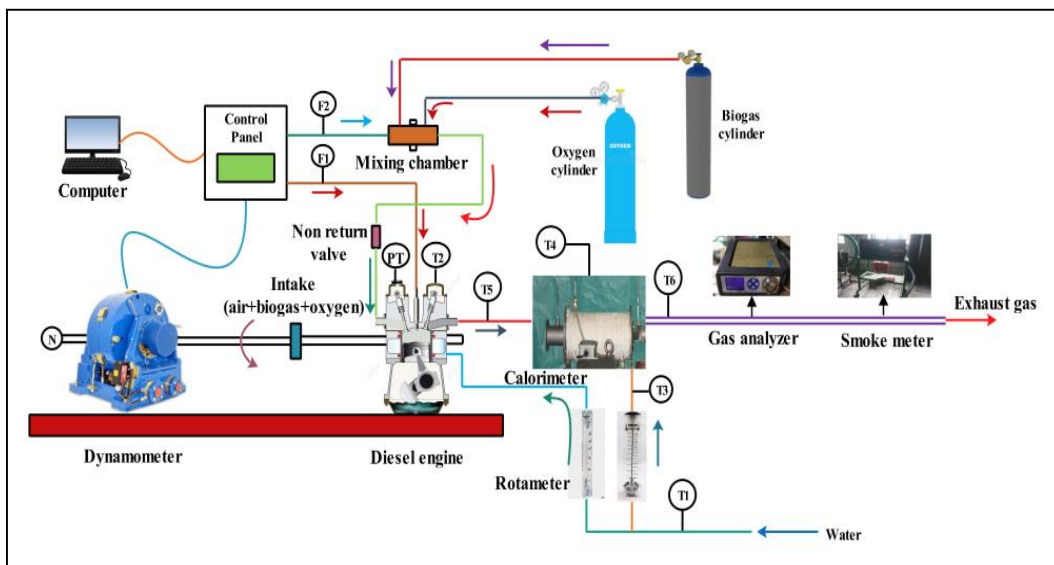
Figure 4.7: Schematic block diagram of the engine test rig

4.5.2 Methodology

The procedure for operating the engine, extracting the results, checking the emission parameters, controlling the various operating conditions are similar and is briefly explained under the section 4.1. The engine characteristics are enhanced by mixing the various levels of oxygen concentration ranging from 21% to 27% (by volume basis) with a step of 2% along with the optimized biogas and intake air and its effects are investigated. The flow rate of the biogas is regulated using the flow meter and the biogas is operated at the required pressure using the pressure regulator. Similarly, the same procedure is followed for oxygen enrichment. The tests are conducted after the engine reaches the constant speed of 1500 rpm and for different load ranging from 25% to 100% load with 25% increment (Jagadish and Gumtapure 2019, 2020). Keeping the injection timing of the fuel to the standard timing of 27.5° bTDC and injection pressure of 180 bar the experiments are conducted by taking the readings once the engine reaches the steady-state condition. The instruments used in the experiment are calibrated before the experiment is conducted and the tests are repeated and the average values are considered for compiling the results.

Initially, the base readings are taken for diesel fuel and then the process is switched over to dual-mode which is achieved by releasing the biogas (BG50) slowly through the flow meter by maintaining the required pressure controlled by using the pressure regulator. The various oxygen concentrations with the required flow rate simultaneously into the intake manifold of the engine through a mixing device situated at the T-junction as shown in Figure 4.6. Further, the released gases mix with the intake air homogeneously before entering into the engine. Figure 4.8 (a) illustrates the oxygen enrichment process and Figure 4.8 (b) represents the engine interfaced to the control panel whereas, Table 4.2 shows the matrix of the experimental work executed in the current research work.

Table 4.2: Matrix of the oxygen enrichment experiment

Method	Fuel used	Oxygen Concentration	Ratios	Load	Speed (rpm)
Diesel mode	Only Diesel	-	100%	0%, 25%, 50%, 75%,100%	1500
Dual-mode	Biogas-Diesel	21% 23% O$_2$ 25% 27%	50% (BG50-Optimized)	25%, 50%, 75%,100%	
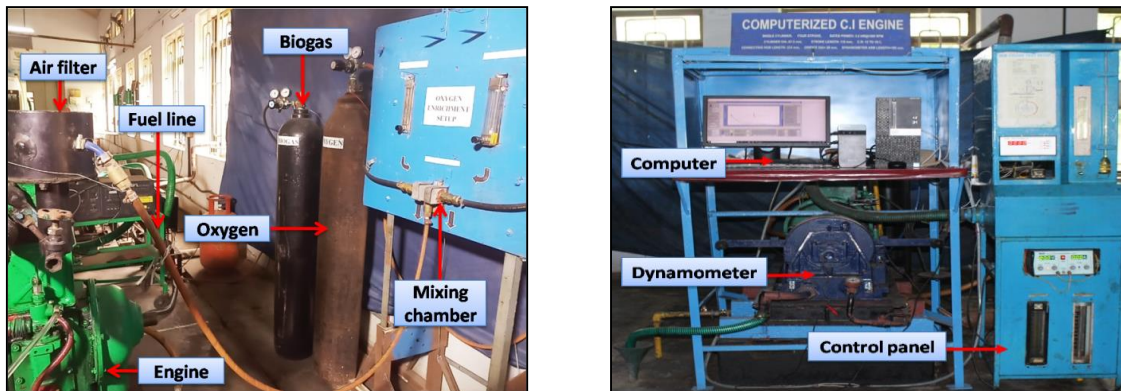
Figure 4.8: (a) Oxygen enrichment process   (b) Engine interfaced to control panel

4.6 Vaporized Water-Methanol Induction System

The oxygen enrichment process has shown enhancement in the performance of the diesel engine fueled with biogas but on the other hand, even though there is a reduction in CO and HC emissions tremendous increase in the NO$_x$ emissions is observed which causes adverse effects on the environment. To overcome this setback in the process, there is a necessity to implement the emission reduction technique to mitigate the NO$_x$ emissions. There are varieties of techniques to reduce the NO$_x$ emissions such as exhaust gas recirculation (EGR), selective catalyst reduction (SCR), turbocharger, water

72

injection, split injections, steam injection, etc. In recent research reveals that the water and steam injection techniques are found to be more effective techniques towards reducing the NO_x emissions. The advancement of steam injection furthermore improved the performance, as well as emission and similar development is observed, if the vaporized water-methanol technique is adapted as revealed in the literature. Henceforth, in the current section, the development and implementation of vaporized water-methanol induction system for optimized biogas along with oxygen enrichment to mitigate the emissions and to improve the performance of the engine for different operating conditions are studied. Figure 4.9 shows the pictorial view of (a) the development of shell and tube heat exchanger, (b) heat exchanger connected to the engine, and (c) generated vapor inducted into the engine manifold.
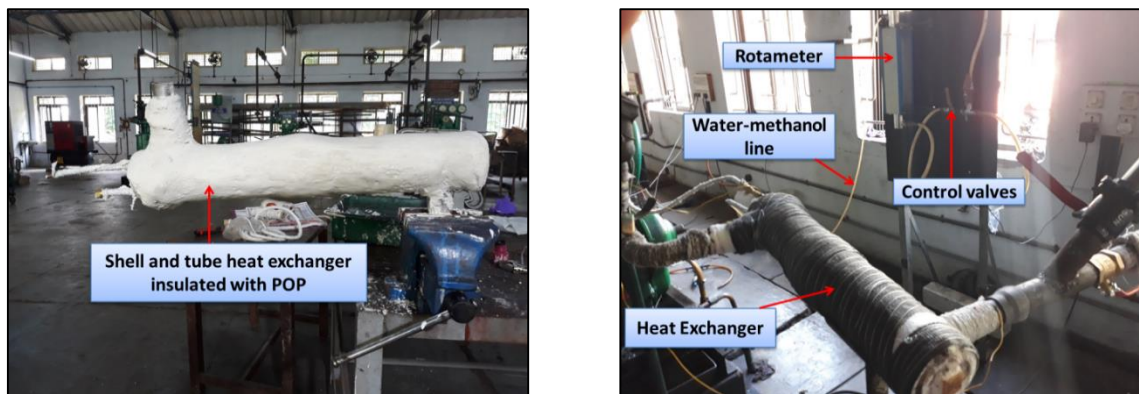
Figure 4.9: (a) Shell and tube heat exchanger   (b) Heat exchanger connected to Engine
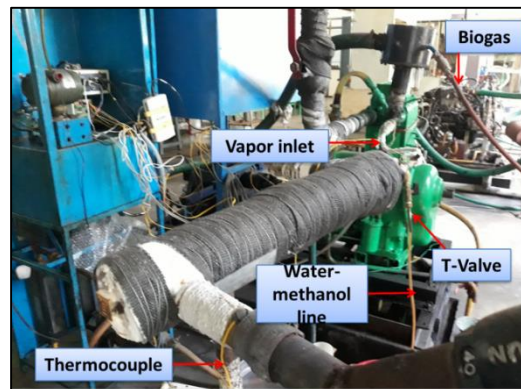
(c) Vapor induction into the intake manifold of the Engine

4.6.1 Design and Development of the Heat Exchanger

A shell and tube heat exchanger is used to convert the liquid into the vapor state of the water-methanol mixture using the waste exhaust gas released from the exhaust pipe of the engine. The shell and tube heat exchanger is designed based on the logarithmic mean temperature difference (LMTD) method and fabricated with the required dimensions as shown in Figure 4.11 and the detailed specification are given in Appendix-II.

A copper tube of length 2.9 m is placed inside the heat exchanger with the aid of baffle plates and is concealed with the horizontally placed shell and tube heat exchanger of length 0.45 m which is firmly fitted to the engine exhaust manifold. The inlet of the heat exchanger is connected to the exhaust pipe and the outlet of the shell is fitted with a long pipe to expel out the exhaust gas from the system. The water-methanol (60:40 ratio) is thoroughly mixed using a stirrer and is stored in a container that is placed at a suitable height. With the aid of a low-pressure pump, the fluid flows into the heat exchanger through the copper tube. The flow rate of the water-methanol is determined and controlled manually through the rotameter of 0.1 to 10 LPH flow range with 0.1 LPH least count. A T-valve is provided between the intake manifold of the engine to the inlet of the heat exchanger to ensure that the fluid mixture is converted into vapor completely and mixed homogeneously along with the optimized biogas and oxygen concentration. A bypass return system is created after the pump such that the excess fluid mixture returns to the container.

4.6.2 Working Methodology

During the combustion process, around 22% to 24% of the heat liberated from the engine is expelled out in the form of a waste exhaust gas. Using the unutilized waste exhaust gas generated, the vapor state of the water-methanol mixture is achieved and the mixture is made to flow with a low flow rate through the inlet of the heat exchanger.
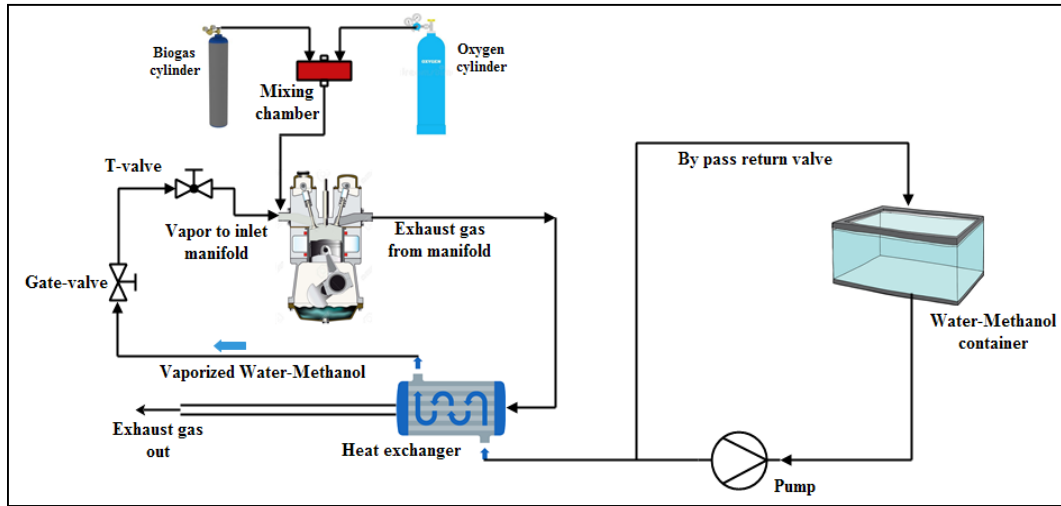
Figure 4.10: Schematic diagram of the vaporized water-methanol induction system

However, before inducting the water-methanol into the intake manifold of the engine it is ensured that the water-methanol mixture is completely converted into the vapor form. The fluid mixture in the liquid form is released to the copper tube and exhaust gases flow across the tube in a counter flow manner, due to the improvement in heat transfer between the two fluids and attainment of higher latent heat the liquid form of the mixture is converted into vapor form. The flow rate of the water-methanol mixture to be inducted into the engine for every operating condition is decided based upon the mass flow rate of the optimized biogas (BG50) and oxygen level (25% O_2) as concluded in the previous section. As per the matrix of the experiment mentioned below, the experiment is conducted with the diesel mode without vapor induction and then for dual-mode with the optimized biogas (BG50) along with oxygen concentration (25% O_2) for different operating conditions. The different flow rate of the water-methanol is achieved using the control valve such that as the flow rate of inducted vapor is increased the mass flow rate of diesel fuel drastically reduces by controlling the governer of the diesel engine. The vapor is inducted continuously into the intake manifold with various flow rates of 10%, 20%, and 30% by the mass basis for every operating condition of the engine. The performance is calculated with a similar procedure as explained in the earlier section and emissions are measured using the AVL gas analyzer as well as with the

smoke meter. Figure 4.10 depicts the schematic diagram of vaporized water-methanol induction system generated using a shell and tube heat exchanger. The matrix of the vaporized water-methanol induction for the present experimental work is given in Table 4.3.

Table 4.3: Matrix of the vapor induction experiment

Method	Fuel used	Vapor induction	Ratios	Load	Speed (rpm)
Diesel mode	Only Diesel	-	100%	0%, 25%, 50%, 75%,100%	1500
Dual-mode	Biogas-diesel	10% 20% 30% (60:40 ratio)	BG50 + 25% O_2 (Optimized)	25%, 50%, 75%,100%	
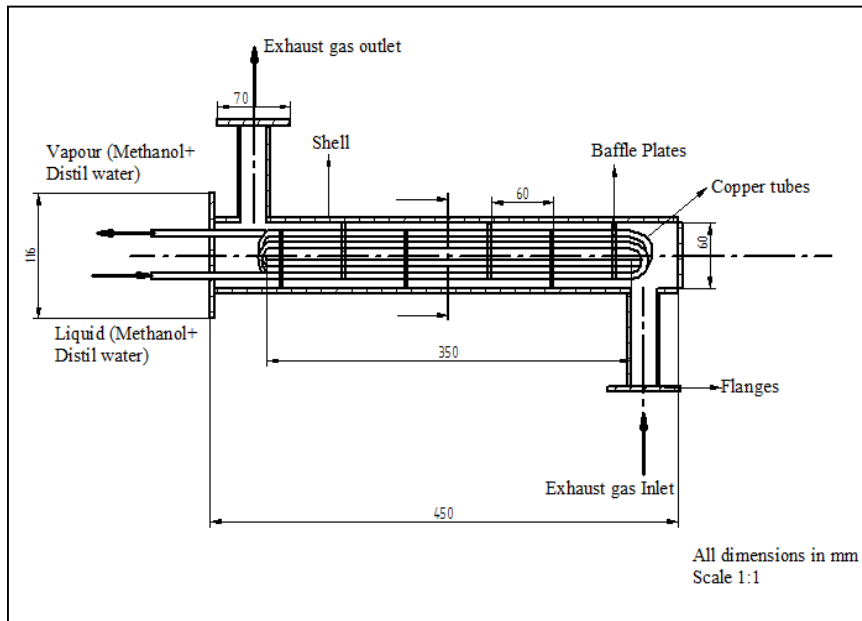
Figure 4.11: Front view of the shell and tube heat exchanger

76

4.7 Calculation of Performance Characteristics

A detailed explanation of determining the various parameters related to performance and combustion along with the corresponding expressions are provided under this section.

4.7.1 Brake Thermal Efficiency (BTE)

Brake thermal efficiency for dual fuel is determined by the following equation:

$$\left[\eta_{th}\right]_{dual\ mode} = \left[\frac{BP}{(m_D \times LHV_D) + (m_{BG} \times LHV_{BG})}\right] \times 100$$

(4.5)

where, η_{th} is the brake thermal efficiency of dual-mode (%), m_D is the mass flow rate of diesel (kg/h), m_{BG} is the mass flow rate of biogas, LHV_D is the lower heating value of diesel and LHV_{BG} is the lower heating value of biogas (MJ/kg). BP is the brake power (kW) of the engine.

4.7.2 Brake Specific Energy Consumption (BSEC)

BSEC for dual fuel mode is determined from the following expression:

$$(BSEC)_{dual\ mode} = \left[\frac{m_D \times LHV_D + m_{BG} \times LHV_{BG}}{BP}\right] \times 100$$

(4.6)

where, $(BSEC)_{DM}$ is the brake specific energy consumption (MJ/kW-h) of dual fuel mode, BP is the brake power (kW), m_D is the mass flow rate of diesel (kg/h), m_{BG} is the mass flow rate of biogas, LHV_D is the lower heating value of diesel and LHV_{BG} is the lower heating value of biogas (MJ/kg)

4.7.3 Volumetric Efficiency (Ƞ$_v$)

Volumetric efficiency for the diesel engine is determined by the following expression:

$$\eta_v = \frac{\overline{m}_a}{\rho^*_a \times V_D \times N^*\!\big/2} \qquad (4.7)$$

where,

ρ^*_a is the density of air inlet.

N^* is the speed of the engine in rpm.

V_D is the displacement volume.

whereas, the volumetric for dual-mode is obtained from the following expression:

$$\left[\eta_v\right]_{dual\,mode} = \left[\frac{\overline{m}_a + m_{BG}}{\rho^*_{(a+BG)} \times V_D \times N_C}\right] \times \left[\frac{\overline{m}_a}{\overline{m}_a + m_{BG}}\right] \times \left[\frac{\rho^*_{(a+BG)}}{\rho^*_a}\right] \times 100 \qquad (4.8)$$

where ρ^*_a is the density of the air

$\rho^*_{(a+BG)}$ is the density of the air and biogas

N_C is the number of cycles/ second= $\left(\dfrac{speed}{2} \times 60\right)$

4.7.4 Energy Share of Biogas (ESB)

Following expression gives the biogas energy contribution operated in a dual fuel mode:

$$\text{Energy share of Biogas} = \left[\frac{\text{Energy supplied from biogas}}{\text{Energy supplied from (diesel+biogas)}}\right] \times 100 \qquad (4.9)$$

where,

$$\text{Energy supplied from biogas} = \frac{m_{BG} \times LHV_{BG}}{3600} \qquad (4.10)$$

where m_{BG} is the mass flow rate of biogas.

Energy supplied from diesel $= \dfrac{m_D \times LHV_D}{3600}$

$$(4.11)$$

where m_D is the mass flow rate of diesel fuel.

4.7.5 Net Heat Release Rate (NHRR)

The net heat release rate for dual fuel operation is obtained based upon the correlations related to the first law of thermodynamics, such that the NHRR for dual fuel mode at every crank angle is determined from the following expression:

$$Q' = W'' + \dfrac{du}{dt} \qquad (4.12)$$

where Q' is the net heat generated (J) during the process and W'' is the rate of work done (J) indicating the displacement done by the system. The equation (4.12) is further modified in terms of ideal gas condition for unit mass system and the expression is as follows:

$$Q' = \left[\dfrac{C'_v}{R'} + 1 \right] \times P' \times \dfrac{dv'}{dt} + \dfrac{C'_v}{R'} \times V' \times \dfrac{dP'}{dt} \qquad (4.13)$$

The equation (4.13) is further modified in terms of ideal gas condition and time (t) is replaced with crank angle (θ) and $\dfrac{C'_P}{C'_V}$ the final expression is as follows:

$$Q' = \dfrac{\gamma^*}{\gamma^* - 1} \times P' \times \left[\dfrac{dv'}{d\theta} \right] + \dfrac{1}{\gamma^* - 1} \times V' \times \left[\dfrac{dp'}{d\theta} \right] \qquad (4.14)$$

where γ^* is the specific heat ratio, P' is the instant cylinder pressure expressed in N/m^2 and V' is the cylinder volume in m^3 and is determined by the values of the crank angle and geometry of the engine. Eventually, the NHRR under dual-mode operation completely depends on the fuel quality of the biogas + air + diesel combination, the mass flow rate as well as Lower Heating Value (LHV) of the fuels (Barik and Murgan 2016,

Heywood 2018). Thus, the final simplified relation to determine the NHRR under dual-mode operation is expressed as below:

$$NHRR = \frac{\overline{m}_f \times LHV_D}{LHV_{(D+BG)}} \tag{4.14}$$

where, $\overline{m}_f$ is the mass fraction of fuel mixture, NHRR is the net heat release rate in J/°CA and LHV is the lower heating value of the fuel (MJ/kg). Whereas, LHV and $\overline{m}_f$ are calculated by the expression:

$$LHV_{BG} = \sigma^* \times (LHV_{CH_4}) \tag{4.15}$$

where

$$\overline{m}_f = \frac{NHRR \times \sigma^* \times (LHV_{CH_4})}{(1\text{-}NHRR) \times LHV_D + \sigma^* \times (NHRR \times (LHV_{CH_4}))} \tag{4.16}$$

$$= \frac{m_{CH_4}}{m_{CH_4} + m_{CO_2}} \tag{4.17}$$

where σ^* is the quality of intake mixture to the engine and m is the flow rate of the fuel in kg/h.

4.7.6 Ignition Delay (ID)

The ID for a naturally aspirated diesel engine operated under the dual-mode operation is obtained by the expression framed by Hardenberg and Hase as follows (Barik and Murgan 2016, Lata and Misra 2011):

$$\theta_d^* = C^* (\overline{O}_{dual})^p \times (0.36 + 0.22 M_P) \exp\left[E_A^* \left(\frac{1}{R' T_m (r_c)^{n-1}} - \frac{1}{17190} \right) + \left(\frac{21.2}{P_m (r_c)^n - 12.4} \right)^{0.63} \right] \tag{4.18}$$

where

C^*, P, $\overline{O}_{dual}$ is the modified coefficients,

M_p is the mean speed of the piston expressed in m/s,

$R^|$ is the universal gas constant (8.314 kJ/kg-K),

E_A^* is the activation energy in kJ/kg,

T_m is the mean temperature in K,

P_m is the mean pressure in the bar of air and biogas mixture in the intake manifold,

n is the polytropic index.

Whereas,

$$\overline{O}_{dual} = \frac{(O_f^|)_{dual}}{(O_f^|)_{diesel}} \qquad (4.19)$$

where,

$O_f^|$ is the mole fraction of oxygen,

$(O_f^|)_{dual}$ is the mole fraction of dual mode,

$(O_f^|)_{diesel}$ is the mole fraction of diesel.

4.8 Uncertainty Analysis

Uncertainty provides the complete details of errors associated with the results or instruments used during the conduction of the experimental work. Uncertainty is caused due to the environment, selection of instruments, calibration, observation, human errors, and experimental procedure. The uncertainty is analyzed for the dependent variables such as BP, BSEC, BTE, etc., and is determined by the partial differential method with uncertainty associated with every instrument used in the current investigation. The determination of uncertainty for the experimental results is presented by Kline and McClintock (1953), which is formulated, based on the Gaussian distribution method and the uncertainty for any parameter to be measured is determined under the confidence limit of ±2σ. The uncertainty of any measured parameter is determined by:

$$W_i = \frac{2\sigma'}{X'} \times 100 \qquad (4.20)$$

By calculating the standard deviation (σ') and mean (X') the uncertainties for independent parameter considered for the overall of the experiment is obtained. The analysis is achieved for the parameters such as load, time, speed, fuel flow rate, the mass flow rate of air, NO_x, CO, etc for the 20 sets of readings at the fixed operating condition. The overall uncertainty is found to be $\pm2.3\%$ in the present investigation and the total uncertainty for the experimental reading is determined is as follows:

$$= \sqrt{(BP)^2 + (BTE)^2 + (BSEC)^2 + (Load)^2 + (speed)^2 + (CO)^2 + (UBHC)^2 + (NO_x)^2 + (SO)^2 + (CP)^2}$$

4.9 Details of the Measuring System

The engine test rig used in the present research work is interfaced with the different instruments. The details about the measuring system of different parameters during the experiment upon the engine test rig are given in this current section.

4.9.1 Measurement of the Engine Speed

The engine is operated at a constant speed, an inductive pickup sensor combined with a digital rpm indicator senses the engine speed and displays it in the control panel. The sensor is placed nearby the eddy-current dynamometer and is controlled accordingly. As the dynamometer shaft rotates at the constant speed of 1500 rpm, the inductive pickup rotary encoder delivers the voltage pulse by converting the frequency into rpm. The readings are displayed across the control panel through the calibrated digital indicator which indicates the speed in the revolution per minute directly. A PCB piezotronics made with a range of 5000 psi using diaphragm stainless steel and hermetic sealed is used to measure the engine speed.

4.9.2 Load Measurements

Using an eddy current dynamometer, the brake load is measured. It consists of several electromagnets mounted on a stator and the engine output shaft is coupled to the rotor disc. The eddy currents are generated across the stator due to the rotation of the rotor and thereby generating the magnetic flux as a result of current flow in the

electromagnets. The loading on the engine is achieved as the rotor motion is opposed by the eddy currents and generates heat. Underneath the dynamometer arm, a strain gauge type load cell is mounted to measure the torque with the aid of a moment arm. The signals from the load cell in the analog form are transmitted through the ADC card PCI 1050 and displayed in the computer in a digital form representing load in kg.

4.9.3 Temperature Measurement

The temperatures required at different locations of the engine test rig are obtained from the Chromel-Alumel thermocouples and are displayed on a digital panel meter. The following temperatures are obtained: Inlet Engine Water Temperature (T1), Outlet Engine Jacket Water Temperature (T2), Inlet Temperature of Calorimeter (T3), Outlet Calorimeter Water Temperature (T4), Exhaust gas Temperature before Calorimeter (T5), Exhaust gas Temperature after Calorimeter (T6). The digital readings of the respective temperatures obtained through the different sensors are connected to the control panel and are also interfaced to the computer through the NI hardware DAQ system.

4.9.4 Varying Injection Timing Measurement

The engine is operated for three different injection timings namely Advance (29.5° bTDC), Actual (27.5° bTDC), and Retard (25.5° bTDC) respectively. The required injection timing is achieved by changing a small part called a shim which is located underneath the fuel pump such that each shim is of 2 mm thickness and 2° CA. The actual injection timing of the diesel engine is 27.5° bTDC consisting of 2 shims, if 1 shim is removed then the injection timing will be advanced to 29.5° bTDC and if the total three shims are included under the fuel pump then the injection timing will be retarded to 25.5° bTDC. The engine makers will provide a marking on the flywheel by fixing the actual timing of 27.5° bTDC. Keeping the punch mark as a reference the required advance and retard injection timings are achieved.

4.9.5 Measurement of Exhaust Gas Emission

A calibrated AVL Digas 444 five gas exhaust gas analyzer is used to measure the various exhaust emissions emitted from the engine during the experiment and the gases

include such as carbon dioxide (CO_2, %volume), carbon monoxide (CO, %volume), oxygen (O_2, % volume), unburnt hydrocarbons (HC, ppm), and oxides of nitrogen (NO_x, ppm). The gas analyzer is maintained with proper care and working condition by cleaning the probe and regularly checking every type of filter used. The most important step to be done in using the gas analyzer is the leakage test and zero adjustments have to be done regularly without fail. Similarly, smoke opacity (SO) is measured by using the AVL smoke meter. Appendix-III provides the detailed specifications of the AVL exhaust gas analyzer used for the research work.

4.9.6 Measurement of Air and Fuel Consumption

The air consumption is measured using an appropriate air-box fitted with an orifice is utilized to fix the pulsations occurring as the air is drawn during the suction stroke. Using a U-tube manometer filled with water and pressure transmitter, the differential pressure (DP) across the orifice is obtained. As the pressure difference is developed across the orifice the DP unit senses the pressure and delivers it to the transmitter. The analog signal delivered to the transducer in the form of DC voltage is converted into the digital signal, which is in turn processed by the software program to obtain the mass flow rate in mm of the water column. Fuel is delivered to the engine filled in the fuel tank and is fitted in the control panel. The time taken for the fuel consumption of 10 CC is measured by determining the product of the density of fuel and the volume flow of the fuel for the given time interval. The measurement of the volume flow of fuel is obtained from a glass burette in ml and the time taken for the engine to consume the fuel is measured by stopwatch manually. The fuel flow is switched out using a control knob connected to the two-way fuel which is kept for measuring position or to the engine through the burette. The DP transmitter unit senses the pressure head difference and delivers the analog signal, through the NI USB-6210 hardware. The final reading of the fuel flow rate in kg/h is represented in the computer display through the *IC Engine Soft*. Before operating the engine, it is important to enter the density value and lower calorific value of every test fuel into the software.

4.9.7 Cylinder Pressure Measurement

The cylinder pressure for consecutive combustion cycles is measured from the piezo-electric transducer (Model HSM111A22) with a 1° crank-angle resolution and it is fixed across the engine cylinder head. The transducer is interfaced to the DAQ (NI-USB-6210) and the data are displayed on the monitor through the IC engine software. Cooling water is circulated continuously across the sensor body to maintain the sensor at a constant temperature. The engine output shaft is fitted with the rotary encoder to attain the crank angle signal. The engine indicator scans the signal instantaneously and it is interfaced to the computer. In the pressure crank-angle (P-θ) and pressure-volume (PV) plots, all the engine properties and combustion properties are evaluated by the software.

4.10 Closure

The current chapter deals with the details about the basic modifications in the engine by converting the diesel mode into dual-mode and also the methodology of the experimental work. The objectives of the research work, such as the basic study of the engine characteristics by dual-mode using biogas, engine behavior under cyclic variations, the influence of injection timing, the effect of oxygen enrichment and study of the vaporized water-methanol induction system are discussed in detail. Also, the details about the uncertainty associated with the devices used and the procedure to use the measuring system for the current investigation are provided. In the next chapter, the results and discussion of the studies incorporated to achieve the research objectives are described.

CHAPTER 5

RESULTS AND DISCUSSIONS

In this section, the performance, combustion, emission characteristics of the engine operated under diesel and dual-mode are investigated. The behavior of the single-cylinder diesel engine under cycle by cycle variations using biogas with different proportions from BG20 to BG60 under dual fuel mode at actual injection timing of 27.5° bTDC is analyzed. The effect of the varying injection timings upon the engine under dual fuel mode is explored such that the biogas and injection timing is optimized based upon the better performance. The work is extended to study the enhancement of engine parameters using oxygen enrichment for optimized biogas at optimized injection timing. To reduce the higher NO_x emissions generated, the vaporized water-methanol method is incorporated and the experimental results are analyzed with the standard base readings.

5.1 Performance Characteristics

The corresponding relations for measuring the performance characteristics such as BTE, BSEC, Volumetric efficiency, and Biogas energy contribution for the dual-mode of operation are given in the equations 4.5, 4.6, 4.8, and 4.9.

5.1.1 Brake Thermal Efficiency (BTE)

Brake thermal efficiency for diesel as well as dual mode at all loads are shown in Figure 5.1. Overall, the BTE trend for the biogas proportions ranging from BG20 to BG60 increases as the load is increased. On the other hand, the efficiency of the dual-mode is lower than the diesel. At actual injection timing of 27.5° bTDC, the biogas BG60 showed a decrease in brake thermal efficiency at all loads compared to other biogases. Whereas, at the full load the BTE decreases due to the increase in friction in the engine for diesel and dual-mode. This drop-in brake thermal efficiency is due to the introduction of biogas at the intake manifold which causes a reduction in oxygen supply, lower calorific value of the biogas and increased negative compression work. This development is also because of lower flame propagation of the biogas, increased negative compression work and incomplete combustion due to the decrease in intake air, as a

result volumetric efficiency decreases (Barik and Murgan 2014). At 3/4th load brake thermal efficiency for BG20, BG30, BG40, BG50, and BG60 is 8.34%, 12.15%, 15.58%, 21.7%, and 24.18% lower than diesel respectively. Whereas, at full load, the brake thermal efficiency of BG20, BG30, BG40, BG50, and BG60 is 11.9%, 14.5%, 15.62%, 22.75%, and 23.13% lower than diesel.
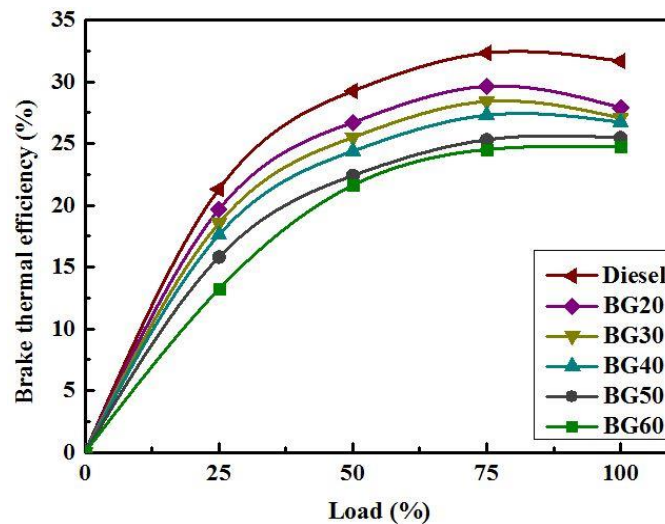
Figure 5.1: Brake thermal efficiency variations for diesel and dual mode

5.1.2 Brake Specific Energy Consumption (BSEC)

Comparison of BSEC with engine load for diesel and the biogas mode is shown in Figure 5.2. Among different biogases, BG60 showed more BSEC as compared to the remaining biogases for all the loads. Whereas, diesel showed less fuel consumption compared to the biogas mode at all loads. At 3/4th load, the BSEC for B20, BG30, BG40, BG50 and BG60 is 9.09%, 18.18%, 27.27%, 38.18% and 45.45% higher than diesel respectively. Whereas, at the full load, the BSEC for B20, BG30, BG40, BG50 and BG60 is 8.33%, 16.66%, 25%, 33.33% and 37.5% respectively. This development resembles that the energy conversion efficiency of biogases increased at higher loads, which can be accredited to the quantity as well as the composition of diesel-biogas fuel induced at the intake stroke. It is also attributed due to the lower energy density and lower cylinder temperature. At lower loads, most of the biogas will be filled inside the cylinder and get combusted due to the heat liberated from the combustion of the diesel fuel. As a result

due to the poor combustion of the biogas-air mixture, the ID gets increased (Heywood 2018). The effect gets extended because of CO_2 concentration present in the biogas which contributes to the lower flame propagation speed and quick quenching of the flame (Badr et al. 1999).
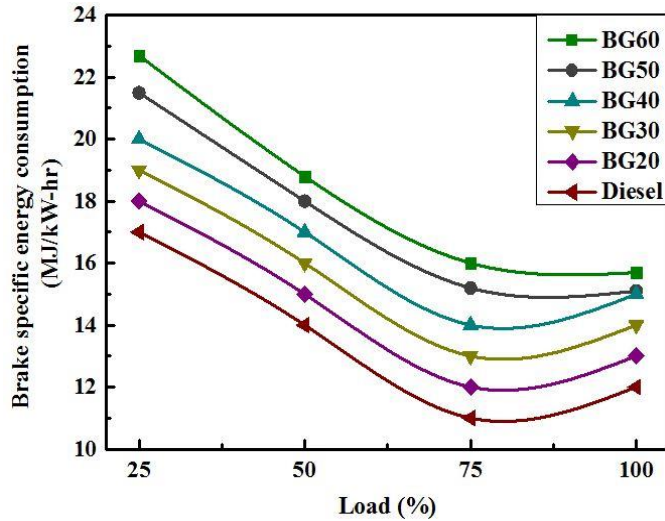
Figure 5.2: Brake specific energy consumption variations for diesel and dual mode

5.1.3 Volumetric Efficiency (η_v)

Volumetric efficiency is a very crucial aspect for deciding the performance of diesel, petrol and gas engines. It is identified that better utilization of the air determines the delivery of higher power output of the engine. Volumetric efficiency is defined as the flow rate of air volume inducted into the intake system divided by the rate of volume displacement done by the system (Ganesan 2003). Variations of volumetric efficiency for diesel as well as biogas from BG20 to BG60 are shown in Figure 5.3. From Figure 5.3, it is observed that as biogas proportion increases the volumetric efficiency decreases, on the other hand even as the load increases both for diesel as well as dual-mode the volumetric efficiency decreases. In conclusion, the diesel mode showed higher volumetric efficiency compared to dual-mode for varying loads. The reason for the decrease in volumetric efficiency for the dual-mode of operation is due to the induction of the biogas along with air at intake manifold causes reduction of fresh air as a result air density decreases. On

the other hand, the increase in temperature of the cylinder wall causes a rise in the temperature of inducted air, so thus the decrease in volumetric efficiency of dual-fuel mode is observed (Barik and Murgan 2014). At full load, the volumetric efficiency of BG20, BG30, BG40, BG50, and BG60 is lower than diesel by 0.93%, 1.68%, 2.51%, 3.30%, and 3.64% respectively.
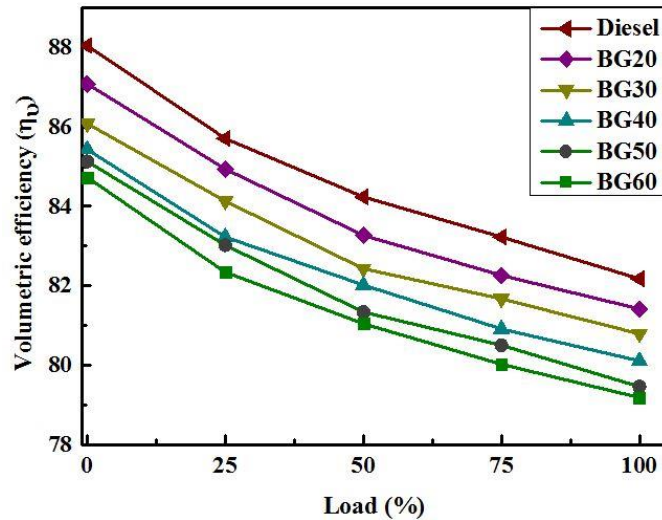
Figure 5.3: Volumetric efficiency variations for diesel and dual mode

5.1.4 Energy Share of Biogas (ESB)

To explore the premixed lean combustion in a diesel engine operated with dual fuel mode, the energy share of the prime fuel is considered to be a significant factor. Major energy contribution is attained by both the biogas as well as diesel fuel generating a definite amount of power. As the combustion process takes place, the biogas, and diesel consumption gets fluctuate correspondingly as the load gets varied. Based on the fuel consumption rate and calorific value, the energy contribution of fuel can be obtained. For the dual-fuel mode, the energy contribution is defined as the ratio of energy delivered by the biogas to the sum of the energy delivered by the biogas and diesel (Barik and Murgan 2014). The ESB from BG20 to BG60 for varying loads (25%, 50%, 75%, and 100%) is shown in Figure 5.4. Observing the results, it is concluded that as the load increases ESB increases. The reason for the increase in energy share is because of the induction of more

biogas into the engine and an increase in diesel replacement is observed. Maximum energy contribution was observed for BG60 compared to lower biogas proportions at all loads. Compared at full load (100%) BG20, BG30, BG40, BG50 and BG60 provides the energy contribution of 34.35%, 45.079%, 51.7%, 63.63% and 69.06% respectively.
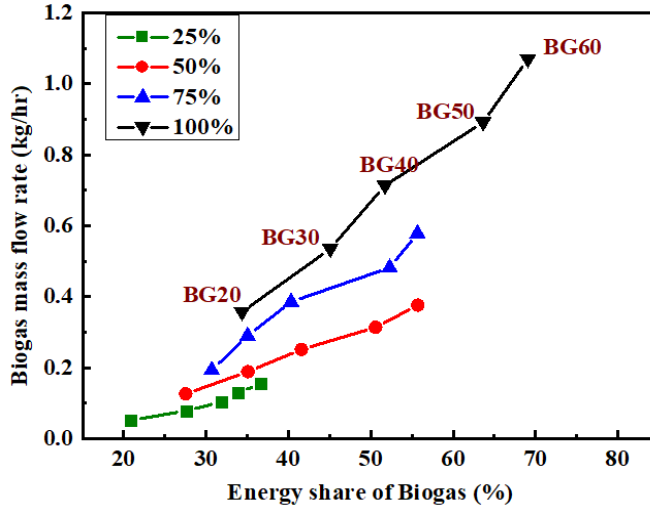
Figure 5.4: Energy Share of Biogas for different mass flow rates

5.2 Combustion Characteristics

Using the IC engine software version 9.0, the combustion parameters such as in-cylinder pressure (P-Ɵ), net heat release rate (NHRR), Ignition delay (ID) are determined and the corresponding expressions are obtained from the equations 4.14 and 4.18.

5.2.1 Cylinder Pressure (P-Ɵ)

The cylinder pressure variations for diesel and dual-mode at full load are shown in Figure 5.5. Peak cylinder pressure for dual-mode is higher than the diesel at full load. Compared to diesel the initiation of ignition gets delayed for all the biogases at full load due to the occurrence of CO_2 in biogas and due to the higher auto-ignition temperature of biogas. Higher peak cylinder pressure is observed for biogas than diesel due to the intake of biogas at intake manifold with intake air causes dilution of oxygen concentration and gradually the air quantity decreases. As a result, at the premixed combustion phase, ID gets extended causing a higher rate of pressure rise, and both peak cylinder pressure and

90

ignition occur little delayed (Barik et al. 2015). At full load, the maximum cylinder pressure for diesel is 56.5 bar, whereas, for biogas mixtures such as BG20, BG30, BG40, BG50, and BG60 are 57.94, 58.72, 59.53, 60.04, and 60.46 bar respectively.
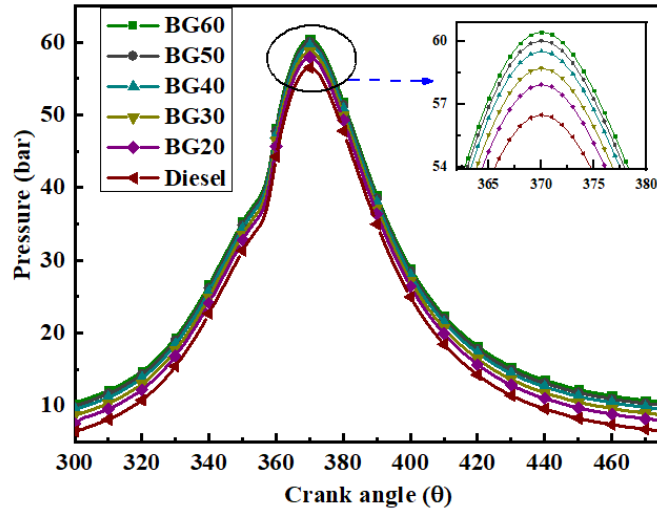
Figure 5.5: Cylinder pressure variations for the fuels at full load

5.2.2 Net Heat Release Rate (NHRR)

Net heat release rate depends upon the fuel mixture quality of diesel, air, and biogas. It also depends on the lower heating value, the mass flow rate of diesel and biogas. Figure 5.6 shows the net heat release rate variations v/s crank angle for diesel and biogas proportions. The heat release rate is influenced by factors such as mixture formation, the rate of combustion, and ID at the preliminary stages as well as at the combustion phase (Heywood 2018). A higher rate of heat release is observed for the biogas mixtures than compared to diesel. This is because at the longer delay period the accumulation of fuel gets increased and due to the larger heating value of the diesel-biogas combination. At full load, the heat release rate occurs earlier for diesel than compared to biogas mixtures and are caused due to the larger specific heat of biogas causing retarded combustion (Barik et al. 2015). For diesel, the maximum heat release rate is found to be 23.75 J/°CA, whereas, the biogas mixtures BG20, BG30, BG40, BG50, and BG60 showed NHRR of 25.31 J/°CA, 26.65 J/°CA, 27.29 J/°CA, 28.61 J/°CA, and 29.14 J/°CA at full load respectively.

91
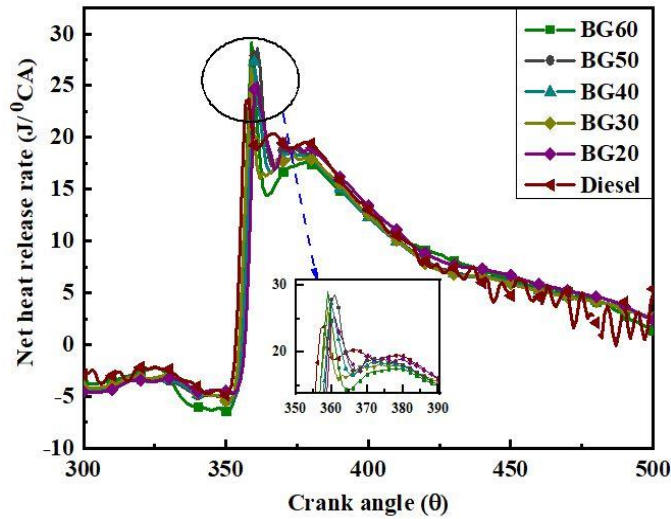
Figure 5.6: Net heat release rate variations for the fuels at full load

5.2.3 Ignition Delay (ID)

The effect of ID is shown in Figure 5.7, ID is affected by various factors such as air-fuel ratio, compression ratio, fuel atomization, type of fuel, quality of the fuel. ID for the dual-mode depends upon the oxygen content in the air. As observed from Figure 5.7, as the load of the engine is increased ID decreases for both diesel and biogas fuels. The delay in the ignition is due to the increase in temperature of the combustion chamber (Lata and Misra 2011). Whereas, due to the induction of biogas at the intake manifold and decrease in the oxygen concentration causes an increase in the duration of ID. It is evident that the increase in the maximum cylinder pressure is due to the induction of biogas with the intake-air charge, causes a decrease and dilution of oxygen concentration. As a result, the longer ID is caused and increase in-cylinder pressure at the premixed combustion stage is witnessed. On the other hand, the higher stoichiometric air requirement of the biogas-air mixture is also the reason to cause an increase in the ID (Prakash et al. 2013). The ID for diesel at full load is 12.2°CA, whereas, BG20, BG30, BG40, BG50, and BG60 showed 13.2°CA, 13.7°CA, 14.2°CA, 14.7°CA, and 14.8°CA delay respectively.
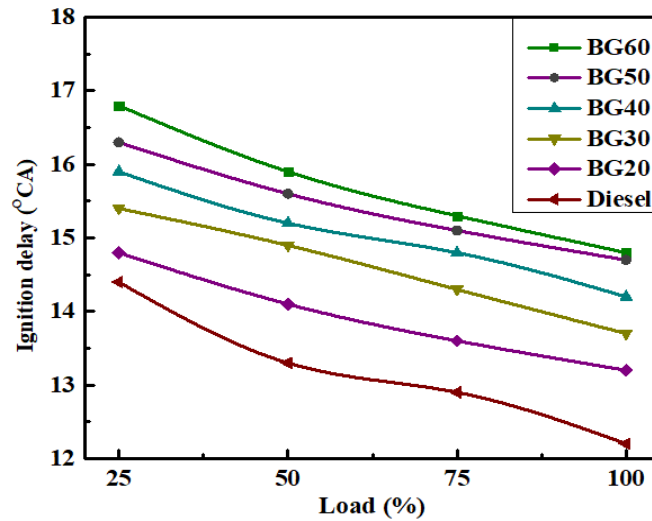
Figure 5.7: Ignition delay variations for diesel and dual mode

5.3 Emission Characteristics

The emission characteristics such as carbon monoxide, unburnt hydrocarbons, nitrogen oxide are measured from the AVL exhaust gas analyzer. While, the smoke opacity or sootness is measured with the aid of the AVL smoke meter and the results are interpreted as mentioned below.

5.3.1 Carbon Monoxide (CO)

Carbon monoxide variations for diesel and biogas mixtures for all loads are shown in Figure 5.8. The trend depicts that CO emission for dual fuel mode is higher than diesel at all loads. Among biogas, BG20 shows less CO emission compared to other higher biogas proportions. At 3/4th load, CO emission for BG20, BG30, BG40, BG50 and BG60 increased by 5%, 7.5%, 12.5%, 20% and 27.5% than diesel. Whereas, at full load CO emission for BG20, BG30, BG40, BG50, and BG60 is higher than diesel by 1.66%, 3.33%, 5%, 8.3%, and 16.6% respectively. For pure diesel, the CO emission is lower compared to dual fuel mode because diesel possesses a higher stoichiometric flame speed than biogas. Whereas, the biogas shows lower stoichiometric flame speed than the diesel, propagation of flame front lags slowly to consume biogas and air (Bora et al. 2014). On the other hand, as the biogas is inducted into the cylinder, oxygen concentration in the air

gets reduced and this causes CO emission to increase as the biogas flow rate is increased. However, CO emission for biogas mode is lower at lower loads (Ambarita 2017).
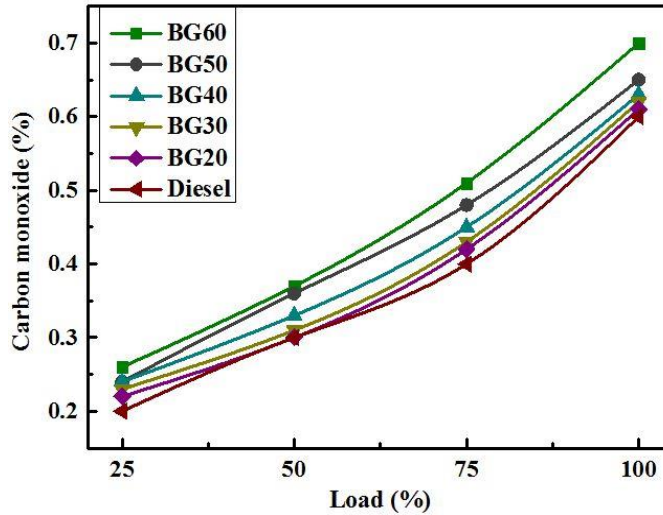
Figure 5.8: Carbon monoxide emission variations for diesel and dual mode

5.3.2 Unburnt Hydrocarbon (UBHC)

Unburnt hydrocarbon emission for diesel and biogas at all the loads is shown in Figure 5.9. UBHC is lower for diesel mode, and UBHC for biogas mode significantly increases. At 3/4th load the UBHC for BG20, BG30, BG40, BG50 and BG60 is 10.86%, 15.21%, 19.56%, 23.91% and 28.26% higher than diesel respectively. At full load, UBHC emission for BG20, BG30, BG40, BG50 and BG60 is 0%, 5.17%, 10.34%, 13.79% and 17.24% higher than diesel. From Figure 5.9 it is observed that UBHC increases as the biogas mixture is increased, this is because when the biogas is injected more inside the combustion chamber causes a rich mixture or less concentration of fresh air. Also, due to the low flame velocity of biogas the UBHC increases, these two factors influence in forming incomplete combustion inside the cylinder and causes larger UBHC within the exhaust gas (Ambarita 2017). Moreover, because of the crevice volumes, the gas-air mixture is strained at the compression stroke and remains unburned (Badr et al. 1999). The overlapping between intake and exhaust valves to promote scavenging is also the reason for UBHC emission to increase for dual fuel mode (Bedoya et al. 2009).

94
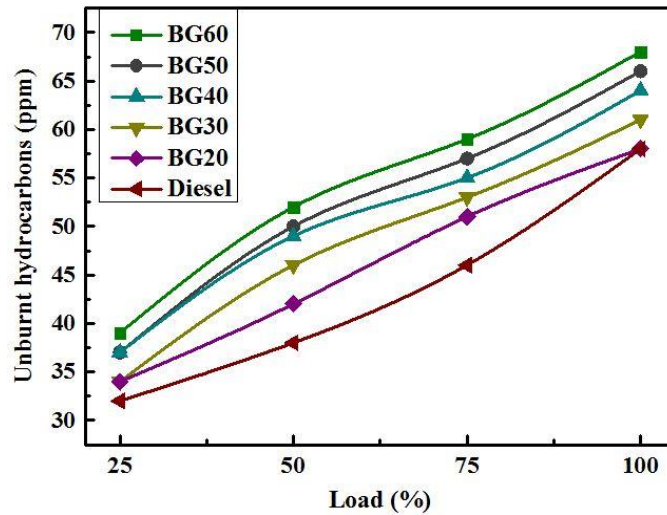
Figure 5.9: Unburnt hydrocarbon emission variations for diesel and dual mode

5.3.3 Nitrogen Oxide (NO$_x$)

Variations of NO$_x$ emissions for both diesel and biogas at all loads are shown in Figure 5.10. In general, the NO$_x$ emission increases as the load increases for both the fuels and compared to diesel, dual fuel mode showed lower NO$_x$ emission for all the loads. This is due to the increase in equivalence ratio for the higher loads (Verma et al. 2017). From Figure 5.10, it is observed that NO$_x$ emissions for dual fuel mode are lower than diesel due to the induction of biogas causing a reduction in oxygen concentrations in the fuel-air mixture, such that the rate of formation of NO$_x$ reduces slowly (Makareviciene et al. 2013). In addition, CO$_2$ presence in the biogas reduces the peak cylinder temperature since CO$_2$ possesses higher specific heat. The combination of these factors promotes lower NO$_x$ emission for biogas mode. On the other hand, the levels of NO$_x$ emissions were found to be equivalent at higher loads due to the enhanced and quick combustion of biogas compared to lower loads ensuing high temperatures and peak pressures (Verma et al. 2017). At 3/4th load, the NO$_x$ emission for BG20, BG30, BG40, BG50, and BG60 is 12.85%, 17.46%, 22.57%, 33.44%, and 45.46% lower than diesel respectively. Whereas, at full load NO$_x$ emission for BG20, BG30, BG40, BG50 and BG60 is 17.59%, 20.6%, 26.6%, 35.33% and 43.65% lower than diesel respectively.
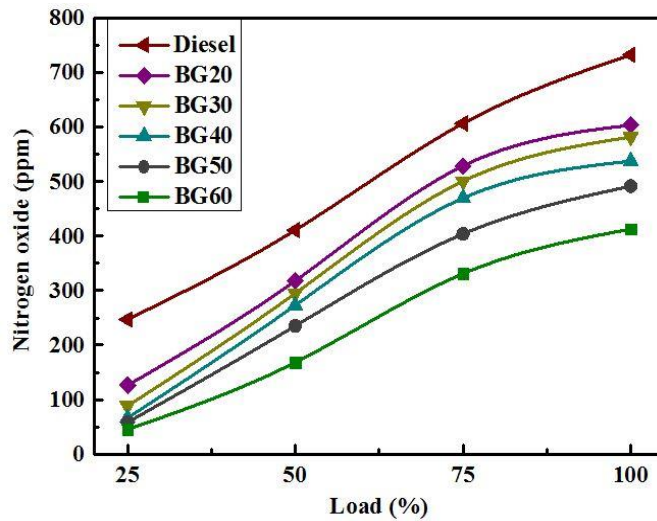
Figure 5.10: Nitrogen oxide emission variations for diesel and dual mode

5.3.4 Smoke Opacity (SO)

Figure 5.11 shows the variations of soot emissions for the diesel and biogases at all loads. The soot emission trend for diesel and biogas fuel is increasing, whereas, the biogas showed lower soot emissions compared to diesel for all loads. The major advantage of biogas operated by dual-mode is the lower smoke emission because the biogas doesn't contain high carbon and aromatic compounds which inhibits soot formation (Wei and Gang 2016). Also, the presence of CO_2 in the biogas decreases the flame temperature, as a result oxidation reaction rate of soot decreases (Verma et al. 2017). Furthermore, combustion period, as well as ID, also contributes to lower smoke emissions in the case of dual fuel mode, such that both these factors promote in proper mixing and combustion of air-biogas fuel causing enhancement of oxidation of soot particles (Sahoo et al. 2009).

Compared to diesel, the smoke opacity for BG20, BG30, BG40, BG50, and BG60 is lower by 10.35%, 20.94%, 29.41%, 30.35%, and 36% respectively at 3/4th load. Whereas, at full load, sootnes for BG20, BG30, BG40, BG50, and BG60 is lower than diesel by 7.82%, 17.69%, 22.71, 28.49%, and 33.14%.
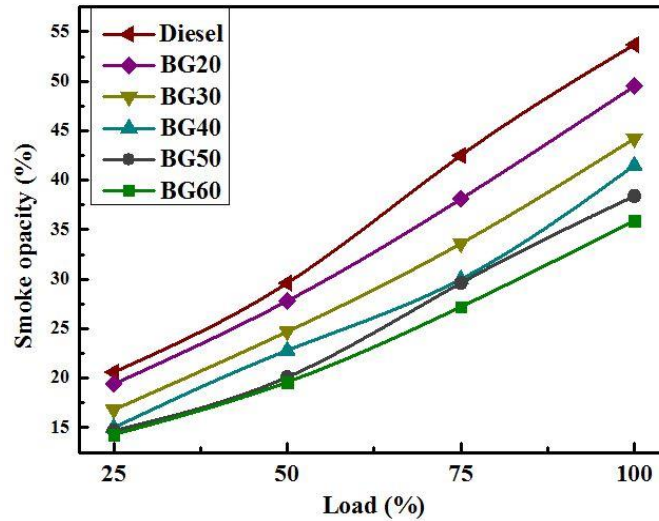
Figure 5.11: Smoke opacity emission variations for diesel and dual mode

5.4 Studies on Cyclic Variations

To study the combustion behavior of biogas operated under the dual-mode in diesel engine, the cyclic variation is explored in this section by studying the nature of coefficient of variance (COV) and time return map of maximum cylinder pressure.

5.4.1 Coefficient of the Variance of Maximum Cylinder Pressure (P_{max})

The maximum peak pressure variations for 100 successive combustion cycles at full load and constant speed of 1500 rpm are observed in Figure 5.12 (a-f). It indicates how the peak pressure variation occurs for diesel as well as biogas from BG20 to BG60 at 100 cycles. Using a high precision piezo-electric pressure transducer the in-cylinder pressure is measured for all operating conditions of the engine. The trends of peak pressure indicate that fluctuations are lower for diesel compared to all the biogas at full load (Maurya and Agarwal 2011). Due to the nature of dominance in non-premixed combustion, lower cyclic variations are caused compared to biogas such that diesel injection first manages the mixing of air-fuel and then combustion. However, instabilities in the injection system of the diesel fuel or to the prolonged ID can also attribute to the higher cyclic variations (Kyrtatos et al. 2016). As the amount of biogas increases the variations in peak combustion pressure increase, BG50 showed higher variations

97

compared to other biogas and diesel fuel. Due to the increase in the amount of biogas, the ID period of the diesel fuel will increase as a result of the combustion of biogas occurring at a higher pressure rate. Moreover, the change in the specific heat of the compressed air-biogas mixture lowered the compression temperature is also the reason for the increase in ID (Selim 2004). The coefficient of variance (COV) of maximum cylinder pressure (P_{max}) for diesel and biogas from BG20 to BG60 is illustrated in Figure 5.13. Cyclic variations are found to be higher for BG50, BG60 and lower for BG20 and BG30 indicating better combustion stability. The COV in P_{max} for all the fuels is below 2% which implies that the diesel engine with biogas will run in stable condition with minute variations in work output and generate less noise (Selim 2004). BG20 showed lower COV of P_{max} by 2.3% than diesel, BG30 showed slightly higher COV of P_{max} by 1.89% than diesel respectively. On the other hand, BG50 and BG60 showed higher COV of P_{max} than diesel by 11.45% and 20.75% respectively.
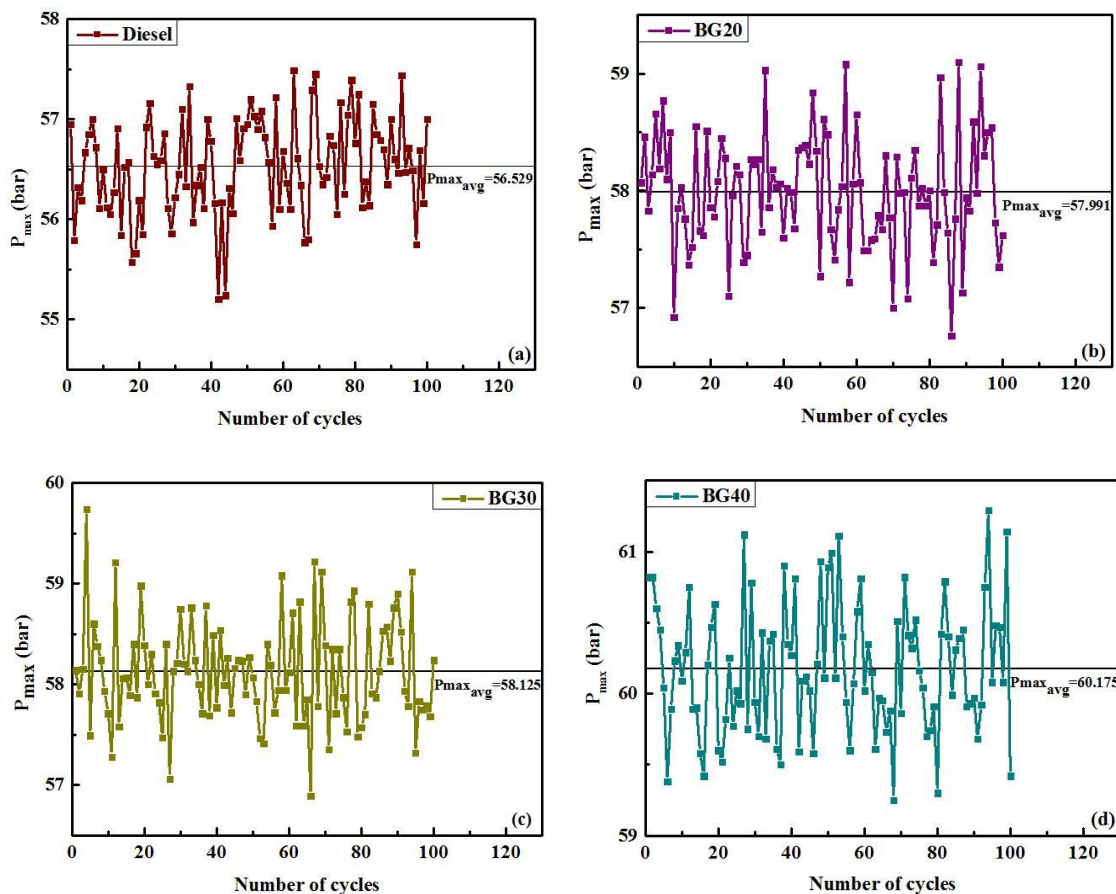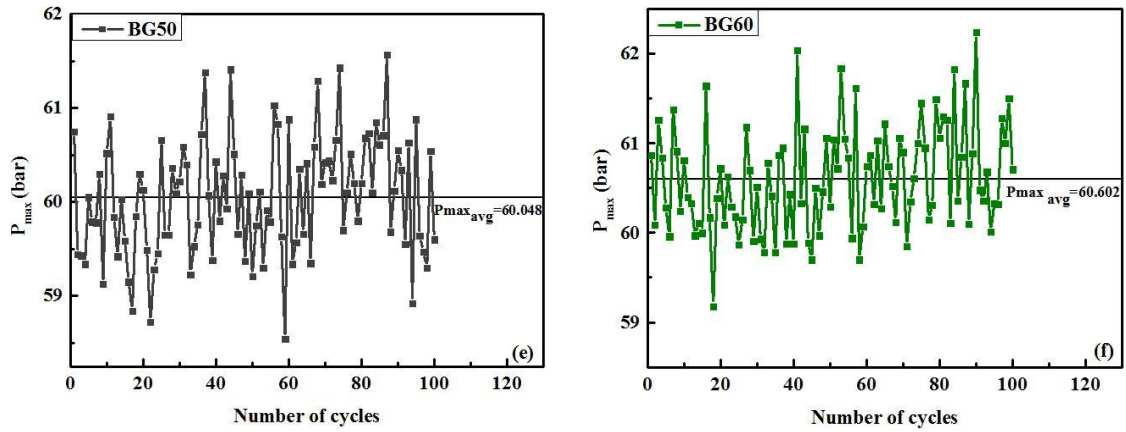
Figure 5.12 (a-f): Maximum cylinder pressures for diesel and dual mode
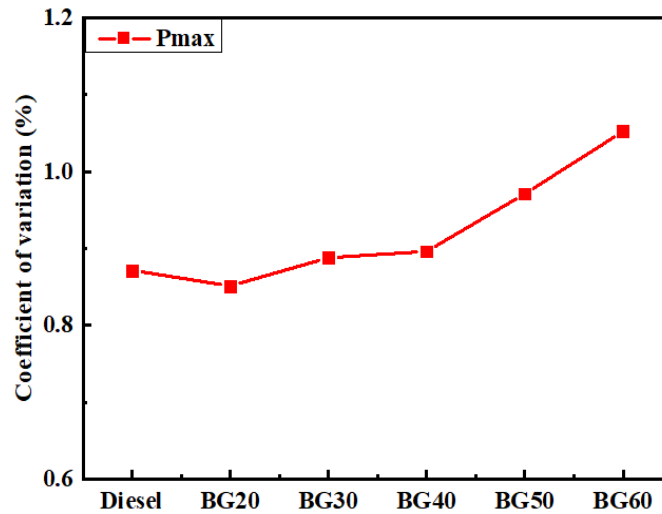
Figure 5.13: Coefficient of maximum cylinder pressure (P_{max}) for the fuels

5.4.2 Time Return Map of Maximum Cylinder Pressure (P_{max})

The nonlinearity of the cylinder pressure (P_{max}) generated from the combustion process for diesel as well as dual fuel mode is analyzed by using a time return map. By plotting the experimental variables against lagging in time, i.e. by plotting the P_{max} for the cycle (i+L) against P_{max} for the ith cycle, such that L is denoted as time return lag and possess a value of 1 (Leach et al. 2019). A circular, unstructured pattern is attained by the means of Gaussian random data which symbolizes the pattern as the existence of

determinism. As the engine generates higher levels of noise indicates that the return map structure is very vigorous for lower dimensional dynamics (Nemoianu et al. 2017).
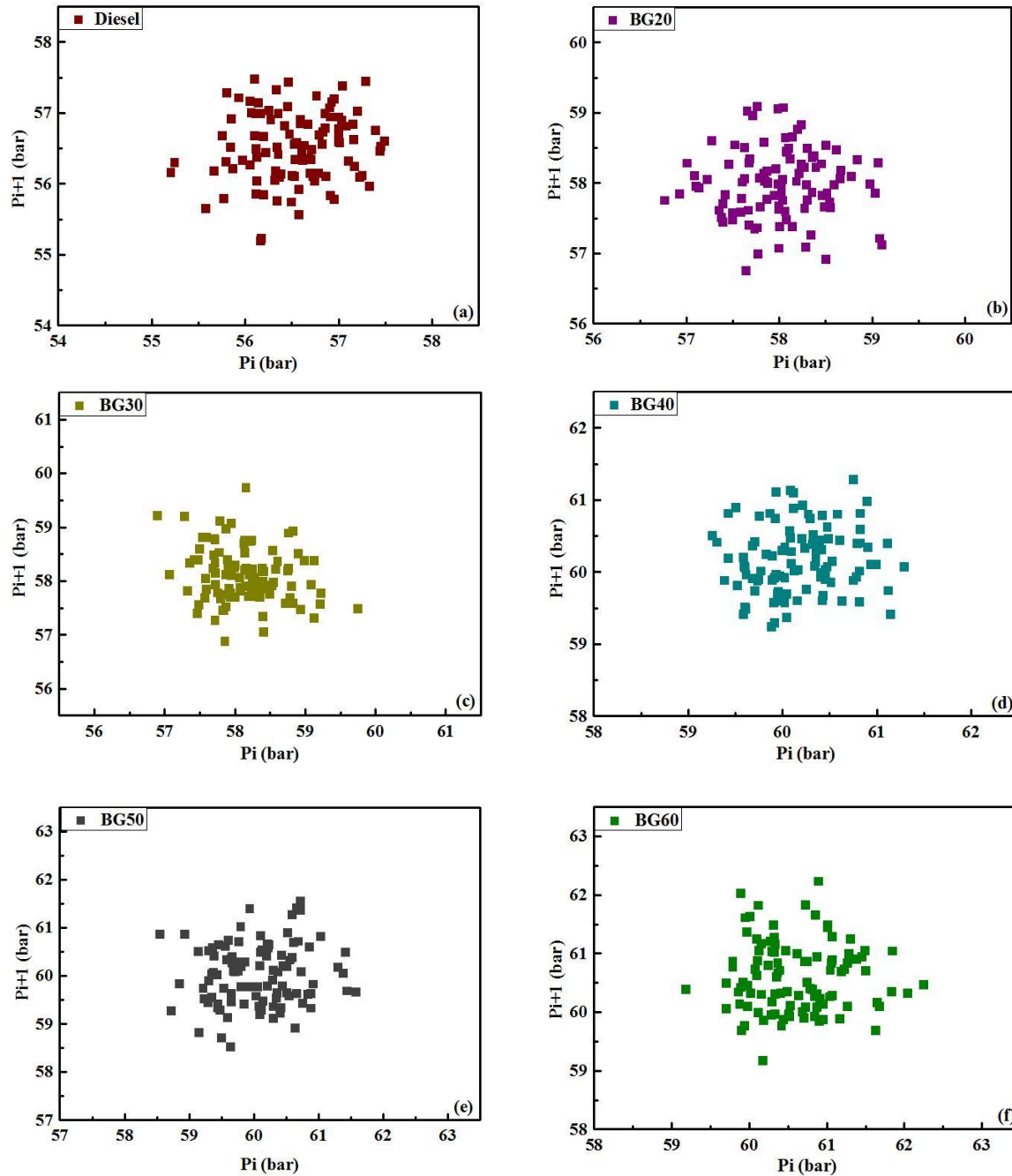
Figure 5.14 (a-f): Time return map of P_{max} for diesel and dual mode

The combustion process of diesel as well as for biogas is said to be stabilized when the grouping of P_{max} is symmetric. Figure.5.14 (a-f) shows the time return map of P_{max} for all the fuels, in detail studies of combustion, is obtained from the P_{max} values which are derived from the signals of cylinder pressure. As the load of the engine increases, the intensity of the P_{max} increases. Compared to diesel, the engine operated with biogas showed larger P_{max} indicating a more scattered and asymmetric pattern except for BG20 and BG30. Observing the return map for the biogas mode, both BG20 and BG30 showed symmetric pattern, less scattered and consistency in power output compared to other fuels.

5.5 Effect of Injection Timing on the Engine Parameters under Dual-Mode

In this current section, the influence of three different injection timing upon the dual diesel engine characteristics using different proportions of biogas is investigated.

5.5.1 Brake Thermal Efficiency (BTE)

The BTE of the biogas proportions ranging from BG20 to BG60 operated at the three injection timings 29.5°, 27.5°, and 25.5° bTDC, along with the diesel at 27.5° bTDC operated for all loads is shown in Figure 5.15 (a-e). As compared to diesel, the engine operated for dual fuel mode using different proportions of biogas showed lower BTE for all three injection timing. The results are analyzed and compared with diesel at operating injection timing of 27.5° bTDC such that the diesel indicated higher BTE compared to dual-mode for respective loads. Considering the different biogas proportions, maximum BTE was observed at advance (29.5° bTDC) injection timing. Whereas, retard (25.5° bTDC) injection timing (IT) showed lower BTE.

This decline in BTE is because of the lower calorific value of biogas, lower flame propagation, and induction of higher rate of biogas-air mixture causing negative compression work which leads to higher consumption of the biogas-air fuel mixture (Bora and Saha 2016, Chandekar and Debnath 2018, Khayum et al. 2020). BG20 showed a maximum BTE of 30.11% at full load but compared to diesel, BG20 showed lower BTE by 4.95% at full load operated at advance injection timing. Whereas, BG60

exhibited a lower BTE of 25.94% and is 28.4% lower than diesel at full load for 29.5° bTDC IT. The trend of reduction in BTE is caused due to the induction of biogas at the intake manifold, as a result, intake air decreases causing a decrease in volumetric efficiency. As observed from Figure 5.15 (a-e), advance injection timing shows maximum BTE compared to actual and retard injection timing at all the loads for every biogas proportion from BG20 to BG60. This is because, at advance timing additional time is accessible for the homogeneous mixing of the air-fuel as compared to actual, retard timings. Also, due to the combination of higher vaporization of the diesel fuel and efficient combustion of biogas-air mixture generates additional power (Bora and Saha 2016, Barik and Murugan 2016).
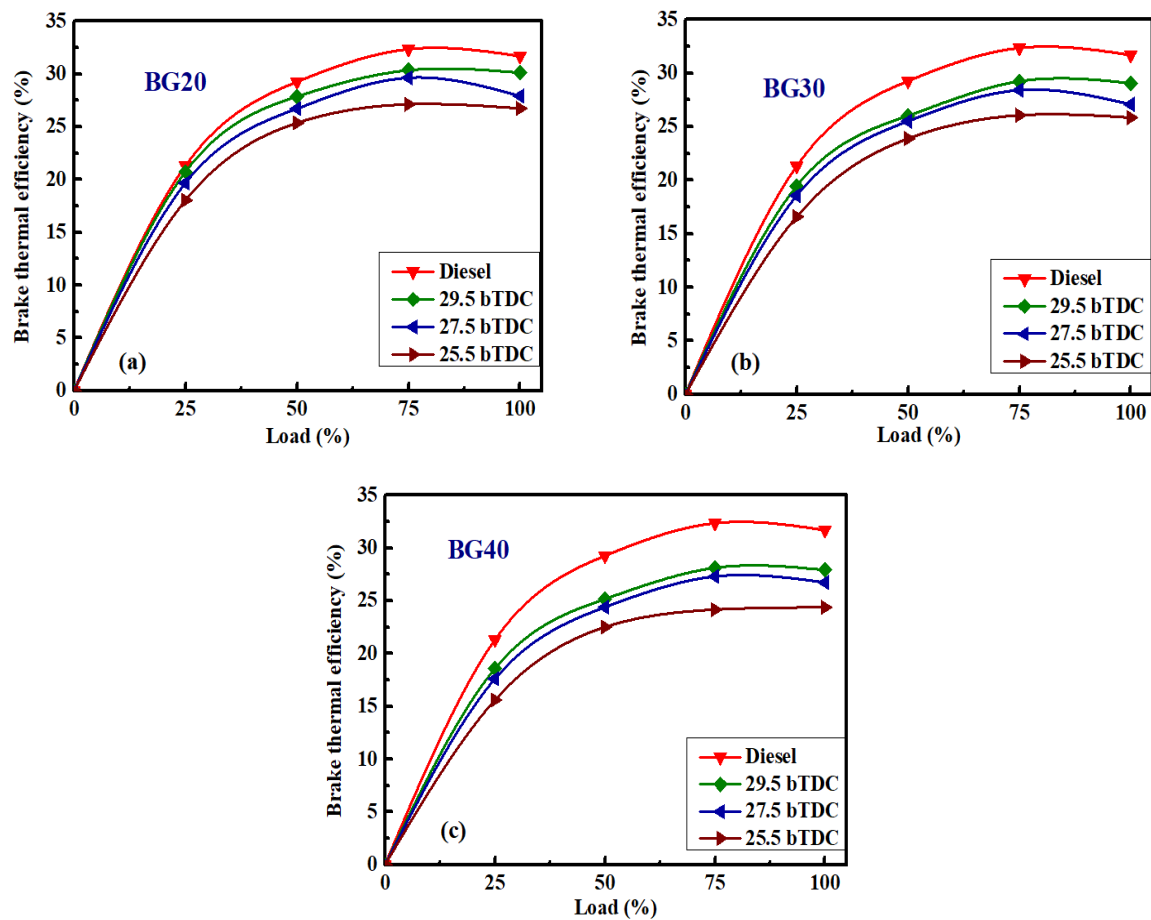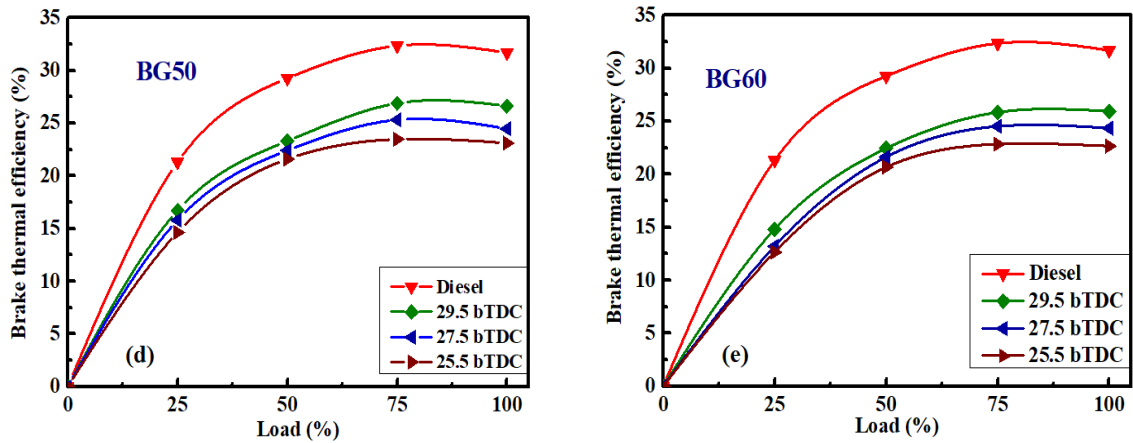
Figure 5.15 (a-e): Influence of injection timings on BTE for different biogas proportions

5.5.2 Brake Specific Energy Consumption (BSEC)

The BSEC variations for diesel and dual-mode at different loads operated at three injection timings are shown in Figure 5.16 (a-e). The plots depict that, the BSEC trend decrease as the load is increased for both diesel and dual-mode. In the case of biogas, the presence of CO_2 causes slower burning of the biogas, lower in-cylinder temperature, and LHV of the biogas (Verma et al. 2017, Jagadish and Gumtapure 2019). Moreover, a significant increase in the BSEC is observed with increase in the flow rate of the biogas. This is caused due to the presence of CO_2 in the biogas creating slow-burning of the biogas-air mixture (Khayum et al. 2020). As the injection timing is advanced, the combustion rate of biogas during the diffusion stage is affected due to the accumulation of diesel in large quantity such that the heat from premixed combustion is released at a higher rate which results in the enhancement of in-cylinder temperature of fuel mixture affecting the burning of the biogas at the second stage of the combustion (Barik and Murugan 2016, Khayum et al. 2020).

However, because of the poor combustion of air-biogas mixture, ID increases as a result heat release rate curve increases at a faster rate indicating higher BSEC as the load is increased (Gumus et al. 2010, Cadavid et al. 2012). BG20 showed lower energy consumption as compared to the rest of the biogas proportions. On the other hand, advance injection timing (29.5° bTDC) consumes less energy compared to actual and

retard injection timing for all the loads (Barik and Murugan 2016). Lower BSEC was observed for BG20 at 29.5° bTDC by 9.09% especially at full load as compared to diesel. At 3/4th load, BG20 showed higher BSEC by 2.6% than diesel. On the other hand, BG60 consumed higher energy density by 14.8% than diesel at full load for 29.5° bTDC injection timing.
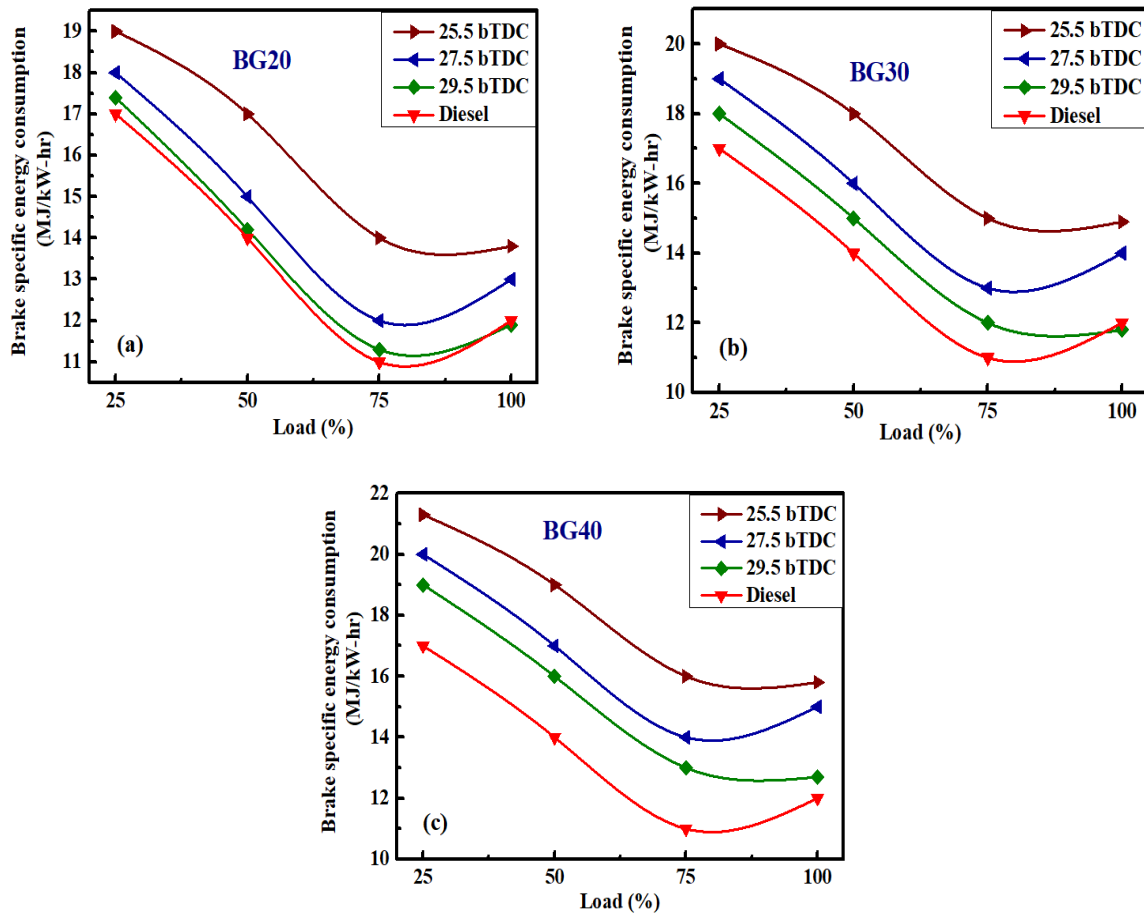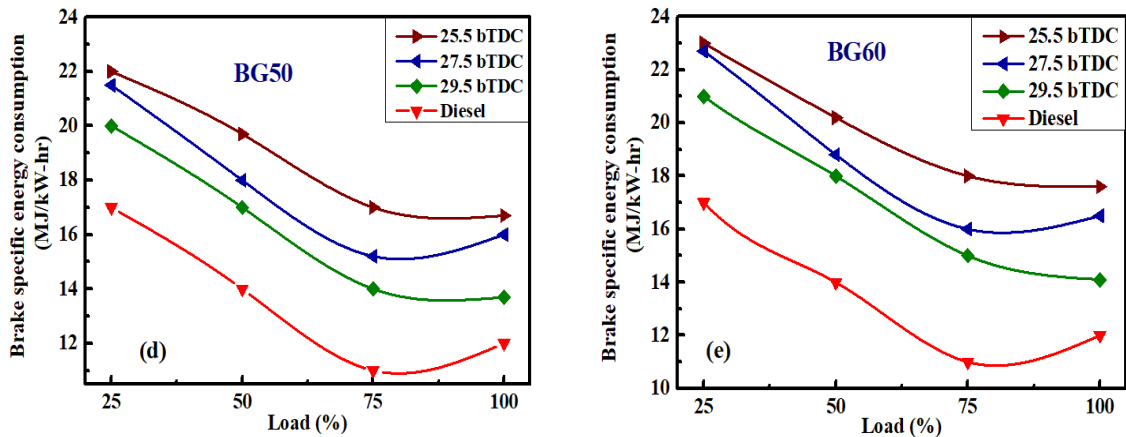
Figure 5.16 (a-e): Influence of injection timings on BSEC under dual mode

5.6 Combustion Characteristics

5.6.1 Cylinder Pressure (P-θ)

The variations of peak cylinder pressure for 100 cycles of both diesel and dual-fuel operated at full load, under the influence of three injection timings are shown in Figure 5.17 (a-e). Generally, it is observed that as the biogas proportions increase the cylinder pressure increases more than the diesel. BG60 shows higher cylinder pressure of 60.46 bar at full load operated at 27.5° bTDC. Whereas, the cylinder pressure of BG20, BG30, BG40 and BG50 is 57.94 bar, 58.72 bar, 59.53 bar, and 60.04 bar respectively. This development at the premixed combustion stage causes the ID to get extended causing peak cylinder pressure to increase at a higher level (Jagadish and Gumtapure 2020, Chandekar and Debnath 2018).

Advance injection timing (29.5° bTDC) showed maximum cylinder pressure for the biogas compared to actual and retard injection timing operated at full load. This is because, as compared to actual and retard injection timing enhanced homogeneous mixing of air-biogas was achieved within the cylinder and due to the development of fuel-rich mixture inside the cylinder. As a result, at the premixed combustion stage, quick burning of the air biogas takes place causing combustion to appear at the earliest such that a large quantity of dual-fuel gets burned before the piston reaches the top dead centre

(TDC) causing the cylinder pressure to reach maximum and appears closer towards TDC (Barik and Murugan 2016, Heywood 2018). BG60 showed a maximum cylinder pressure of 64.15 bar and the cylinder pressure for BG20 is 60.95 bar at advance injection timing. As compared to diesel, BG60 showed an increase in cylinder pressure by 11.9% at 29.5° bTDC. In the case of BG20, BG30, BG40, and BG50 increased by 7.3%, 7.9%, 9.23%, and 11.01% respectively.
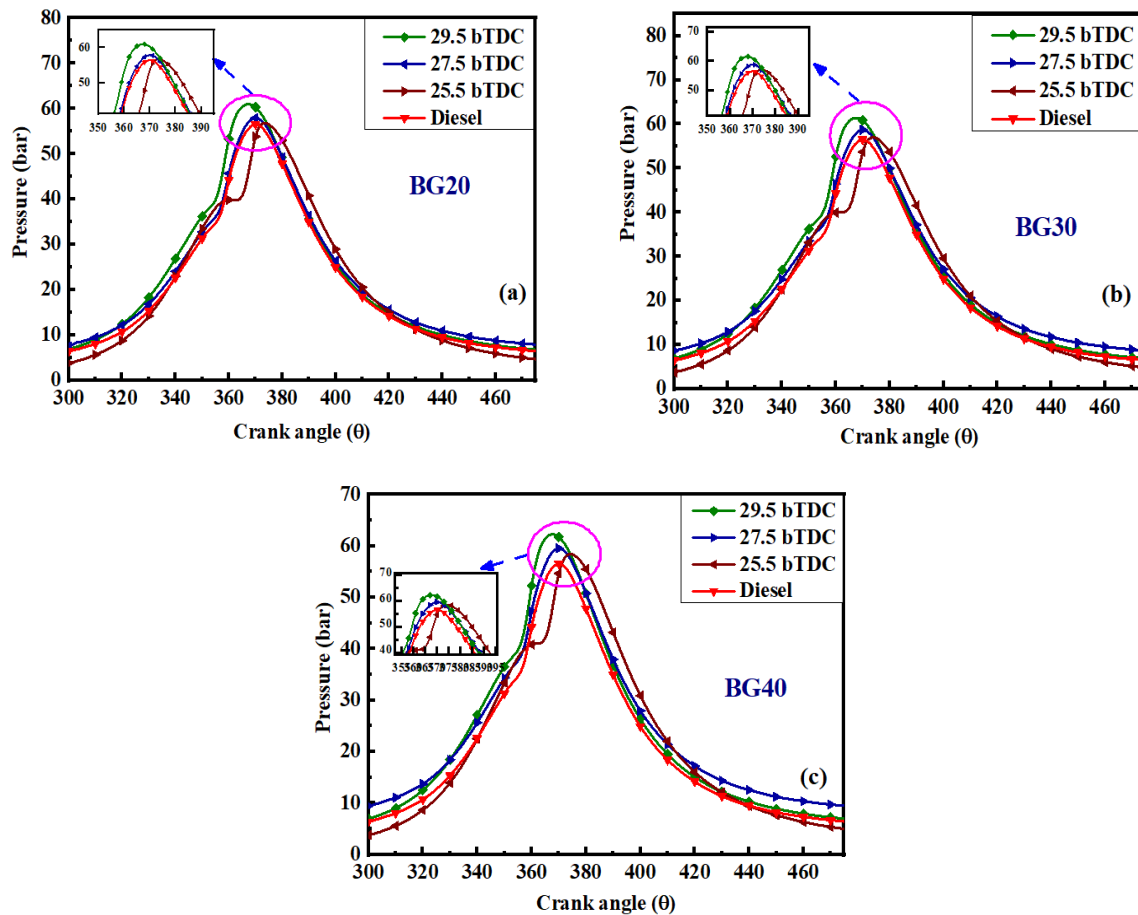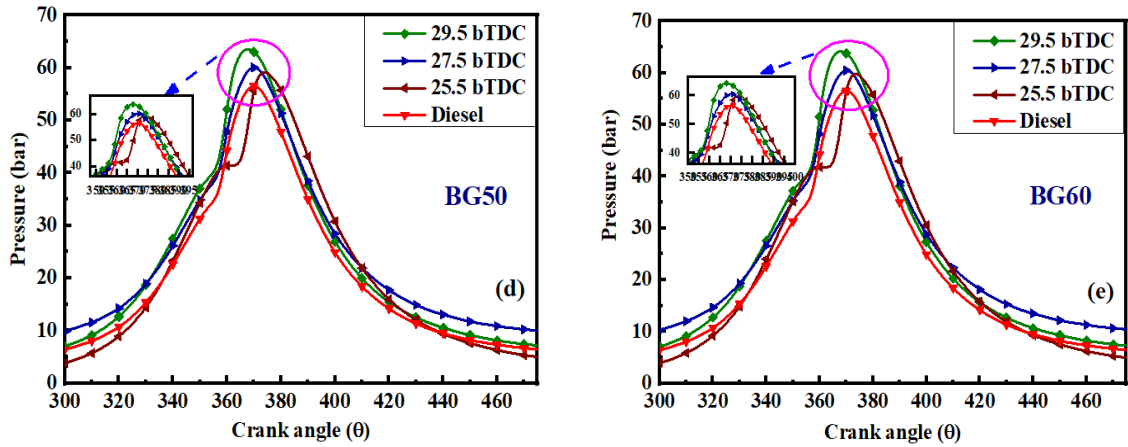
Figure 5.17 (a-e): Influence of injection timings on peak cylinder pressure under dual mode

5.6.2 Net Heat Release Rate (NHRR)

The net heat release rate for the diesel and dual-mode is described in Figure 5.18 (a-e) for the three injection timings operated at full load condition. The concept of NHRR is a difficult process as it includes the combustion of two different fuels having different properties. The NHRR essentially depends on the quality of the inducted air-biogas fuel mixture along with the diesel, also parameters such as energy density, mass flow rate of both the diesel and biogas fuel which depicts the intensity of heat release rate. In dual-mode, HRR is formed due to the three levels of combustion process namely combustion of diesel fuel, combustion of biogas, and the pre-ignition at the consequent flame propagation (Barik and Murugan 2016, Bedoya et al. 2009).

As observed from Figure 5.18 (a-e), the NHRR is maximum for dual-mode than diesel fuel such that the rate of heat release occurring at the premixed combustion phase is influenced by the rate of combustion at the starting stage, formation of the mixture, and ID. In general, dual-mode exhibited a higher rate of heat which is caused because of the gathering of fuel at a higher rate during the elongated ID phase. On the other hand, at the combustion zone of diesel fuel, the flammability increased due to the combined impact of diesel and biogas fuel (Verma et al. 2017, Jagadish and Gumtapure 2019). Moreover, due to the induction of biogas, there is a delay in the appearance of NHRR in the case of dual-

107

mode which is because of CO_2 presence and its higher specific heat. As the injection timing is advanced in the case of dual-mode, the NHRR appears at the early stage which provides more platform for full spray and quantity of the fuel mixture. Because of more time available, the combustion initiates at the earliest burning more amount of fuel and energy is released at the higher rate (Barik and Murugan 2016). Maximum NHRR is observed for BG60 with 33.5 J/°CA and shows an increment in NHRR compared to diesel by 29.10% at advance injection timing operated under full load. Other biogas proportions BG20, BG30, BG40, and BG50 showed NHRR of 27.35 J/°CA, 28.07 J/°CA, 29.04 J/°CA, and 30.91 J/°CA respectively.
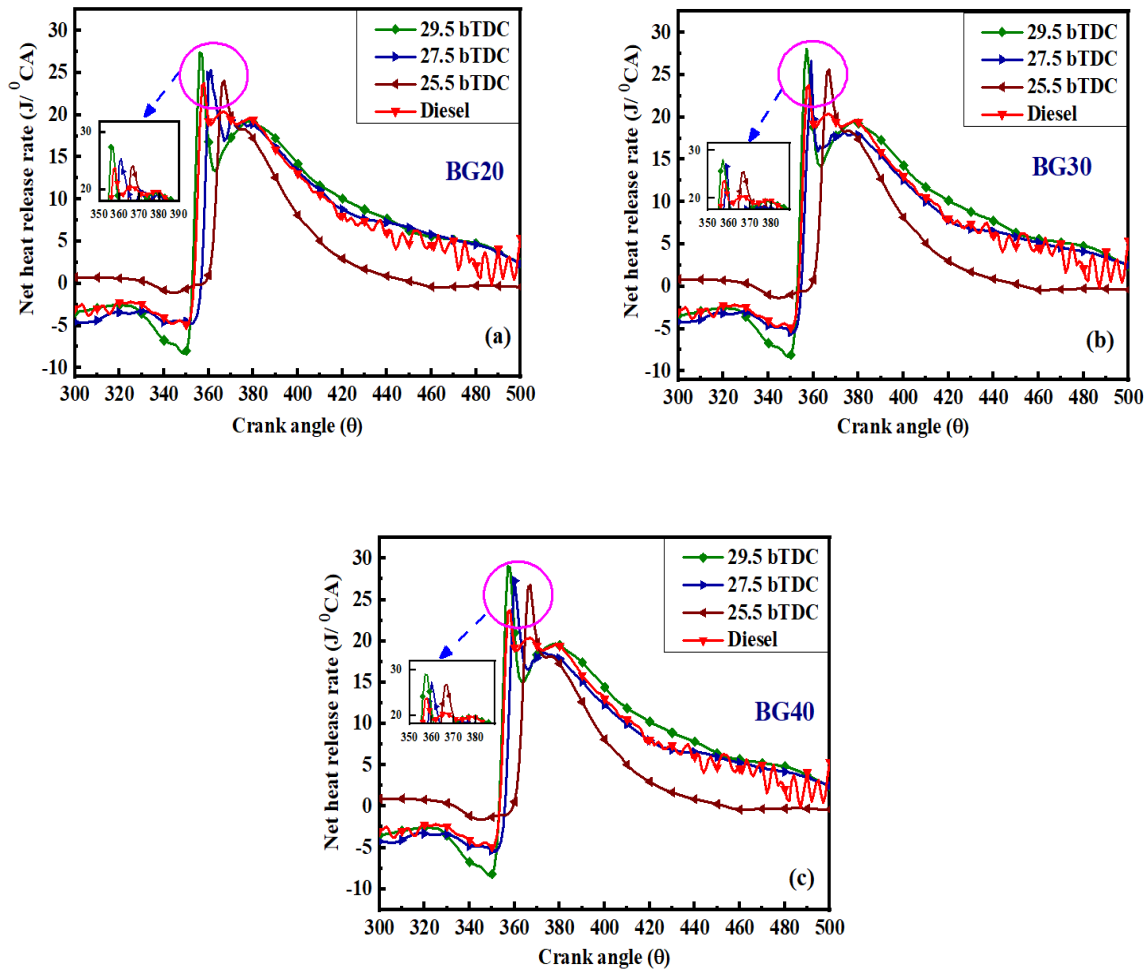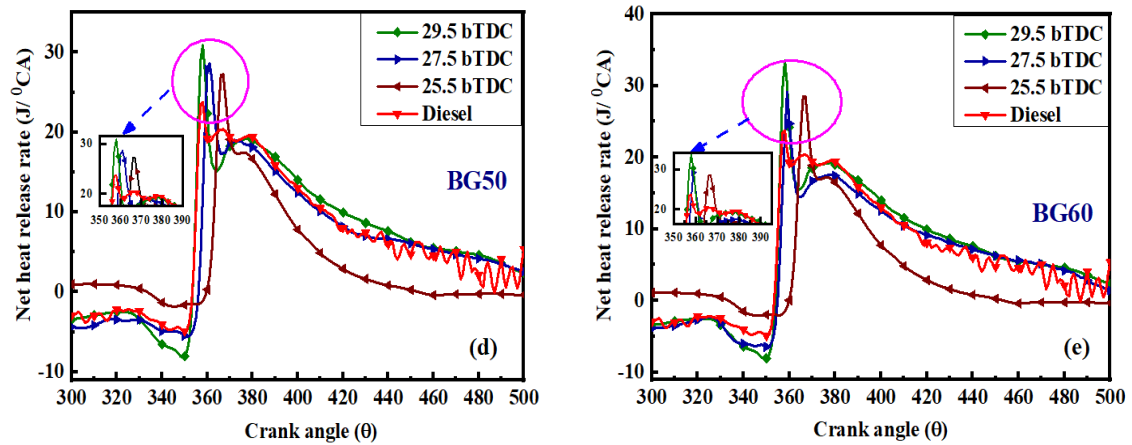
Figure 5.18 (a-e): Influence of injection timings on NHRR under dual mode

5.7 Emission Characteristics

5.7.1 Carbon Monoxide (CO)

Variations in carbon monoxide for diesel and dual-fuel mode operated for the defined injection timings as well as loads are represented in Figure 5.19 (a-e). Among the diesel and dual fuels, CO emission was found to be higher for dual fuels due to the partial combustion, lower intake temperature of the air-gas mixture, higher equivalence ratio, and most important reason is the appropriate time available for complete combustion to take place. On the other hand, the existence of 11.89% CO_2 in biogas causes incomplete combustion by diluting the air-biogas mixture (Barik and Murgan 2014). However, the flame generated from the combustion of diesel fuel is generally retained in the flame zone until the minimum value of self-ignition is attained by the biogas-air mixture causing incomplete combustion.

In the case of injection timings, as observed from Figure 5.19 (a-e), the dual fuel mode showed a decrement in CO emissions as the injection timing is advanced towards 29.5° bTDC, which is due to the maximum temperature attained inside the combustion chamber and improvement in the oxidation reaction taking place between the gas molecules (Verma et al. 2017). Whereas, retard injection timing showed higher CO emission as it underwent poor combustion process due to less availability of oxygen and

less time for complete combustion to take place. Among the three injection timings, advance injection timing showed lower CO emission as compared to actual and retard injection timing for dual-mode operation (Barik and Murugan 2016, Bora et al. 2014). As observed from Figure 5.19 (a-e), BG20 showed lower CO emissions and BG60 showed higher CO emissions for three injection timings. BG60 showed CO emission higher by 20% and 11.76% at $3/4^{th}$, full load than diesel mode. Whereas, BG20 emitted lower CO emissions by 2.56%, 5.26% at $3/4^{th}$ & full load as compared to diesel respectively.
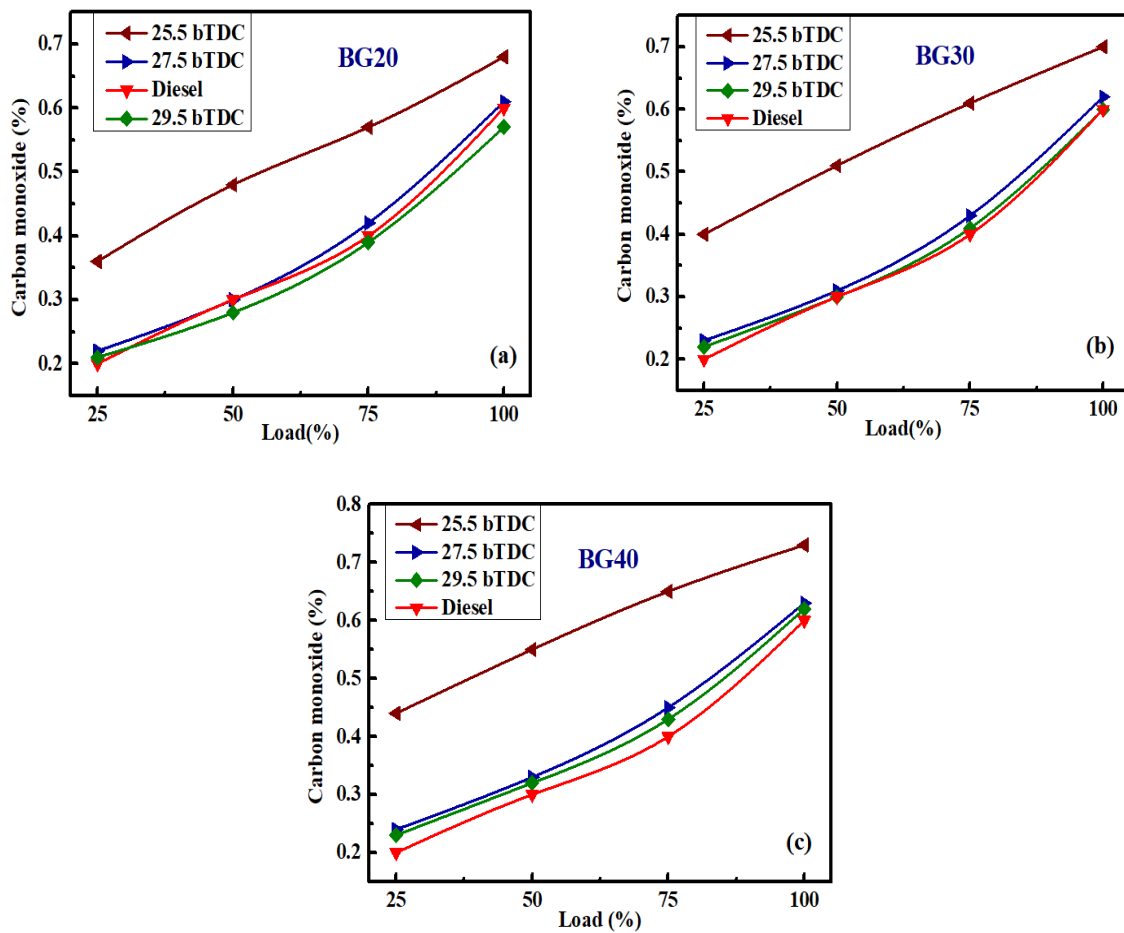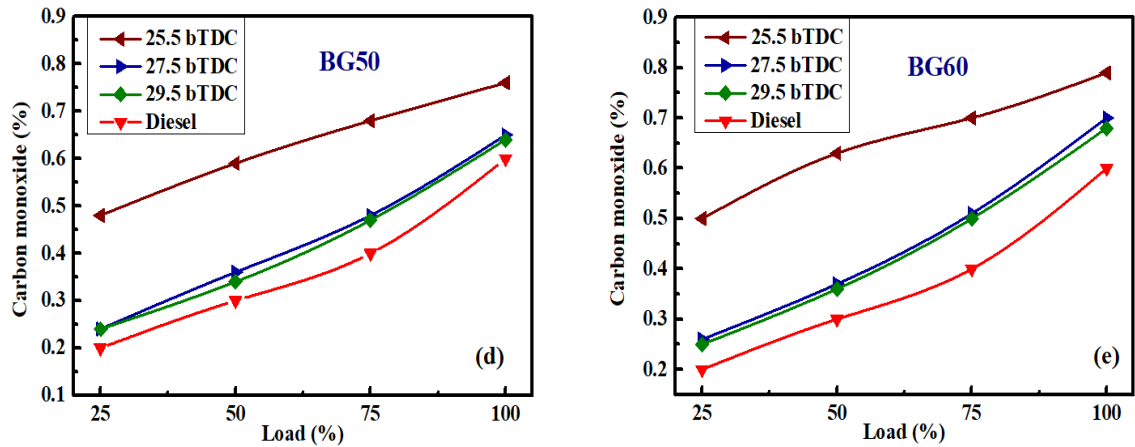
Figure 5.19 (a-e): Influence of injection timings on CO emissions under dual mode

5.7.2 Unburnt Hydrocarbons (UBHC)

Generally, the UBHC is formed as a result of the incomplete combustion of intake air-fuel mixture due to the lack of oxygen concentration, flame quenching, impingement to the cylinder walls, excess mixing of the fuel mixture ahead of the flammability limits. During the dual-mode condition, the trend of UBHC emission keeps on increasing because the biogas is inducted at the intake manifold. Less concentration of fresh air is created inside the cylinder and the biogas possesses low flame propagation (Ambarita 2017). Also, due to the presence of CO_2 in the biogas, the combustion appears to be with lean oxygen concentration which creates higher UBHC emissions. Eventually, few quantities of the air-biogas mixture remain unburned across the fissures which takes place at the compression stroke is also considered to be one of the reasons for the increase in emissions (Khayum et al. 2020).

As the biogas proportions are increased, the accumulation of lesser diesel does not withstand the flame propagation generated during the combustion of dual-fuel and will be concealed at the early stage. The inefficient mixing of diesel and biogas-air fuel will also add up in increasing the UBHC emissions. Various researchers also found the significant reason for the increase in UBHC emission for dual fuel mode is the prolonged ID and excess mixing of air-biogas along with the combusted residues (Verma et al. 2017, Duc and Wattanavichien 2007). The UBHC emissions for the diesel and various biogas

proportions at different loads and injection timing are illustrated in Figure 5.20 (a-e). Under varying load conditions, the dual-fuel mode emitted higher UBHC emissions as compared to the diesel mode which is caused because of biogas intake by dual-mode as a result volumetric efficiency reduces causing incomplete combustion. Lower UBHC emissions were observed at 29.5° bTDC compared to actual and retard injection timings. This development is because of the early beginning of combustion causing the in-cylinder temperature to increase such that complete combustion of dual-mode will take place. (Barik and Murugan 2016) Also, the smooth operation of the engine occurs as a result of higher temperature at the early stage of the combustion (Khayum et al. 2020). At 3/4th and full load, higher UBHC emissions were observed for BG60 compared to diesel by 22.03% and 13.43% at 29.5° bTDC respectively. BG20 emitted lower UBHC emission than diesel by 5.17% at full load and advanced injection timing.
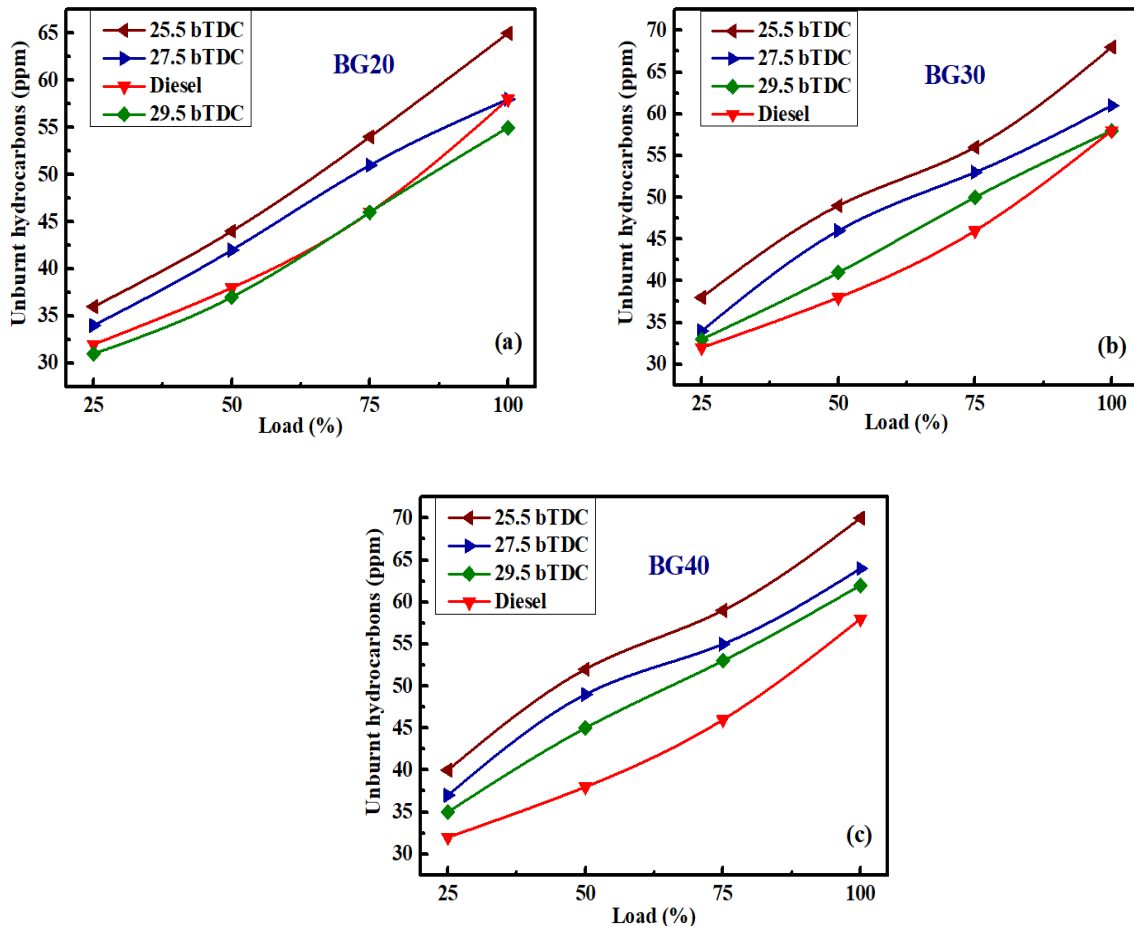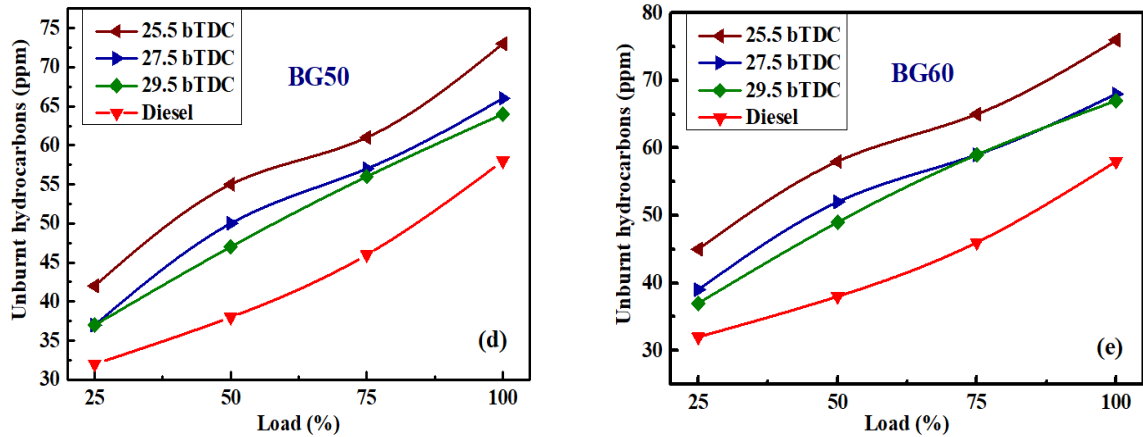
Figure 5.20 (a-e): Influence of injection timings on UBHC emissions under dual mode

5.7.3 Nitrogen Oxide (NOₓ)

The influence of injection timings on NO_x emissions emitted from the diesel engine operated in diesel and dual-mode is shown in Figure 5.21 (a-e). In general, the NO_x formation is analyzed from zeldovich mechanism which indicates factors such as the high temperature of the combustion chamber, presence of adequate air concentration, retention time and nitrogen molecules are responsible for NO_x formation (Jagadish and Gumtapure 2020). Additionally, the NO_x formation depends on the operating factors of the engine such as compression ratio, injection timing, and injection pressure as well as properties such as viscosity, cetane number, density, etc (Khayum et al. 2020). Eventually, in the dual-mode operation, a significant reduction in NO_x emission than diesel mode is observed because as the biogas is inducted at the intake manifold the volumetric efficiency decreases as a result of lack of oxygen concentration. However, due to the higher equivalence ratio, a trend of increase in NO_x emission is observed as the load is increased in the case of both diesel and dual-mode. On the other hand, the maximum cylinder temperature is observed to be decreased because biogas consists of CO_2 which has higher molar specific heat and acts as diluents. As a result, the NO_x emission decreases (Verma et al. 2017, Lata and Misra 2011). In the case of the three injection timings, retard injection timing of 25.5° bTDC showed less NO_x emission compared to diesel mode. Increase in pressure and temperature is observed in the

113

combustion chamber operated at advance injection timing for different proportions of biogas. This development is due to the early injection of the diesel fuel, such that more time is available for homogeneous mixing with the biogas-air mixture and complete combustion to take place (Barik and Murugan 2016, Hyun and Sik 2011).

The retard injection timing of 25.5° bTDC with BG60 emitted lower NO_x emissions than diesel at actual injection timings by 52.05% and 45.02% at $3/4^{th}$ and full load respectively. Whereas, BG20 showed higher emissions among other biogas proportions at 25.5° bTDC but showed lower NO_x emissions than diesel by 23.46% at full load. Even though advance injection timing showed higher emissions than other injection timings, less NO_x emission than diesel at actual timing was observed by 39.86% and 27.83% at $3/4^{th}$ and full load respectively.
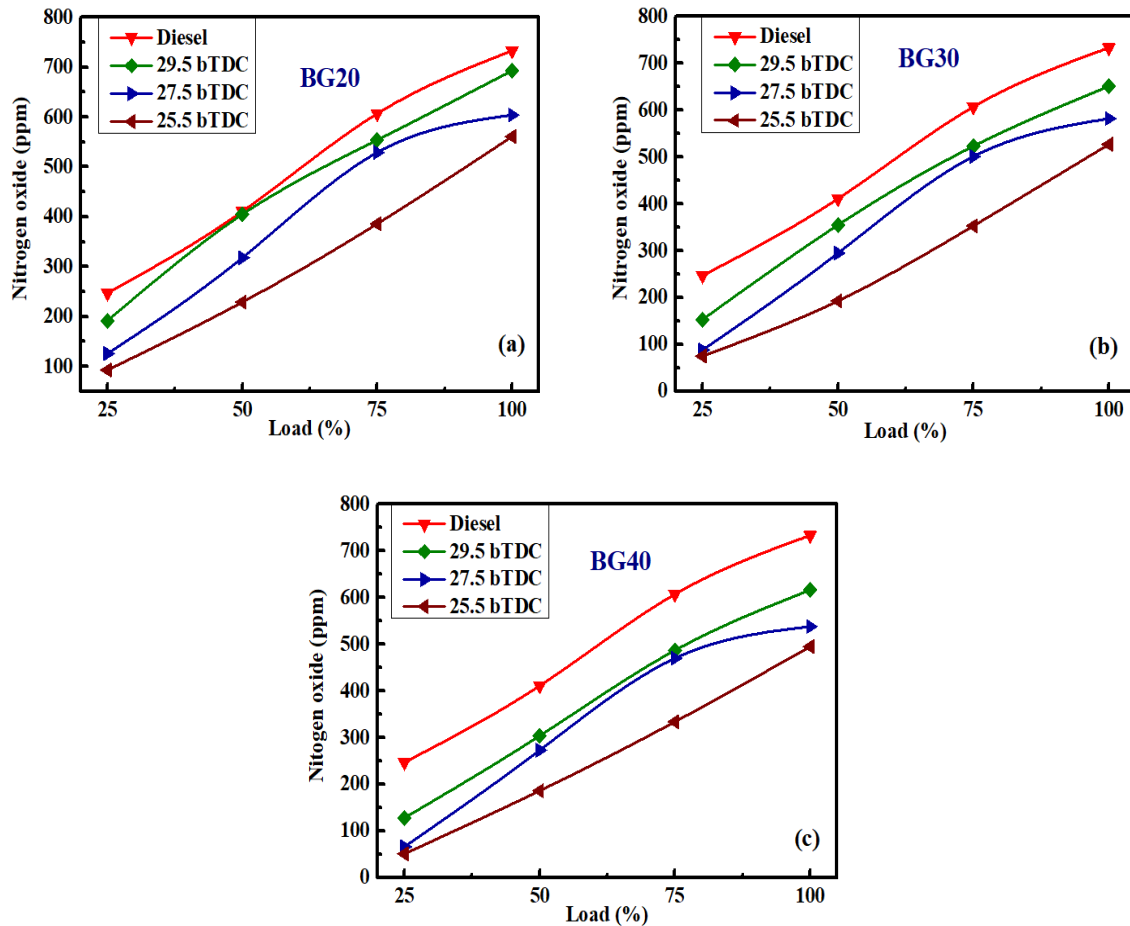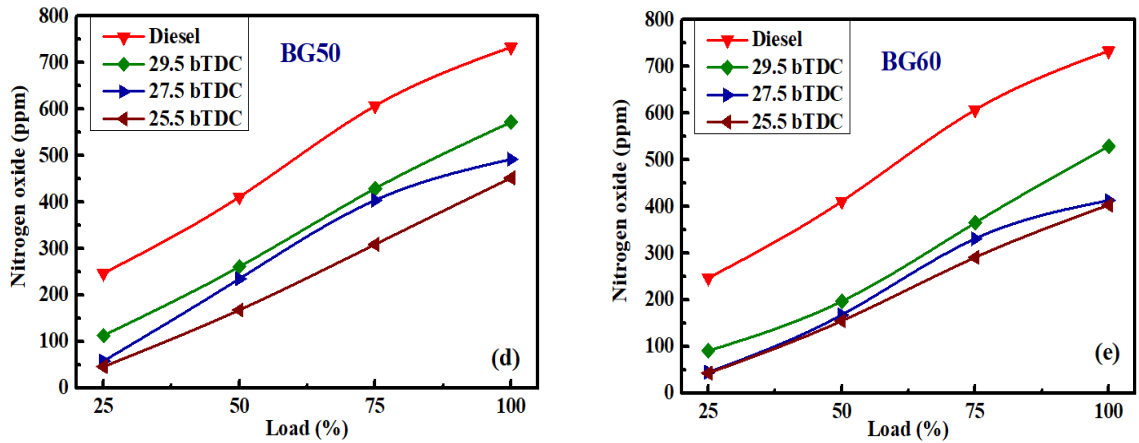
Figure 5.21 (a-e): Influence of injection timings on NO_x emissions under dual mode

5.7.4 Smoke Opacity (SO)

Variations of smoke opacity or sootness for diesel and dual-fuel mode for the three injection timings operated at various loads are depicted in Figure 5.22 (a-e). The engine operated with biogas has discrete advantage over diesel mode with lower emission of the sootness which directly depends on the fuel-rich region occurring at the diffusion stage as a result of incomplete combustion and on the fuel consumption (Khayum et al. 2020). As it is well known, diesel consists of higher aromatic compounds which are responsible for higher SO emissions. These kinds of compounds are absent in the biogas instead it contains higher methane composition and has less affinity towards soot formation (Verma et al. 2017, Wei and Gang 2016). The plots indicate that, as the load is increased the SO emission increases in the case of dual fuel mode for all the biogas proportions but lower than diesel.

The reason behind this development is due to the increase in ID, such that the higher oxidation of soot particles formed is suppressed by the presence of CO_2 in the biogas as a result the temperature of the flame front decreases. The diesel mode operated at 27.5° bTDC showed higher soot emissions at all loads and other injection timings compared to dual-mode operation. Moreover, lower soot emissions were observed for the IT 29.5° bTDC compared to diesel and other injection timings which is caused due to the superior combustion rate, more time available for oxidation of soot particles inside the

cylinder (Barik and Murugan 2016, Tippayawong et al. 2007). However, the accumulation of additional fuel inside the cylinder facilitates proper mixing of the air-biogas mixture and thereby increases the reaction rate to enrich the oxidation process leading to the formation of lower soot emissions (Khayum et al. 2020). BG60 showed lower SO emission compared to diesel by 45.64% and 41.34% respectively at 3/4th and full load with 29.5° bTDC injection timing. On other hand, BG20 showed higher SO emissions among other biogas proportions but less than diesel by 20.94% & 18.62% respectively at 3/4th and full load.
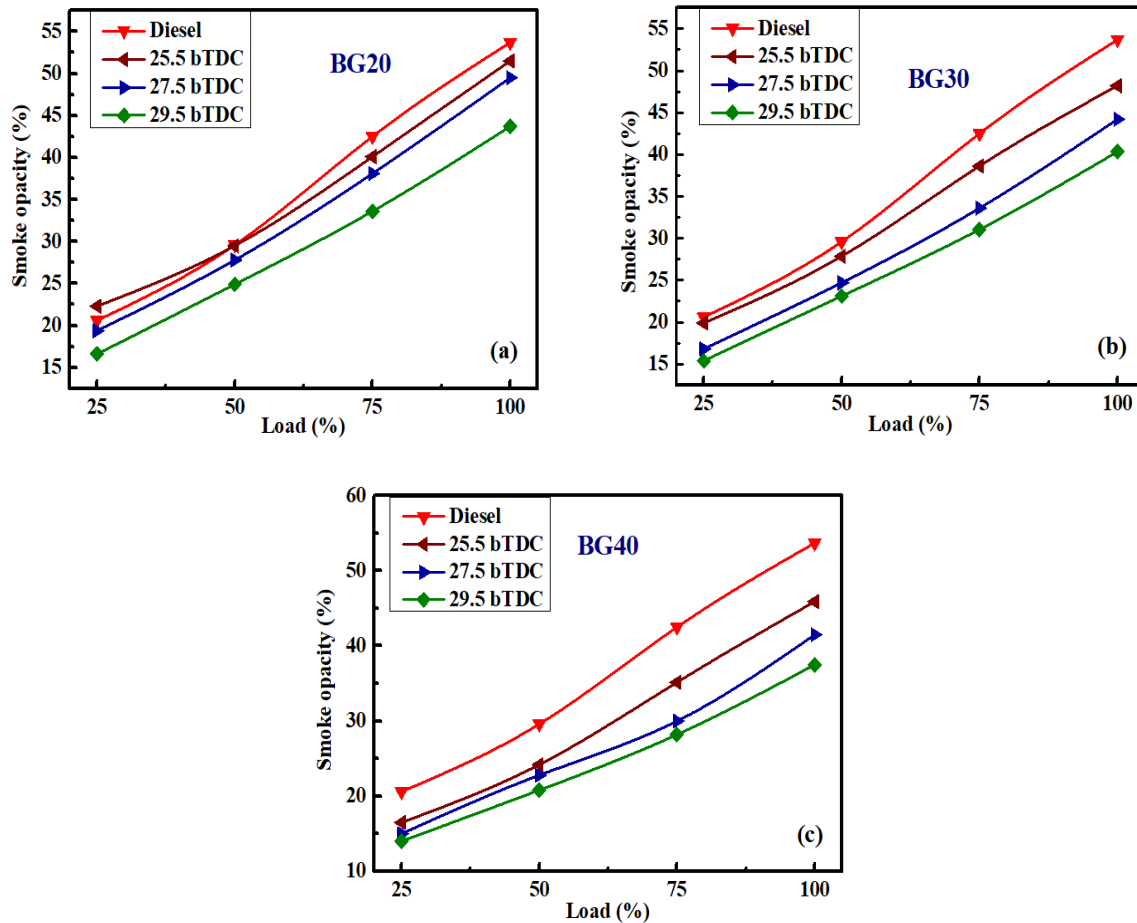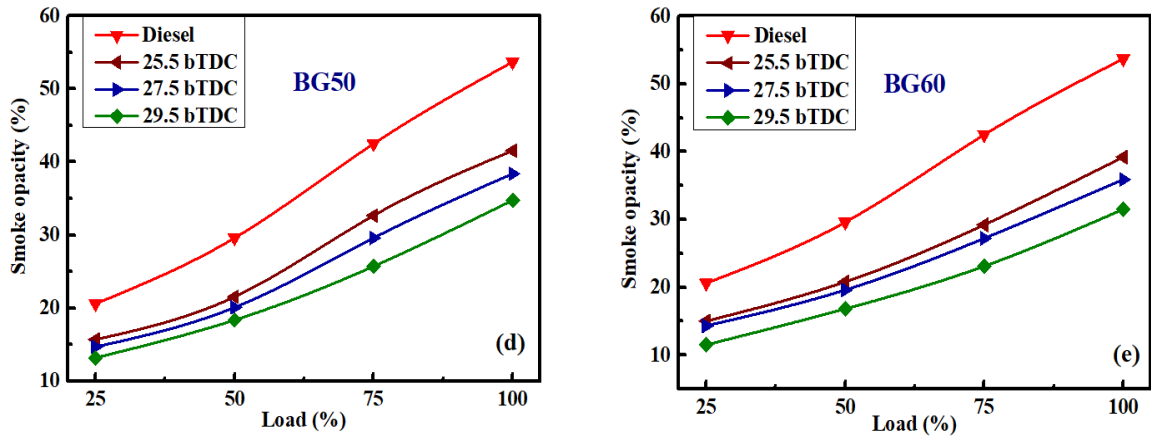
Figure: 5.22 (a-e): Influence of injection timings on sootness under dual mode

5.8 Oxygen Enrichment Mechanism

In the previous section both the injection timing and biogas proportion are optimized based upon the experimental results and to enhance the properties of the engine using the optimized biogas (BG50), the oxygen enrichment method is implemented and studied under the current section.

5.8.1 Brake Thermal Efficiency (BTE)

Figure 5.23 depicts the variation of brake thermal efficiency against load for diesel, optimized biogas (BG50), and with different levels of oxygen concentration (21%-27%). Maximum BTE is observed for diesel fuel compared to BG50 and oxygen concentration at varying loads. The least BTE was observed for BG50 without the oxygen enrichment, such that as the oxygen enrichment is inducted into the intake manifold from 21% to 27% with an increment of 2%, the BTE gradually increased as seen in Figure 5.23.

This improvement in the engine efficiency is attributed to the betterment of partial oxidation reactions causing an advance in flame propagation velocities of the fuel mixture. Along with these two factors, the reduction in ID of the diesel fuel contributes to an increase in thermal efficiency for optimized biogas (BG50) along with the oxygen enrichment (Cadavid et al. 2012, Jagadish and Gumtapure 2019). However, a substantial

117

improvement is developed in the engine efficiency due to the increment in the ratio of specific heats of the mixture formed. As a result, the thermal energy of the mixture is converted into the effective work output (Baskar and Senthilkumar 2016, Jagadish and Gumtapure 2020). Predominantly, the combustion of the gaseous mixture is improved because of the oxygen enrichment such that improved fuel economy, improvement in the power of the engine, and enhanced BTE are observed owing to the stability in the combustion reaction. As the load is increased, more quantity of biogas and air-fuel is inducted into the engine cylinder thus the strength of the mixture improves. This development causes stability in the flame consequently no impact is observed in the fuel economy and the betterment of the engine efficiency is achieved (Abdelaal et al. 2013, Gómez Montoya et al. 2018, Hotta et al. 2019, Banapurmath and Tewari 2009, Lee et al. 2013). Maximum BTE was achieved at 27% oxygen concentration which is higher by 15.28% and 18.37% than BG50 without oxygen enrichment at 3/4th and full load but shows lower BTE by 7.57% and 5.36% than diesel at 3/4th and full load respectively.
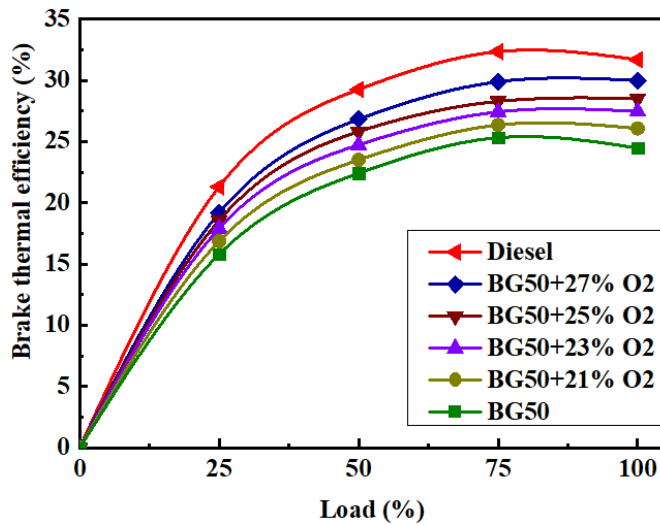
Figure 5.23: Variation of BTE under the oxygen enrichment technique

5.8.2 Brake Specific Energy Consumption (BSEC)

BSEC depicts the ability of the engine to convert the chemical energy of the fuel into heat energy during the combustion to generate adequate brake power. In this research

work, two types of fuels are used namely Diesel and Biogas. These test fuels possess different lower heating values and densities such that it will be inappropriate to use BSFC (Brake specific fuel consumption) and hence BSEC is used as it provides the clear exploration of how well the fuel energy is utilized and converted into the engine power at various working conditions. The experimental result as depicted in Figure 5.24 indicates that as the oxygen concentration is increased gradual reduction in BSEC is observed as a result of better energy conversion and utilization of the fuel. This development is due to the induction of oxygen enrichment which causes a faster reaction rate, increases the laminar flame propagation and accelerates the burning rate of the gas mixture.

After the enlarged combustion takes place, the larger section of gaseous fuel is incorporated during the oxidation process because of a boost in the reaction activity which promotes reduction in BSEC gradually. On the other hand, due to the oxygen induction, the ID period decreases, such that the heat generated from the combustion of the fuel occurs at the end of the compression stroke and the start of the power stroke. This indicates the maximum portion of the fuel energy getting converted into the effective work output (Abdelaal et al. 2013, Deheri et al. 2020).

Optimized biogas (BG50) showed higher BSEC as compared to the BG50 along with oxygen enrichment. BG50 with 27% oxygen concentration showed lower BSEC by 25.62% and 25.83% at 3/4th and full load respectively. However, an insignificant increase in BSEC was observed for 27% O_2 as compared to diesel fuel by 9.09% at 3/4th load but no difference was observed at full load.
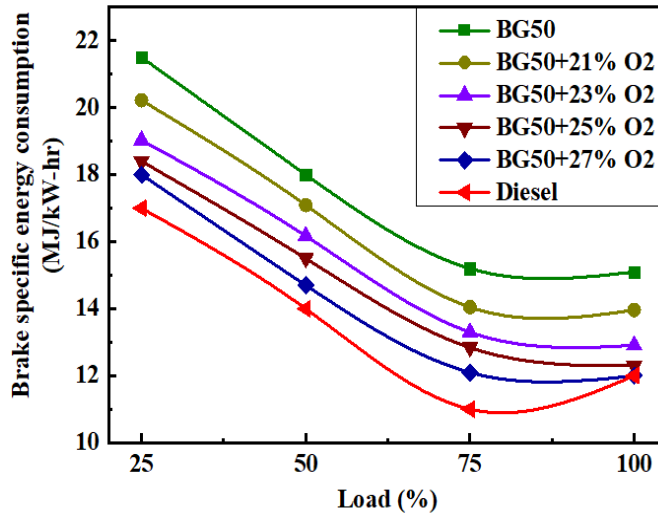
Figure 5.24: Variation of BSEC under the oxygen enrichment technique

5.9 Combustion Characteristics

5.9.1 Cylinder Pressure (P-θ)

The variation in-cylinder pressure for optimized biogas (BG50) resultant to the full load for different oxygen concentrations operated for 100 cycles is shown in Figure 5.25. Maximum cylinder pressure was found to be for 27% O_2, however, BG50 without O_2 concentration showed lower pressure and lies at the last level but above the diesel fuel. It is evident that as the oxygen enrichment is increased from a lower concentration of 21% to a higher concentration of 27% with an increment of 2% the maximum cylinder pressure gradually increased at full load. This development owes to the improvement in the reaction rate of both BG50 and O_2 fuels which take place at the premixed combustion phase and apparently due to the reduction in ID (Cadavid et al. 2012, Baskar and Senthilkumar 2016).

Moreover, the flame region gets strengthened during the induction of oxygen enrichment as a result of improved combustion is attained such that the heat transfer gets decreased and temperature inside the cylinder is improved. Besides, the lack of local oxygen level available in the diesel fuel spray substantially decreases due to the application of oxygen enrichment which improves the stability of the combustion process

120

by mitigating the deficiencies inter associated with the flame zone. As observed from Figure 5.25, the peak cylinder pressure appears to be very much closer to the TDC during the premature phases of the power stroke which is attributed to the shorter ID period as a result the entire combustion process gets forwarded. Thus, it is evident that an increase in the oxygen enrichment enhances the cylinder pressure due to the improvement in-cylinder temperature and decrease in the ID period (Abdelaal et al. 2013, Maizonnasse et al. 2013). Maximum cylinder pressure was achieved at 27% O_2 of 69.53 bar compared to other O_2 levels and BG50 such that 27% O_2 concentration showed higher peak cylinder pressure by 27.16% and when compared with diesel the cylinder pressure is 18.74% higher at full load respectively.
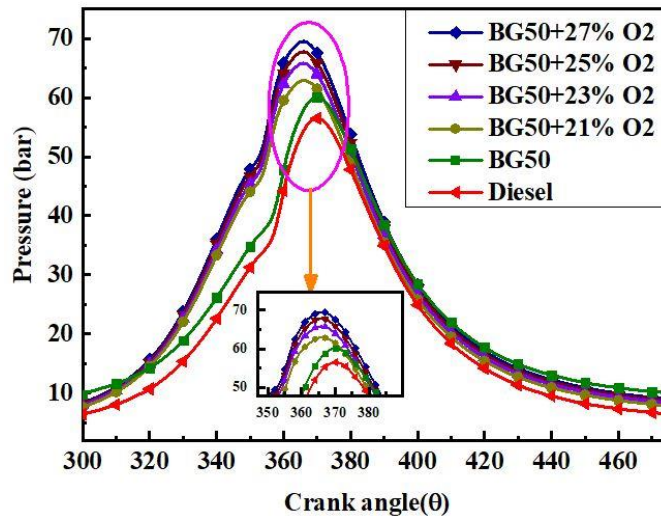
Figure 5.25: Variation of cylinder pressure under the oxygen enrichment technique

5.9.2 Net Heat Release Rate (NHRR)

The net heat release rate v/s crank angle for diesel, optimized biogas (BG50), and BG50 with oxygen enrichment at full load are represented in Figure 5.26. The trend of the graph indicates as the oxygen concentration is increased the NHRR increases gradually due to the reduction in the ID period and the combustion phenomenon initiated at the earlier stage causes a drastic rise in the HRR curve (Abdelaal et al. 2013). This is caused due to the reduction in the ID and decreases in the premixed combustion stage as

121

the oxygen induction is increased stipulating more energy liberated and a higher combustion rate (Cadavid et al. 2012, Poola and Sekar 2003). The accumulation of the diesel fuel in the combustion chamber gets reduced because of the decrease in the ID period. The very first peak NHRR curve is generated due to the faster auto-ignition of the gathered diesel fuel within a certain crank angle. A maximum heat release rate of 41 J/°CA was observed for BG50 with 27% O_2 concentration at full load as compared to diesel as well as other concentrations of oxygen. As compared to BG50 without oxygen levels, the BG50 at 27% O_2 level showed an improvement of 30.22% rise in heat release rate. As compared with diesel, BG50 with 27% O_2 showed significant improvement by 42.07% at full load respectively.
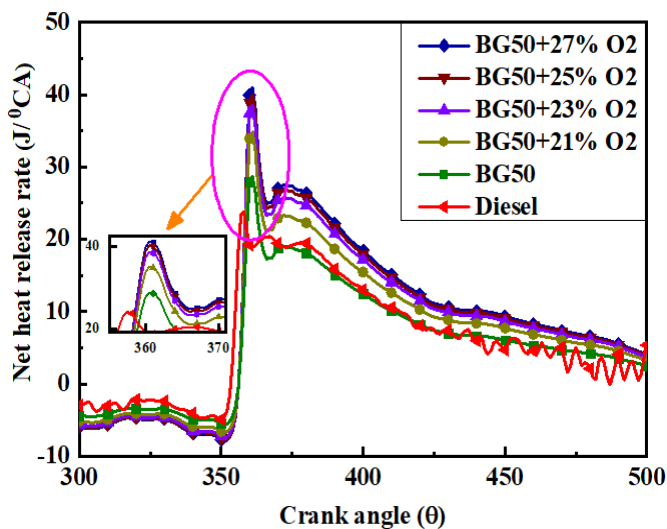
Figure 5.26: Variation of NHRR under the oxygen enrichment technique

5.9.3 Ignition Delay (ID)

The variation of ID period for the test fuels along with the different levels of oxygen concentration at all loads is shown in Figure 5.27. The ID was found to be lower as the oxygen levels were enriched promoting efficient combustion due to the more availability of the oxygen and this creates the rapid formation of pre-ignition effects of the diesel fuel. The combustion process gets advances with the induction of even a small amount of the oxygen concentration causing improvement in performance as well as

reduction in ID period (Cadavid et al. 2012, Bedoya et al. 2009). The oxygen concentration of 27% showed lower ID as compared to optimized biogas and remaining O_2 levels which is 12.58% and 14.28% lower than BG50 at $3/4^{th}$ and full load. However, the ID for BG50 with 27% O_2 showed 2.27% and 3.17% higher compared to diesel at $3/4^{th}$ and full load.
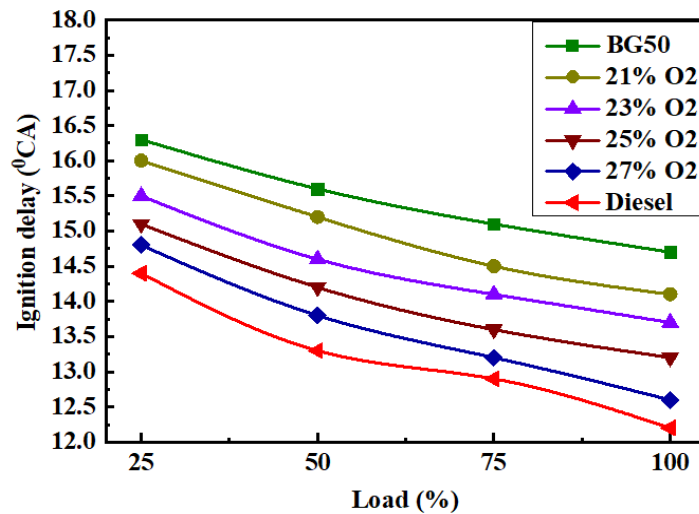
Figure 5.27: Variation of ID under the oxygen enrichment technique

5.10 Emission Characteristics

5.10.1 Carbon Monoxide (CO)

Generally, in the dual fuel mode, the CO is formed due to the induction of the biogas causing less availability of the oxygen level for complete combustion (Baskar and Senthilkumar 2016) and the formation of CO depends on the temperature of the mixture formed as well as the availability of unburned gases (Abdelaal et al. 2013). Besides, under the leaner air-fuel condition the exhaust elements at elevated temperature further contribute to higher CO emission. However, a drastic reduction in CO emission was developed after the induction of oxygen into the cylinder which promotes enhanced combustion, and an increase in the trend is observed as the load is increased. With oxygen enrichment being implemented pre-ignition reactions of the biogas are achieved at a faster rate as a result of enhanced air-fuel ratio. Also, the amount of the fuel mixture

ahead of the limit of lean flammability is considerably reduced which is unable to auto-ignite or uphold the higher reaction rate of the flame front. This development plays a vital role in reducing CO emissions and increasing combustion efficiency. Figure 5.28 depicts the nature of the curve to be increasing in trend as the load increases for all the cases. BG50 without oxygen enrichment emitted maximum CO emission as compared to the rest of the fuels at different loads (Baskar and Senthilkumar 2016). Whereas, BG50 with 27% O_2 emitted lower CO emission by 29.16% and 20% at 3/4th and full load as compared to BG50. On the other hand, BG50 with 27% O_2 showed lower CO emission than diesel by 17.64% and 15.38% at 3/4th and full load respectively.
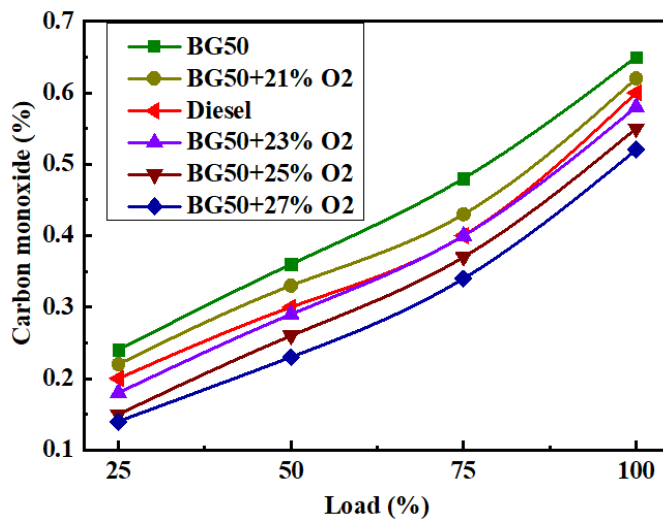
Figure 5.28: Variation of CO under the oxygen enrichment technique

5.10.2 Unburnt Hydrocarbons (UBHC)

During the dual-mode operation, the biogas is injected at larger quantity into the combustion chamber with less oxygen concentration. Due to incomplete combustion, lower flame propagation of the biogas, crevice volumes, layers of the oil accumulation, overlapping of inlet and exhaust valves during scavenging causes the larger formation of the UBHC emission. However, a reduction in UBHC emission was observed after the induction of oxygen enrichment which provides more intake of oxygen inside the cylinder causing complete combustion. It also reduces the amount of fuel mixed beyond

the lean flammability limit that is not able to auto-ignite or sustain a fast reaction front (Verma et al. 2017, Duc and Wattanavichien 2007). On the other hand, the quenching distance of the mixture was decreased as a result flame temperature decreased due to the enhancement in oxygen level. This significant improvement in the flame propagation causes the flame to propagate in the vicinity of the cylinder wall and causes a reduction in UBHC emissions (Abdelaal et al. 2013). Improvement in the flame propagation is attributed to the betterment in the combustion process, enhancement in the oxidation of crevice, elevation in the in-cylinder temperature, and deposition of the hydrocarbon layer. Also, ID contributes a significant role in improving the UBHC emission by avoiding unnecessary fuel impingement across the cylinder walls and eradicating the over-penetration of the diesel fuel (Abdelaal et al. 2013, Berlini et al. 2020). Figure 5.28 demonstrates the effect of O_2 concentration upon the UBHC emission for all the fuels and at different loads of the engine. Oxygen level with 27% showed lower UBHC emission compared to other remaining fuels at all the engine loads such that an improvement in UBHC emission by 31.57% and 27.27% at 3/4th and full load compared to BG50 was achieved. Whereas, BG50 with 27% O_2 is compared with diesel, UBHC emission reduced by 17.94% and 20.83% at 3/4th and full load respectively.

Figure 5.29: Variation of UBHC under the oxygen enrichment technique

5.10.3 Nitrogen Oxide (NO$_x$)

Systematic variation of NO$_x$ emission for diesel as well as BG50 along with different levels of oxygen enrichment operated for various engine loads is illustrated in Figure 5.30. It is evident from several studies that NO$_x$ formation involves two different mechanisms namely thermal NO$_x$ and prompt NO$_x$ (Jagadish and Gumtapure 2020). The thermal NO$_x$ formed is the most significant factor which occurs inside the combustion chamber at the post-flame gas region across the high-temperature zone as clearly explained by Zeldovich mechanism (Baskar and Senthilkumar 2016) with the following reactions:

$O + N_2 \leftrightarrow NO + N$,

$N + O_2 \leftrightarrow NO + O$,

$N + OH \leftrightarrow NO + H$
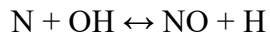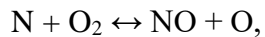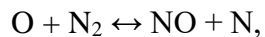
The rate of thermal NO$_x$ increases during the combustion process due to the presence of oxygen concentration and higher flame temperature. In short, the NO$_x$ is directly related to the induction of oxygen concentration inside the cylinder and exponentially related to the in-cylinder temperature. On the other hand, sufficient quantities of active radicals are formed in the fuel-rich region during the small residual time leading to the formation of prompt NO$_x$. This is portrayed by the Fenimore prompt mechanism and is not an important basis for NO$_x$ formation in the case of diesel engines. Generally, in dual-mode operation, the NO$_x$ emission trend decreases in nature due to the higher equivalence ratio, decrease in volumetric efficiency as well as due to the presence of CO$_2$ which possess higher specific heat and reduce the cyclic temperature by diluting the fuel mixture (Abdelaal et al. 2013, Lee et al. 2013).

As the oxygen enrichment is initiated, the NO$_x$ emission drastically increases compared to the increase in oxygen levels from 21% to 27% O$_2$ with an increment of 2% for all the engine loads. It is observed from Figure 5.30 that, the NO$_x$ intensity rises by three times the ambient air as the oxygen concentration reaches 27% which is a foremost

disadvantage about the oxygen enrichment process. A higher rate of thermal NO_x is formed throughout the combustion process as a result of higher oxygen concentration and post-flame temperatures such that the flame zone appears at a higher intensity. This development promotes a significant rise in the cylinder temperature. Consequently, thermal NO_x increases linearly due to oxygen induction. Similarly, prompt NO_x also increases as a formation of the higher quantity of active radicals and due to the occurrence of pre-ignition reactions (Baskar and Senthilkumar 2016). BG50 without oxygen enrichment showed the lowest NO_x emission among the remaining fuels for every operating load and is increasing in nature. However, BG50 inducted with 27% O_2 showed maximum NO_x emission of 1373 ppm at full load. Compared to diesel, optimized BG50 inducted with 27% O_2 emitted more NO_x emission by 47.03% and 46.61% at $3/4^{th}$ and full load. On the other hand, BG50 at 27% O_2 emitted higher NO_x emission compared to BG50 without oxygen enrichment by 64.74% and 64.16% at $3/4^{th}$ and full load respectively.
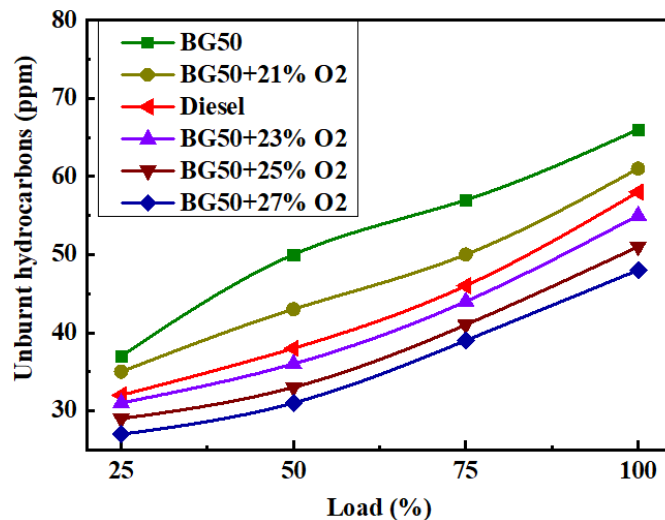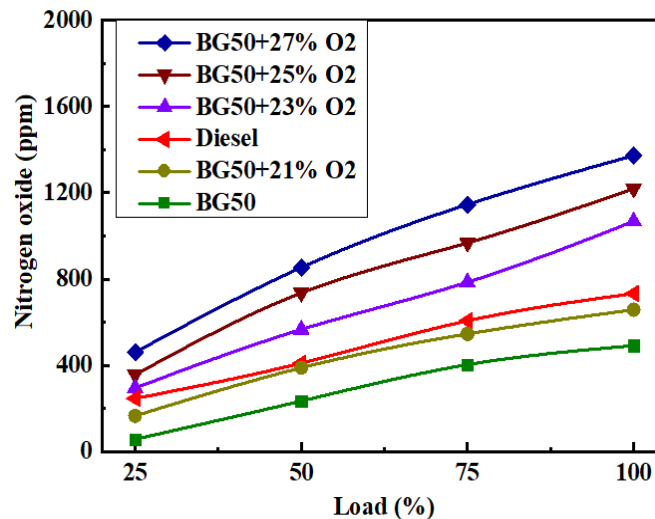

Figure 5.30: Variation of NO_x under the oxygen enrichment technique

5.10.4 Smoke Opacity (SO)

The diesel engine emits an enormous quantity of particulate matter measured in terms of smoke opacity or sootness which is caused due to the fractional combustion of

hydrocarbons (Madhankumar et al. 2020). However, the sootness is reduced with a larger difference as the diesel engine is operated in the dual-mode due to the less presence of high aromatic and carbon compounds. Also, the flame temperature inside the combustion chamber decreases due to the existence of CO_2 causing the rate of oxidation of soot particles to decrease (Jagadish and Gumtapure 2019, Verma et al. 2017). Conversely, the sootness was further improved on implementing the different levels of oxygen concentration for the optimized biogas inducted at the intake manifold. It is observed that sootness is drastically reduced at various load conditions signifying a lower rate of particulate matter which is a natural phenomenon due to the enhancement in the oxidation process due to the increment in the in-cylinder temperature and oxygen levels as observed in Figure 5.31. Complete combustion was developed even at the fuel-rich flame across the core of the diesel fuel as the induction of oxygen levels is increased. Conversely, the oxidation reaction is further improved for already created soot particles (Abdelaal et al. 2013). However, the inducted oxygen levels improve the residence period of soot particles and reduce the ID in an elevated temperature zone and contribute to complete and clean burning of the fuel (Madhankumar et al. 2020).

BG50 inducted with 27% O_2 concentration showed lower smoke opacity as compared to remaining fuels for different loads with the lowest emission of 20.1% and 26.8% at 3/4th and full load. As compared with BG50 without oxygen enhancement, the sootness was improved for BG50 at 27% O_2 by 47.26% and 43.28% at 3/4th and full load respectively. On the other hand, diesel showed maximum emission among other fuels and emitted sootness of 43% and 54% at 3/4th and full load.
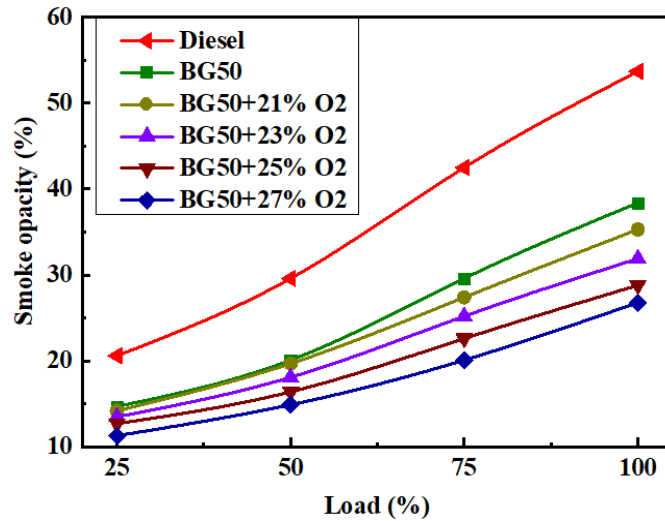
Figure 5.31: Variation of SO under the oxygen enrichment technique

5.11 Vaporized Water-Methanol Induction

Based upon the higher NO_x emissions emitted for the optimized biogas (BG50) with increment in oxygen levels as observed from the experimental results in the previous section, the study of vaporized water-methanol induction to bring down the NO_x emission intensity for BG50 with 25% O_2 as well as to enhance the performance of the dual engine is accomplished in the present section.

5.11.1 Brake Thermal Efficiency (BTE)

The engine efficiency or BTE variations for diesel, BG50 along with 25% O_2 and with different fractions of water-methanol combination in the form of vapor for every load are depicted in Figure 5.32. Major improvement in the efficiency is observed as the percentage of water-methanol increases to 30% and then drastically decreases as the fluid proportion is further increased. The reason to justify this development in the BTE is due to the increment in the enthalpy of the vaporized form, mixing process, and attainment of better atomization from the exchange of latent heat energy of the exhaust gas through the heat exchanger (Patnaik et al. 2016). In addition to this, the combustion process was enhanced due to the oxygen liberation from the vapor of methanol along with raise in the steam that occurred in the cylinder indicating fuel consumption to decrease causing the

129

BTE to increase. On the other hand, as the water-methanol flow rate increased beyond 20%, the volumetric efficiency decreases intensively causing more fuel consumption, a significant reduction in BTE was observed (Gonca and Sahin 2017). Slight improvement in BTE is achieved for 30% methanol vapor induction (MVI) specifically at 25% and 50% load, conversely as the load is increased further to 75% and full load BTE decreased. The reason for the development can be attributed to the combination of water-methanol which reduces the temperature and lower the calorific value of the charge and similar observations were attained by several researchers (Masimalai et al. 2018). Henceforth, the mass flow rate of the vaporized water-methanol is not increased further and is limited to 30%.

A maximum BTE of 31.32% was observed for BG50 at 25% O_2 with 20% MVI at full load. Significant improvement in terms of BTE is achieved for BG50 at 25% O_2 with 20% MVI but lower than compared to diesel by 4.42% and 1.14% at $3/4^{th}$ and full load. However, BG50 at 25% O_2 with 20% MVI showed an affirmative increase in BTE as compared to BG50 at 25% O_2 without vapor induction by 8.51% and 9% at $3/4^{th}$ and full load respectively. Whereas, BG50 showed improvement in BTE for 25% O_2 with 30% MVI at 25% and 50% load but decreased suddenly at 75% and full load. On the other hand, the efficiency of BG50 at 25% O_2 with 30% MVI increased by 7.73% and 8.15% compared to BG50 at 25% O_2 without vapor induction.
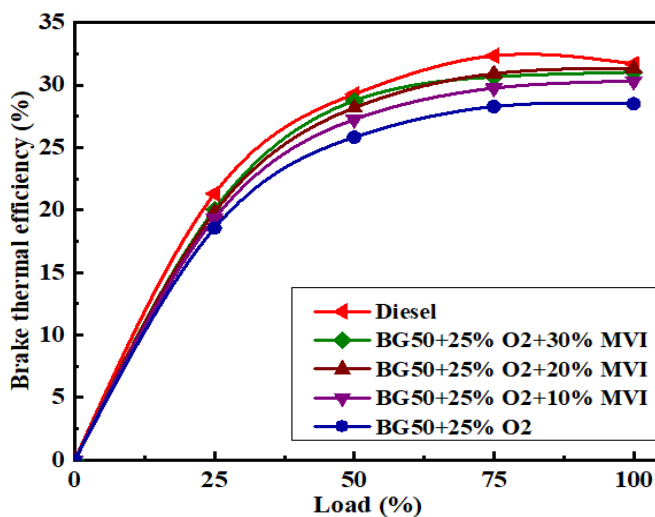
Figure 5.32: Variation of BTE under the influence of vapor induction

5.11.2 Brake Specific Energy Consumption (BSEC)

The fuel economy of the engine fuelled with BG50 with 25% O_2 & 20% vapor induction is determined by the means of BSEC and is indicated in Figure 5.33 for the different mass flow rates of vaporized water-methanol induction for various load conditions. It is evident from the nature of the graph that as the vapor ratio is increased the amount of energy consumed to generate engine power will drop down signifying less consumption of the fuel. This improvement is caused because inducting the vapor of the water-methanol combination directs to a smaller reaction rate of the combustion as a result of appropriate mixing of the fuel and enhanced atomization (Patnaik et al. 2016). Moreover, due to the existence of additional oxygen radicals in the water-methanol in the form of steam will advance the combustion process is also the reason for BSEC to decrease (Masimalai et al. 2018). BSEC for BG50 at 25% O_2 with 20% MVI is lower than the BG50 at 25% O_2 without vapor induction by 6.12% and 6.03% at 3/4th and full load. Whereas, compared to BG50 at 25% O_2 without vapor induction, BSEC was lower for BG50 at 25% O_2 with 30% MVI by 4.39% and 5.13% for 3/4th and full load conditions respectively.
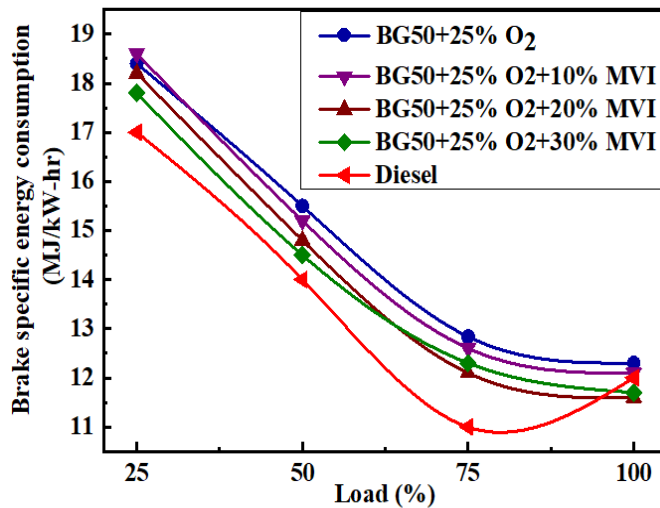
Figure 5.33: Variation of BSEC under the influence of vapor induction

5.12 Combustion Characteristics

5.12.1 Cylinder Pressure (P-Ө)

The in-cylinder pressure comparison for diesel, BG50 with oxygen enrichment as well as different ratios of methanol vapor induction system at full load is represented in Figure 5.34. As the vapor induction flow rate is increased from 10% to 30%, the cylinder pressure reduces considerably as compared to diesel and BG50 with oxygen enrichment. This major development is caused due to the reduction in the combustion temperature by the effect of the water-methanol combination (Gonca and Sahin 2017). Moreover, higher partial pressure of the oxygen and higher molar capacity of the vapor induction system as well as occurrence of maximum pressure away from TDC is also the reason for the decline in-cylinder pressure (Masimalai et al. 2018, Adnan et al. 2012). Maximum cylinder pressure is achieved for BG50 at 25% O_2 with 10% MVI with 62.02 bar and lower is for BG50 at 25% O_2 with 30% MVI with 54.3 bar which is lower than diesel at full load. BG50 at 25% O_2 without vapor induction showed higher in-cylinder pressure compared to diesel by 16.62%. BG50 at 25% O_2 with 10%, 20% MVI showed higher pressure by 8.9%, and 2.89% than diesel. However, BG50 at 25% O_2 with 30% MVI showed a decrease in pressure by 4.05% than diesel at full load. On the other hand, as compared to BG50 with 25% O_2, cylinder pressure decreased by 9.26%, 16.47%, and 24.79% for BG50 at 25% O_2 with 10%, 20%, and 30% MVI at full load respectively.
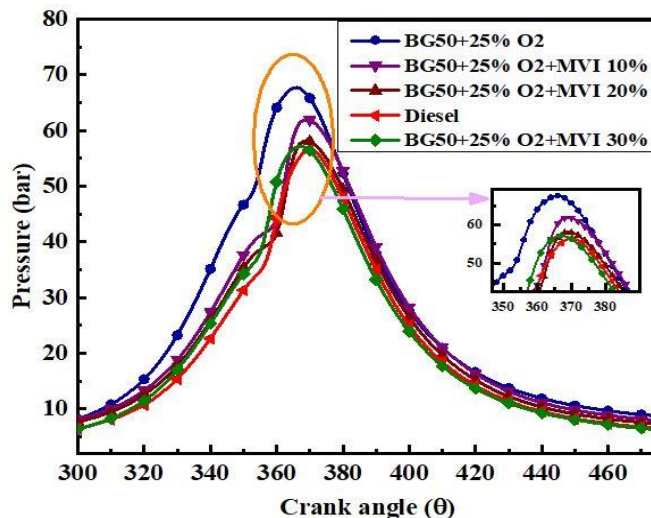
Figure 5.34: Variation of Cylinder pressure under the influence of vapor induction

5.12.2 Net Heat Release Rate (NHRR)

Figure 5.35 illustrates the net heat release rate for diesel, BG50 with 25% O_2 and different flow rates of methanol vapor induction operated at full load condition. From the observation of the nature of the graph, it indicates that before the initiation of ignition the heat release rate curve appears at the negative locality because of diesel and the vapor form of water-methanol combination causing furthermore to vaporize by absorbing the heat accumulated at the cylinder charge (Adnan et al. 2012). Within the vapor induction method, the combustion process completely depends on various factors such as the quality of the diesel spray, superior mixing nature of the oxygen-enriched biogas with vapor form of water-methanol combination inside the cylinder charge (Patnaik et al. 2016). Due to the vapor induction, the heat release rate decreased causing a cooling effect at the premixed combustion zone and restricting the transmission of turbulent flame to the diesel fuel region to the cylinder charge.

Overall, with this preliminary development in the premixed zone, the concentration of heat released during the combustion process is affected (Tesfa et al. 2012). At the constant engine speed of 1500 rpm and at full load condition the heat release rate decreases as the flow rate of vapor induction increases such that, BG50 at 25% O_2 with 10% vapor induction showed a maximum heat release rate of 34.16 J/°CA and is higher than diesel but lower than BG50 at 25% O_2 without vapor induction. Among vapor induction systems, the least heat release rate of 27.68 J/°CA was observed for BG50 at 25% O_2 with 30% MVI. Compared to diesel, BG50 at 25% O_2 with 10%, 20% & 30% MVI showed higher heat release rate by 30.47%, 24.82%, and 14.2% at full load. Whereas, compared to BG50 at 25% O_2, BG50 at 25% O_2 with 10%, 20% & 30% MVI the heat release rate was lower by 12.47%, 21.62%, and 38.8% at full load respectively.
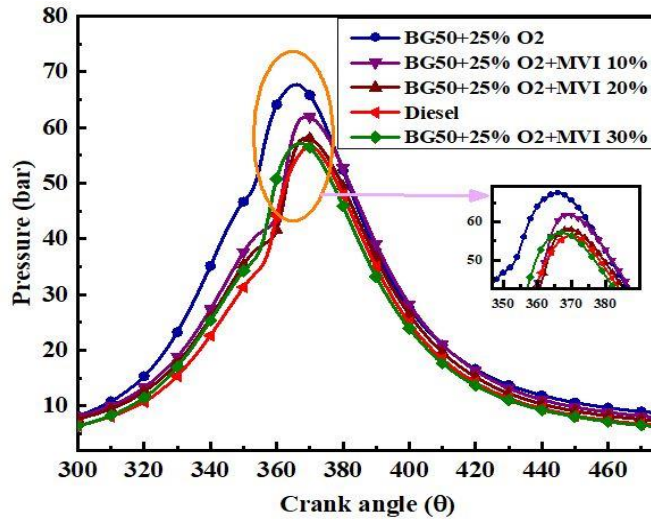
Figure 5.35: Variation of NHRR under the influence of vapor induction

5.12.3 Ignition Delay (ID)

The effect of vapor induction upon the ID for dual-mode operations with enriched oxygen is shown in Figure 5.36. Generally, the ID is obtained from heat release rate curves considering from the start of the diesel injection to the start of the combustion. For oxygen enrichment, the ID decreased in nature for dual-mode but as the vapor induction is incorporated for optimized biogas the ID increased. A longer delay period for dual-mode with oxygen enrichment is because of the cooling effect of water-methanol vapor induction upon the air intake temperature causes the temperature of charge to decrease at the interval of injecting the fuel (Adnan et al. 2012, Masimalai et al. 2018). Also, the process of diesel combustion gets elongated by reallocating to retard condition caused due to the presence of vapor in the cylinder charge as a result the turbulence mixing of the burnt flame is affected. From this development, it is more evident to the Arrhenius function indicating that ID solely depends upon the temperature of the intake charge and is concluded that as the vapor induction increases ID increases for every case (Tesfa et al. 2012). BG50 at 25% O_2 with 30% MVI showed longer ID and minimum delay is attained for BG50 at 25% O_2 with 10% MVI for all the operating engine loads. BG50 at 25% O_2 with 10% MVI exhibited a small increase in ID by 3.10% and 4.92% at $3/4^{th}$ and full load

as compared to diesel. However, BG50 at 25% O_2 with 10% MVI showed lower ID than the remaining vapor inductions. Eventually, BG50 at 25% O_2 with 30% MVI showed higher ID by 12.4% & 15.5% compared to diesel at $3/4^{th}$ and full load. Significant reduction in delay period for BG50 at 25% O_2 with 10% MVI was achieved by 2.26% and 3.12% compared to BG50 at 25% O_2 without vapor induction at $3/4^{th}$ and full load. Conversely, as the vapor induction increased to 30% with BG50 at 25% O_2, ID increased subsequently by 6.62% and 6.82% compared to BG50 at 25% O_2 without vapor induction at $3/4^{th}$ and full load respectively.
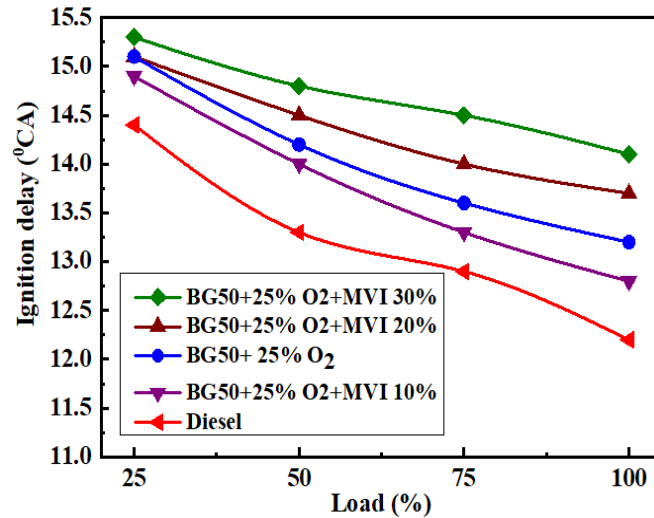
Figure 5.36: Variation of ID under the influence of vapor induction

5.12.4 Carbon Monoxide (CO)

As the flow rate of vapor induction increases the effect upon CO emissions has positive development for dual-mode with a decrement in nature as depicted in Figure 5.37. It is evident from the result that as the vapor induction increases, the CO emission decreases but to some extent CO emission starts increasing marginally particularly for BG50 at 25% O_2 with 30% MVI after the half load. This type of drastic change is due to the presence of methanol with the water will boost up the oxygen content inside the cylinder and as a result the CO emission increases (Patnaik et al. 2016, Adnan et al. 2012). On the other hand, the volumetric efficiency decreases as the vapor induction

135

percentage are increased consequently there are not many differences in the CO emission. The prominent cause for improvement in CO emission is because of two major reasons, the very first is the fast chemical conversion from CO to CO_2 due to the presence of vapor in the combination, such that the temperature of pre-combustion decreases significantly. The next reason says that the CO and H_2O formation was enhanced as a result of solid carbon reaction taking place at elevated temperature along with the water-methanol vapor occurring inside the cylinder.

Various researchers' observation also says that an increase in the air-fuel equivalence ratio amplifies the temperature of in-cylinder gas kinetic reaction rate to increase from CO to CO_2 (Tesfa et al. 2012, Mingrui et al. 2017). Maximum CO emission was observed for BG50 at 25% O_2 with 10% MVI compared to other vapor induction for all operating loads but lower than diesel by 17.65% and 20% at 3/4th and full load. However, as the vapor induction increased to 30%, CO emission decreased significantly for 25% and half load but emission increased for 3/4th & full load. A subsequent decrement in the CO emission was found for BG50 at 25% O_2 with 30% MVI compared to diesel by 29.03% and 25% at 3/4th and full load. On the other hand, as compared to BG50 at 25% O_2 without vapor induction, CO emission reduced for BG50 at 25% O_2 with 30% MVI by 19.35% and 14.58% at 3/4th and full load respectively.
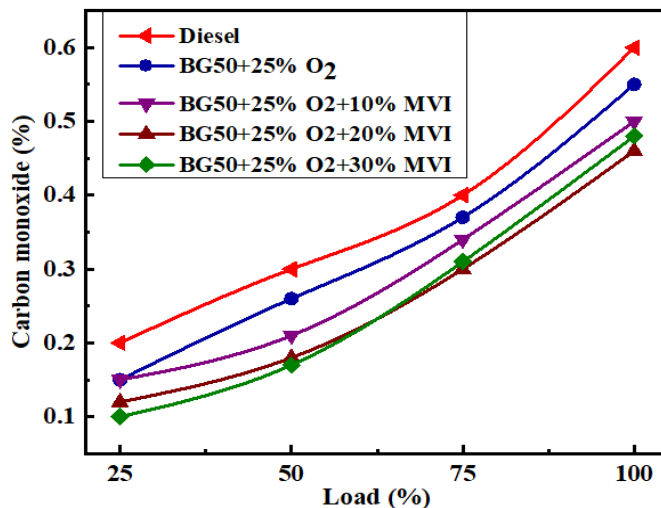
Figure 5.37: Variation of CO emissions under the influence of vapor induction

5.12.5 Unburnt Hydrocarbon (UBHC)

Figure 5.38 illustrates the variation of UBHC emission under the influence of a vapor induction system. Encouraging results were achieved with a decrease in HC emission with the increase in vapor induction rate as compared to diesel and BG50 without vapor induction. This significant improvement is caused due to the existence of a fuel vapor interface with lower interfacial tension generating improved atomization of the injected fuel (Tesfa et al. 2012, Adnan et al. 2012). The better atomization of fuel results in longer contact along with the inducted air endorses finer dispersion of the fuel droplets during the combustion process. Also, many researchers' finding depicts that a shorter combustion reaction rate occurs as a result of advancement in the vaporization and proper mixing process is the reason behind attaining lower HC emissions (Mingrui et al. 2017). However, as the flow rate of vapor induction is increased the BG50 at 25% O_2 with 30% MVI showed considerable reduction in HC emissions for 25% and half load but at the 75% and full load, the HC emission raised marginally which is attributed to the quenching of the flame occurred during the combustion process (Masimalai et al. 2018, Patnaik et al. 2016).

Maximum UBHC emissions were observed for BG50 at 25% O_2 with 10% MVI compared to other ratios of vapor induction at all respective operating loads but showed lower HC emissions compared to diesel by 24.32% and 34.88% at $3/4^{th}$ and full load. On the other hand, HC emission reduced for BG50 at 25% O_2 with 30% MVI compared to diesel by 35.29% and 45% at $3/4^{th}$ and full load. Successive reduction in HC emission was achieved for BG50 at 25% O_2 with 30% MVI as compared to BG50 at 25% O_2 without vapor induction by 20.59% and 27.5% at $3/4^{th}$ and full load respectively.
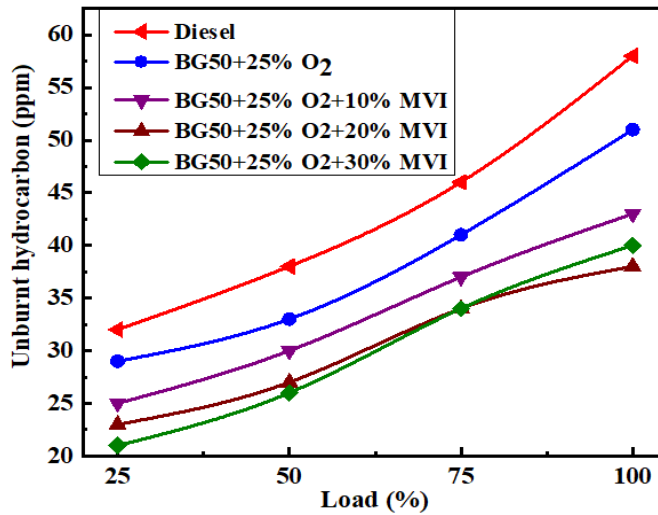
Figure 5.38: Variation of UBHC emissions under the influence of vapor induction

5.12.6 Nitrogen Oxide (NO$_x$)

During the oxygen enrichment mechanism, the NO$_x$ emission increased enormously for optimized biogas such that positive development is achieved after the implementation of vaporized water-methanol induction which acts as a diluent and causes a simultaneous reduction in NO$_x$ emission by regulating the in-cylinder temperature during the combustion (Mingrui et al. 2017). Variation of NO$_x$ emission under the influence of vapor induction for BG50 along with oxygen enrichment is revealed in Figure 5.39. The trend of NO$_x$ emission showed a decrease in nature as the rate of vapor induction increased. The reason for this trend is attributed to the water-methanol mixture entering into the combustion chamber in the form of minute-sized droplets influences upon the fuel combustion and particularly on NO$_x$ emissions (Tesfa et al. 2012, Patnaik et al. 2016). Furthermore, the thermo-physical properties of the water-methanol mixture get altered inside the cylinder which has a higher influence upon the heat transfer coefficient of gas formed and makes it easier for heat to dissipate through the cylinder wall. Similar outcomes such as, reduction in the NO$_x$ emission and improvement in engine efficiency were observed for vapor induction upon diesel engine as experienced by several researchers who have worked upon the impact of water injection systems upon the

138

engines. Inside the combustion chamber, atomized droplets in the finest form mix with the air instantaneously and form a homogenous mixture. The factors such as higher latent heat of vaporization, higher molar heat capacity of water-methanol mixture as well as reduction in partial pressure of oxygen create fewer chances of nitrogen to combine with oxygen. Thereby, the in-cylinder temperature and the rate of NO_x formation decreases (Masimalai et al. 2018).

The vaporized water-methanol induction through the intake manifold shows lower NO_x emission for BG50 at 25% O_2 with 30% MVI compared to other flow rates of vapor induction for all the engine loads. As compared to diesel, lower NO_x emission was attained for BG50 at 25% O_2 with 30% MVI by 13.25% and 20.76% at $3/4^{th}$ and full load. Whereas, BG50 at 25% O_2 with 20% and 30% vapor induction showed higher NO_x emission than diesel for all the loads. Conversely, a drastic reduction in NO_x emission was observed for BG50 at 25% O_2 with 30% MVI as compared to BG50 at 25% O_2 without vapor induction by 80.6% and 86.82% at $3/4^{th}$ and full load respectively.
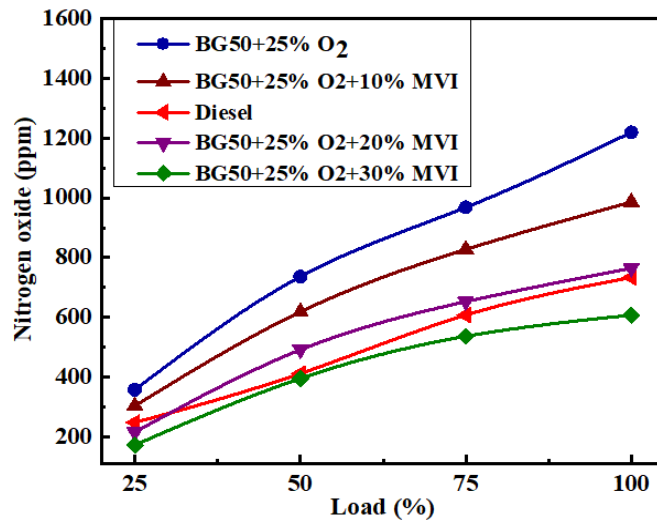
Figure 5.39: Variation of NO_x emissions under the influence of vapor induction

5.12.7 Smoke Opacity (SO)

Factors such as higher temperature and fuel-rich zone favor the fuels to form higher sootness which generally takes place at the initial phase of the combustion process

appears in depletion form as a result of oxidation at the zone consisting higher level of oxygen. The formation of particulate matter includes several numbers of chemical and physical processes such that oxidation takes place at elevated temperatures along with carbonaceous particles. Also, local air/fuel ratio, temperature, reaction time, and pressure are the factors that affect the process of particulate formation (Tesfa et al. 2012, Masimalai et al. 2018). In this study, the sootness of oxygen-enriched optimized biogas reduced drastically as the induction of vaporized water-methanol increased because of the combustion process taking place at a lower temperature, and the nature of the curve is illustrated in Figure 5.40.

After the vapor induction surges inside the combustion chamber, the steam decomposes into oxygen and hydrogen at elevated temperatures. The OH and O radical concentrations increase, which leads to the formation of a higher oxidation rate. This development further endorses the aromatic hydrocarbons as well as sootness emission to reduce significantly (Mingrui et al. 2017). BG50 at 25% O_2 with 30% MVI showed lower sootness as compared to other flow rates for all the engine loads. As compared to diesel, BG50 at 25% O_2 with 30% MVI showed lower sootness by 52.98% & 48.61% at 3/4th and full load. Whereas, compared to BG50 at 25% O_2 without vapor induction, sootness decreased for BG50 at 25% O_2 with 30% MVI by 58.05% and 56.46% for 3/4th and full load respectively.
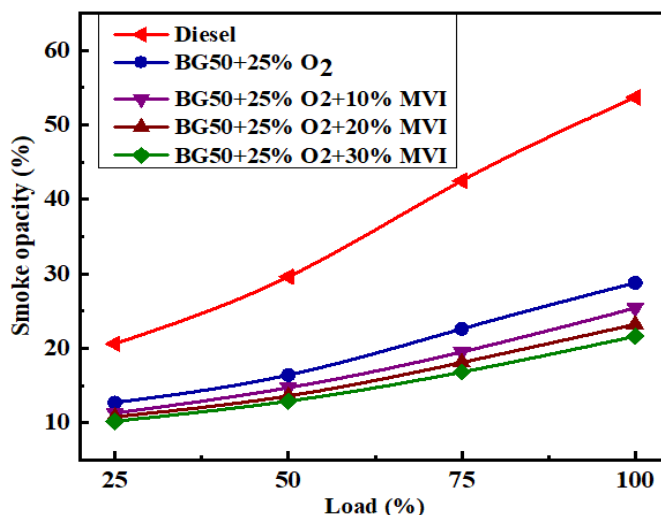
Figure 5.40: Variation of SO emissions under the influence of vapor induction

5.12.8 Exhaust Gas Temperature (EGT)

The variation of exhaust gas temperature for biogas with different flow rates of vapor induction with all engine operating loads shows the decrease in trend as shown in Figure 5.41. As observed from the graph, it is evident that as the vapor induction fraction increased the EGT gradually reduces. This may be attributed to the lower temperature occurring for concurrent cycles which are fundamentally due to the addition of vapor induction such that this factor is also one of the reasons for lower NO_x emission (Mingrui et al. 2017). Enhanced vaporization, appropriate mixing process, and evaporative cooling of water-methanol combination contribute a pivotal role in the kinetics of the combustion by reducing the charge temperature significantly.

Also, the proper mixing of vapors with the intake air and gradual enhancement inside the combustion region during the late combustion segment causes in-cylinder charge temperature to decline, and hence, EGT decreases (Adnan et al. 2012, Patnaik et al. 2016). Among the different flow rates of vapor induction, BG50 at 25% O_2 with 30% MVI showed lower EGT for different engine loads. As compared to diesel, EGT is lower for BG50 at 25% O_2 with 30% MVI by 19.07% and 23.36 at 3/4th and full load. Whereas, furthermore improvement was observed for BG50 at 25% O_2 with 30% MVI which exhibited lower EGT compared to BG50 at 25% O_2 without vapor induction by 19.07% and 23.36% for 3/4th and full load respectively.
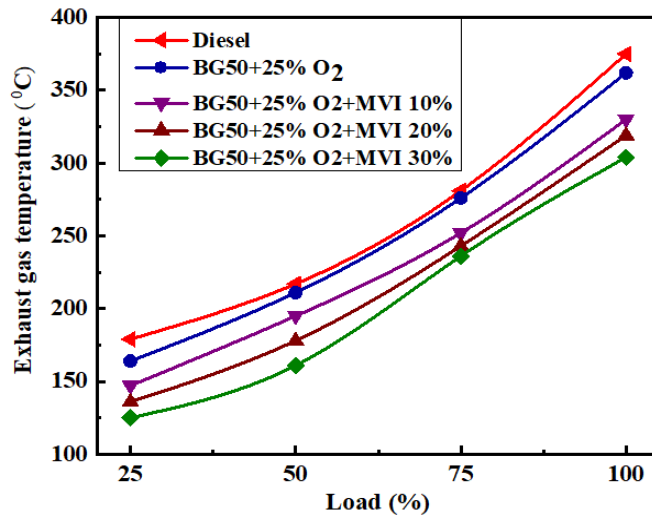
Figure 5.41: Variation of EGT under the influence of vapor induction

5.13 Closure

The result analysis of the modified diesel engine performance operated under dual-mode using higher proportions of biogas ranging from 20% to 60% with a step of 10% are provided in detail. The nature of the engine behavior when it is exposed to cyclic variations for dual fuel mode operation has been investigated. Studies related to the influence of the advanced injection timing on engine characteristics using biogas are reported in this chapter. To improve the engine performance, the method of oxygen enrichment is implemented along with optimized biogas (BG50) and the engine behavior is analyzed. The behavior of the engine under the vaporized water-methanol method to reduce the NO_x emissions generated from the engine is studied. In the next chapter, the overview of the present investigation, conclusions and scope of future work have been discussed.

CHAPTER 6

CONCLUSIONS

Throughout the world, food waste disposal has become a major issue for proper storage and dissipation without disturbing the ecological cycle and living creatures on the planet. Effective measurements and techniques have to be implemented for better management of waste as well as to extract the energy and utilize it in an essential manner for several applications. One such approach has been executed in this present investigation, the biogas generated using waste food from the biogas digester monitored by MCC Mangalore is used as an alternative fuel for operating diesel engine. The present chapter includes a description about the major outcomes of studies related to the performance, combustion and emission characteristics of diesel and dual-fuel mode. Brief summary of results about the engine behavior under cyclic by cycle variation conditions for diesel and dual-fuel mode is provided. The engine performance under the influence of varying injection timing and the effect of oxygen enrichment is highlighted. The research is concluded by analyzing the impact of vaporized water-methanol induction on the engine performance and to reduce emissions.

Following outcomes are drawn and concluded based upon the experimental results:

- ➢ The optimized biogas (BG50) exhibited better performance and lower emissions compared to other biogas ratios, indicating superior conversion of energy into work.

- ➢ Significant improvement in peak cylinder for dual mode was observed than diesel at full load, due to the longer ID and higher auto-ignition temperature. As a result of larger heating value of diesel–biogas combination, higher NHRR is witnessed for dual mode.

- ➢ On account of incomplete combustion, BG50 emitted higher CO emissions than diesel by 8.3% at full load. Due to the inadequate supply of air, BG50 indicated higher UBHC emissions by 13.79% than diesel at full load respectively.

➢ Phenomenal reduction in the NO_x emission for BG50 is attained than diesel by 35.33% at full load. The rapid decrease in the flame temperature for dual mode, contributed to lower soot emission than diesel by 28.49% at full load.

➢ The cyclic variations measured in terms of cylinder maximum pressure (P_{max}) increased as the biogas proportion is increased from BG20 to BG60.

➢ Higher cyclic variations of P_{max} was observed for BG50 and BG60, as a result of lower flame propagation causing instabilities in combustion.

➢ Lower biogas proportions showed lower COV of P_{max} and higher biogas proportion's showed higher COV of P_{max}.

➢ From the return map, it is evident that BG20 and BG30 showed greater combustion stability compared to other biogas proportions.

➢ Lower biogas proportion BG20, with the 29.5° bTDC IT caused early combustion and exhibited higher BTE by 7.3% compared to other IT's. But depicted lower efficiency compared to diesel for the same operating load.

➢ The presence of CO_2 in biogas caused higher BSEC per power output than diesel at 29.5° bTDC IT.

➢ The outcome from the investigation suggest, that increasing IT provides more platform for homogeneous mixing of air-biogas and creates more turbulence inside the chamber resulting in higher cylinder pressure.

➢ As the IT is advanced, improved oxidation reaction taking place between the gas molecules prevented in emitting higher CO emission for dual mode. Inefficient mixing of diesel and biogas-air fuel will contribute higher UBHC emissions at retard IT.

➢ Retardation of IT has proved lower NO_x emissions for higher biogas ratios. Further, the dual mode showed discrete advantage with the three IT's exhibiting lower sootness compared to diesel.

➢ Overall, 27.5° bTDC injection timing showed optimum results as compared to other injection timings and BG50 is optimized compared to other biogas ratio's in terms of better engine performance and lower emissions.

- The oxygen enrichment has shown promising results with enhanced BTE for BG50, which is attributed to the betterment of partial oxidation reactions causing an advance in flame propagation velocities of the fuel mixture.

- A favorable improvement in peak cylinder pressure was developed at full load which is 27.16% higher for BG50 at 27% O_2, as a result of improved reaction rate and reduction in ID.

- Drastic increment in NHRR was witnessed with increased oxygen levels for dual mode, which is attributed to the reduced ID and higher combustion rate.

- Lower ID was observed for BG50 at 27% oxygen concentration, because of adequate supply of O_2 leading to complete combustion.

- Oxygen enrichment has a significant influence on CO emissions, which promotes complete combustion owing to the more availability of oxygen and higher reaction rate.

- Reduction in UBHC emission was observed after the induction of oxygen enrichment, which provides more intake of oxygen inside the cylinder causing complete combustion. BG50 showed lower UBHC emission with oxygen level compared to BG50 without enrichment.

- NO_x intensity increases by three times the ambient air as the oxygen concentration reaches 27% and lower emission is attained for BG50 with lower oxygen levels. Hence, the oxygen level is limited to 27% and not exceeded beyond the limit. Improved reaction rate exhibits lower smoke emissions for dual mode with the increased oxygen levels.

- Significant improvement in the BTE is achieved for BG50 at 25% O_2 with 20% MVI. However, BG50 at 25% O_2 with 20% MVI showed affirmative increase in BTE due to the increment in the enthalpy of the vaporized form.

- Prior to the improvement in BTE, BSEC for BG50 at 25% O_2 with 20% MVI reduces by 6.03% at full load, as a result of the enhanced atomization the energy consumption per power output drops.

- The combined effect of water-methanol and higher partial pressure of oxygen contributed lower peak cylinder pressure for BG50 at 25% O_2 with various ratios of MVI.

- Similarly, the water-methanol combination provided superior cooling effect, hence the NHRR decreases and BG50 at 25% O_2 with 30% MVI showed lower heat release rate.

- With the increased rate of vapor induction, the ID for BG50 at 25% O_2 with various levels of MVI showed significant improvement due to the reduced intake charge temperature.

- Compared to BG50 at 25% O_2 without vapor induction, CO emission reduced for BG50 at 25% O_2 with different levels of MVI, which is attributed due to the higher combustion rate. Similarly, as a result of better atomization of the injected fuels and better mixing process the rate of UBHC emissions for BG50 at 25% O_2 with different levels of MVI decreased.

- Induction of MVI has delivered lower NO_x emission for BG50 at 25% O_2, which owes to the enhanced atomization and drastic reduction in in-cylinder temperature.

- In this study, because of the combustion process taking place at a lower temperature, the sootness drastically reduced as a result of higher oxidation rate.

- Induction of higher vapor fraction for concurrent cycles, aided in the lower EGT for BG50 at 25% O_2 with 30% MVI by 23.36% at full load.

Overall, the experimental investigation has proved that the biogas derived from food waste showed promising results in the diesel engine application as a prominent alternative fuel. The base experiment results showed lower emissions from the engine using higher biogas proportions with marginal performance. However, by optimizing the injection timing parameter has shown improvement in the enhanced performance, combustion characteristics with the significant reduction in the emissions. Besides, the induction of the oxygen enrichment to the biogas-driven engine has shown

positive development in the performance results but the engine emitted higher NO_x emissions. With the incorporation of vaporized water-methanol technique to the engine operated with the oxygen enriched-biogas, drastic reduction in the NO_x emission was achieved. In general, BG50 with 25% O_2 and 20% MVI showed exceptional results in terms of engine characteristics, operated under dual mode.

Scope of the future work

➤ Biodiesel which is not explored can be used in place of diesel to operate in dual mode along with biogas to study the engine parameters.

➤ To enhance the engine parameters other gaseous fuels such as producer gas, syngas, hydrogen, LPG & CNG with appropriate proportionate can be used along with biogas.

➤ Apart from conventional diesel engine biogas can be used and compared in advanced engines such as turbocharged petrol and CRDI, HCCI, RCCI with necessary modifications.

➤ Direct injection of biogas into the combustion chamber using gas injector interfaced to programmable ECU and the results can be analyzed with the dual-mode operation.

➤ Other engine parameters such as injection pressure, varying compression ratio, the higher mass flow rate of the biogas, etc can be incorporated and study the effects.

➤ With more than 500 cycles combustion studies can be explored.

➤ Biogas can be driven with turbocharger operation to enhance the engine parameters and compare them with the oxygen enrichment process.

➤ Techniques such as exhaust gas recirculation (EGR), selective catalyst reduction (SCR), thermal barrier coating (TBC), Emulsion technology, low-temperature combustion, combustion chamber modification can be implemented to reduce NO_x emissions and compared with vaporized water-methanol induction fueled with biogas.

➤ Studies related to computer simulation of biogas combustion along with NO_x reduction by water-methanol induction can be executed.

LIST OF PUBLICATIONS

International Journals:

1) **Jagadish C** and Veershetty Gumtapure. "Experimental investigation of methane enriched biogas in a single-cylinder diesel engine by dual mode". **Energy Sources, Part A: Recovery, Utilization, and Environmental Effects**. https://doi.org/10.1080/15567036.2019.1647314-**Taylor & Francis**. Status: **Published, (IF-3.447)**.

2) **Jagadish C** and Veershetty Gumtapure. "Experimental studies on cyclic variations in a single-cylinder diesel engine fuelled with raw biogas by dual mode of operation". **Fuel, Elsevier**. Status: **Published, (IF-6.609)**.

3) **Jagadish C** and Veershetty Gumtapure. "Experimental study on the effect of injection timing on a dual fuel diesel engine operated with biogas derived from food waste". https://doi.org/10.1115/1.4054586. **Journal of Energy Resource and Technology, ASME**. Status: **Published**, **(IF-2.903)**.

4) **Jagadish C** and Veershetty Gumtapure. "Experimental studies of biogas in a single cylinder diesel engine by dual fuel mode of operation"- **Applied Mechanics and Materials**- #514491714-24/10/19, 06:57:44- **Scientific.net**. Status: **Published**.

5) **Jagadish C** and Veershetty Gumtapure. "Effect of oxygen enrichment on cyclic variations and parameters of diesel engine propelled with biogas derived from food waste" - **Industrial Crops & Products, Elsevier**. Status: **Under review**.

International Conferences:

1) **Jagadish C** and Veershetty Gumtapure. "Experimental studies of biogas in a single cylinder diesel engine by dual fuel mode of operation". Green Trends in Mechanical Engineering Sciences, (**GTMES-2018**), MCE Hassan, Karnataka, 3-5 October, 2018.

2) **Jagadish C** and Veershetty Gumtapure. "Experimental investigation of methane enriched biogas in a single-cylinder diesel engine by dual mode". International Conference on Advanced Materials, Energy & Environmental Sustainability, (**ICAMEES-2018**), UPES Dehradun, Uttarkhand, 14-15 December, 2018.

3) **Jagadish C** and Veershetty Gumtapure. "Influence of raw biogas operated in a single cylinder diesel engine by dual fuel mode". International Symposium on Advanced Materials for Industrial and Societal Applications (**NMD ATM-2019**) at Hotel uday samudra, kovalam, Trivandrum, on 13-16 November 2019.

REFERENCES

Abdelaal, M. M., Rabee, B. A., and Hegab, A. H. (2013). "Effect of adding oxygen to the intake air on a dual-fuel engine performance, emissions, and knock tendency." *Energy*, 61, 612–620.

Achinas, S., Achinas, V., Jan, G., and Euverink, W. (2017). "A Technological Overview of Biogas Production from Biowaste A Technological Overview of Biogas Production from Biowaste." *Engineering*, 3(3), 299–307.

Adnan, R., Masjuki, H. H., and Mahlia, T. M. I. (2012). "Performance and emission analysis of hydrogen fueled compression ignition engine with variable water injection timing." *Energy*, 43(1), 416–426.

Ambarita, H. (2017). "Performance and emission characteristics of a small diesel engine run in dual-fuel (diesel-biogas) mode." *Case Stud. Therm. Eng*., 10, 179–191.

Awogbemi, Omojola, Adeyemo, Babatunde, S. (2015). "Development and testing of biogas-petrolblend as an alternative fuel for spark ignition engine." *International Journal of Scientific & Technology Research*, 4 (9), 179–186.

Badr, O., Karim, G., A and Liu, B. (1999). "Examination of the flame spread limits in a dual fuel engine." *Appl. Therm. Eng*., 19, 1071–1080.

Banapurmath, N. R., and Tewari, P. G. (2009). "Comparative performance studies of a 4-stroke CI engine operated on dual fuel mode with producer gas and Honge oil and its methyl ester (HOME) with and without carburetor." *Renew. Energy*, 34(4), 1009–1015.

Barik, D., and Murugan, S. (2014). "Investigation on combustion performance and emission characteristics of a DI (direct injection) diesel engine fueled with biogas-diesel in dual fuel mode." *Energy*, 72, 760–771.

Barik, D., Satapathy, A. K., and Murugan, S. (2015). "Combustion analysis of the diesel–biogas dual fuel direct injection diesel engine – the gas diesel engine." *Int. J. Amb.*

Energy, 38 (3), 259-266.

Barik, D., and Murugan, S. (2016). "Experimental investigation on the behavior of a DI diesel engine fueled with raw biogas-diesel dual fuel at different injection timing." *Journal of the Energy Institute*, 89 (3), 373–388.

Barik, D., Murugan, S., Sivaram, N. M., Baburaj, E., and Sundaram, P. S. (2017). "Experimental investigation on the behavior of a direct injection diesel engine fueled with Karanja methyl ester-biogas dual fuel at different injection timings." *Energy*, 118, 127–138.

Baskar, P., and Senthilkumar, A. (2016). "Effects of oxygen enriched combustion on pollution and performance characteristics of a diesel engine." *Eng. Sci. Technol. an Int. J.*, 19(1), 438–443.

Bhatia, S. K., Kim, S. H., Yoon, J. J., & Yang, Y. H. (2017). Current status and strategies for second generation biofuel production using microbial systems. *Energy Conversion and Management*, *148*, 1142–1156.

Bedoya, I. D., Arrieta, A. A., and Cadavid, F. J. (2009). "Bioresource technology effects of mixing system and pilot fuel quality on diesel – biogas dual fuel engine performance." *Bioresource Technology*, 100 (24), 6624–6629.

Bedoya, I. D., Saxena, S., Cadavid, F. J., Dibble, R. W., and Wissink, M. (2012). "Experimental evaluation of strategies to increase the operating range of a biogas-fueled HCCI engine for power generation." *Applied Energy*, 97, 618–629.

Berlini, R., Molina, R., Hernández, J. J., César, A., Malaquias, T., Coronado, C. J. R., José, F., and Pujatti, P. (2020). "Experimental investigation on the potential of biogas / ethanol dual-fuel spark-ignition engine for power generation : combustion , performance and pollutant emission analysis." *Appl. Energy*, 261, 114438.

Bhatia, R. K., Ramadoss, G., Jain, A. K., Dhiman, R. K., and Bhatia, S. K. (2020).

"Conversion of waste biomass into gaseous fuel : Present status and challenges in India." *BioEnergy Research*, 13:1046–1068.

Bhaskor, J. B., Saha, U. K. (2015). "Estimating the theoretical performance limits of a biogas powered dual fuel diesel engine using emulsified rice bran biodiesel as pilot fuel." *Journal of Energy Resource and Technology*, 138, 021801-1.

Bora, B. J., Saha, U. K., Chatterjee, S., and Veer, V. (2014) "Effect of compression ratio on performance, combustion and emission characteristics of a dual fuel diesel engine run on raw biogas." *Energy Conversion and Management*, 87, 1000–1009.

Bora, B. J., and Saha, U. K. (2015). "Comparative assessment of a biogas run dual fuel diesel engine with rice bran oil methyl ester, pongamia oil methyl ester and palm oil methyl ester as pilot fuels." *Renewable Energy*, 81, 490–498.

Bora, B. J., and Saha, U. K. (2016). "Optimisation of injection timing and compression ratio of a raw biogas powered dual fuel diesel engine." *Applied Thermal Engineering*, 92, 111–121.

Bora, B. J., and Saha, U. K. (2016). "Experimental evaluation of a rice bran biodiesel - biogas run dual fuel diesel engine at varying compression ratios." *Renewable Energy*, 87, 782–790.

Cadavid, F.,Amell, A., and Cacua, K. (2012). "Effects of oxygen enriched air on the operation and performance of a diesel-biogas dual fuel engine." *Biomass and Bioenergy*, 45, 0–8.

Chandra, R., Vijay, V. K., Subbarao, P. M. V, and Khura, T. K. (2011). "Performance evaluation of a constant speed IC engine on CNG, methane-enriched biogas and biogas." *Applied Energy*, 88 (11), 3969–3977.

Chandekar, A. C., and Debnath, B. K. (2018). "Computational investigation of air-biogas mixing device for different biogas substitutions and engine load variations." *Renew. Energy*, 127(X), 811–824.

Cengel, Y. A. (2013). "*Thermodynamics An Engineering Approach*." McGraw-Hill, Inc.,

Chinwan, D., and Pant, S. (2014). "Waste to Energy in India and its Management." *Journal of Basic and Applied Engineering Research,* 1(10), 89–94.

Cheng, Q., Ahmad, Z., Kaario, O., & Martti, L. (2019). "Cycle-to-cycle variations of dual-fuel combustion in an optically accessible engine". *Applied Energy*, *254*, 113611.

Debnath, B. K., Bora, B. J., Sahoo, N., and Saha, U. K. (2013). "Influence of emulsified palm biodiesel as pilot fuel in a biogas run dual fuel diesel engine." *Journal of Energy Engineering*, 140 (3).

Deheri, C., Acharya, S. K., Thatoi, D. N., and Mohanty, A. P. (2020). "Review article A review on performance of biogas and hydrogen on diesel engine in dual fuel mode." *Fuel*, 260, 116337.

Duc, P. M., and Wattanavichien, K. (2007). "Study on biogas premixed charge diesel dual fuelled engine." *Energy Conversion and Management*, 48, 8, 2286-2308.

Fermoso, F. G., Serrano, A., Alonso-Fariñas, B., Fernández-Bolaños, J., Borja, R., & Rodríguez-Gutiérrez, G. (2018). Valuable Compound Extraction, Anaerobic Digestion, and Composting: A Leading Biorefinery Approach for Agricultural Wastes. *Journal of Agricultural and Food Chemistry*, *66*(32), 8451–8468.

Ganesan, V. (2003). "*Internal combustion engines*." Tata McGraw-hill.

Gao, A., Tian, Z., Wang, Z., Wennersten, R., and Sun, Q. (2017). "Comparison between the technologies for food waste treatment." *Energy Procedia*, 105, 3915–3921.

Gonca, G. (2014). "Investigation of the effects of steam injection on performance and NOx emissions of a diesel engine running with ethanol-diesel blend." *Energy Conversion and Management*, 77, 450–457.

Gonca, G., and Sahin, B. (2017). "Effect of turbo charging and steam injection methods

on the performance of a Miller cycle diesel engine (MCDE)." *Appl. Therm. Eng.*, 118, 138–146.

Gómez Montoya, J. P., Amador Diaz, G. J., and Amell Arrieta, A. A. (2018). "Effect of equivalence ratio on knocking tendency in spark ignition engines fueled with fuel blends of biogas, natural gas, propane and hydrogen." *Int. J. Hydrogen Energy*, Volume 43, 51, 20, 23041-23049.

Gumus, M., Sayin, C., and Canakci, M. (2010). "Effect of Fuel Injection Timing on the Injection , Combustion , and Performance Characteristics of a Direct-Injection (DI) Diesel Engine Fueled with Canola Oil Methyl Ester - Diesel Fuel Blends." *Materials Today: Proceedings*. Volume 2, Issues 4–5, 1316-1325 (13), 3199–3213.

Hadia, F., Wadhah, S., Ammar, H., and Ahmed, O. (2017). "Investigation of combined effects of compression ratio and steam injection on performance, combustion and emissions characteristics of HCCI engine." *Case Studies in Thermal Engineering*, 10, 262–271.

Heywood, J. B. (2018). "*Internal Combustion Engine Fundementals*." McGraw-Hill, Inc.,

Hotta, S. K., Sahoo, N., Mohanty, K., and Kulkarni, V. (2019). "Ignition timing and compression ratio as effective means for the improvement in the operating characteristics of a biogas fueled spark ignition engine." *Renew. Energy*., Volume 150, 854-867.

Hyun, S., and Sik, C. (2011). "Experimental investigation on the combustion and exhaust emission characteristics of biogas – biodiesel dual-fuel combustion in a CI engine." *Fuel Processing Technology*, 92 (5), 992–1000.

Jagadish, C., and Gumtapure, V. (2020). "Experimental studies on cyclic variations in a single cylinder diesel engine fuelled with raw biogas by dual mode of operation." *Fuel*, 266, 117062.

Kalsi, S. S., and Subramanian, K. A. (2017). "Effect of simulated biogas on performance,

combustion and emissions characteristics of a bio-diesel fueled diesel engine." *Renewable Energy*, 106, 78–90.

Kannan, G. R., and Anand, R. (2011). "Experimental evaluation of DI diesel engine operating with diestrol at varying injection pressure and injection timing." *Fuel Process. Technol.*, 92(12), 2252–2263.

Khayum, N., Anbarasu, S., and Murugan, S. (2020). "Combined effect of fuel injecting timing and nozzle opening pressure of a biogas-biodiesel fuelled diesel engine." *Fuel*, 262, 116505.

Kumar, M. H., Raju, V. D., Kishore, P. S., and Venu, H. (2018). "Influence of injection timing on the performance , combustion and emission characteristics of diesel engine powered with tamarind seed biodiesel blend." *Int. J. Ambient Energy*, 0(0), 1–9.

Kumar, S., Smith, S. R., Fowler, G., Velis, C., Kumar, S. J., Arya, S., Kumar, R., and Cheeseman, C. (2017). "Challenges and opportunities associated with waste management in India." *Royal society open science,*4:160764.

Kumari, S., & Das, D. (2016). Biologically pretreated sugarcane top as a potential raw material for the enhancement of gaseous energy recovery by two stage biohythane process. In *Bioresource Technology* (Vol. 218, pp. 1090–1097).

Kyrtatos, P., Brückner. C., and Boulouchos. K., (2016). "Cycle-to-cycle variations in diesel engines." *Applied Energy* . 171, 120–32.

Lata, D. B., and Misra, A. (2011). "Analysis of ignition delay period of a dual fuel diesel engine with hydrogen and LPG as secondary fuels." *Int. J. Hydrogen Energy*, 36(5), 3746–3756.

Li, H., Biller, P., Hadavi, S. A., Andrews, G. E., Przybyla, G., and Lea-Langton, A. (2013). "Assessing combustion and emission performance of direct use of SVO in a diesel engine by oxygen enrichment of intake air method." *Biomass and Bioenergy*, 51,

43–52.

Leach, F., Davy, M., and Peckham, M. (2019). "Cycle-to-Cycle NO and NOx Emissions from a HSDI Diesel Engine." *Journal of Engineering for Gas Turbines and Power*. 141(x): 1–9:1–9.

Lee, T. H., Huang, S. R., and Chen, C. H. (2013). "The experimental study on biogas power generation enhanced by using waste heat to preheat inlet gases." *Renew. Energy*, 50, 342–347.

Madhankumar, S., Stanley, M. J., Thiyagarajan, S., Geo, V. E., Karthickeyan, V., and Chen, Z. (2019). "Effect of oxygen enrichment on CI engine behavior fueled with vegetable oil: an experimental study." *J. Therm. Anal. Calorim.*, 142(3), 1275–1286.

Maizonnasse, M., Plante, J. S., Oh, D., and Laflamme, C. B. (2013). "Investigation of the degradation of a low-cost untreated biogas engine using preheated biogas with phase separation for electric power generation." *Renew. Energy.*, 55 (2013) 501-513.

Makareviciene, V., and Sendzikiene, E., Pukalskas, S., Rim-kus, A., and Vegneris, R. (2013). "Performance and emission characteristics of biogas used in diesel engine operation." *Energy Con-vers. Manag.*, 75, 224–233.

Masimalai, S. K., Ganesan, N., Pasupathiraju, S., and Mohanraj, T. (2018). "Investigations on the Combined Effect of Oxygen Enrichment and Water Injection Techniques on Engine's Performance, Emission and Combustion of a Mahua Oil Based Compression Ignition Engine." *SAE Tech. Pap.*, 01, 0929.

Maurya, R. K., and Agarwal A. K. (2011). "Experimental investigation on the effect of intake air temperature and air – fuel ratio on cycle-to-cycle variations of HCCI combustion and performance parameters." *Applied Energy*. 88, 1153–63.

Mingrui, W., Thanh Sa, N., Turkson, R. F., Jinping, L., and Guanlun, G. (2017). "Water injection for higher engine performance and lower emissions." *J. Energy Inst.*, 90(2), 285–299.

Nemoianu , L., Pana, C., Negurescu, N., Cernat., A, Fuiorescu., D, and Nutu., C. (2017). "Study of the cycle variability at an automotive diesel engine fuelled with LPG." *MATEC Web of Conferences*, 112:1–6.

Nirendra, N. M.(2006). "The use of biogas in internal combustion engines: A Review." *Proceedings., Technical.conference. on Internal combustion engine*, ASME, Aachen, Germany., 1-10.

Nathan, S. S., Mallikarjuna, J. M., and Ramesh, A. (2010). "An experimental study of the biogas – diesel HCCI mode of engine operation." *Energy Conversion and Management*, 51 (7), 1347–1353.

Park, C., Park, S., Lee, Y., Kim, C., and Lee, S. (2011). "Performance and emission characteristics of a SI engine fueled by low calorific biogas blended with hydrogen." *International Journal of Hydrogen Energy*, 36 (16), 10080–10088.

Patnaik, P. P., Acharya, S. K, Padhi, D and Mohanty, U. K (2016). "Experimental investigation on CI engine performance using steam injection and ferric chloride as catalyst." *Eng Sci Technol and Int J*, 19:2073–80.

Porpatham, E., Ramesh, A., and Nagalingam, B. (2007). "Effect of hydrogen addition on the performance of a biogas fuelled spark ignition engine." *International Journal of Hydrogen Energy*, 32, 2057–2065.

Poola, R. B., and Sekar, R. (2003). "Reduction of NO_X and particulate emissions by using oxygen-enriched combustion air in a locomotive diesel engine." *J. Eng. Gas Turbines Power*, 125(2), 524–533.

Prakash, R., Singh, R. K., and Murugan, S. (2013). "Experimental investigation on a

diesel engine fueled with bio-oil derived from waste wood-biodiesel emulsions." *Energy*, 55, 610–618.

Prabakar, D., Suvetha K, S., Manimudi, V. T., Mathimani, T., Kumar, G., Rene, E. R., & Pugazhendhi, A. (2018). Pretreatment technologies for industrial effluents: Critical review on bioenergy production and environmental concerns. *Journal of Environmental Management*, 218, 165–180.

Rahman, K. A., and Ramesh, A. (2019). "Studies on the effects of methane fraction and injection strategies in a biogas diesel common rail dual fuel engine". *Fuel*, 236, 147–165.

Raj, C. S., Arul, S., Sendilvelan, S., and Saravanan, C. G. (2009). "Biogas from textile cotton waste - An alternatefuel for diesel engines." *The open waste management journal*, 2, 1–5.

Rodriguez, C., Alaswad, A., Benyounis, K. Y., & Olabi, A. G. (2017). "Pretreatment techniques used in biogas production from grass". *Renewable and Sustainable Energy Reviews*, 68, 1193–1204. https://doi.org/10.1016/j.rser.2016.02.022.

Rossetto, C., Nelson, S., Souza, M. De, Santo, R. F., Souza, J. De, and Klaus, O. L. (2013). "Performance of an Otto cycle engine using biogas as fuel." *African Journal of Agricultural Research*, 8 (45), 5607–5610.

Salve, N. D., Kolekar, A. H., and Jadhav, K. M., (2016). "Experimental evaluation of dual fuel CI engine using synthesized biogas." *International Engineering Research Journal*, 1223–1229.

Salvi, B.L., Subramanian, K.A. and Panwar, N.L.,(2013). "Alternative fuels for transportation vehicles: A technical review." *Renewable and Sustainable Energy Reviews*, 25, 404–419.

Sagar Aryal (2018)." Gas chromatography- definition, principle, working, uses", http:// https://www.microbenotes.com/gas-chromatography/ (Oct. 22, 2018).

Sahoo, B. B., Sahoo, N., and Saha, U. K., (2009). "Effect of engine parameters and type of gaseous fuel on the performance of dual-fuel gas diesel engines — A critical review." *Renewable and Sustainable Energy Reviews*, 13, 1151–1184.

Sahoo, N., Debnath, B.K., Bhaskor, J. B., and Saha, U. K. (2014). "Influence of Emulsified Palm Biodiesel as Pilot Fuel in a Biogas Run Dual Fuel Diesel Engine." *Journal of Energy Engineering*. 140 (3), 1–9.

Santoso, W. B., Bakar, R. A., Ariyono. S., Cholis. (2012) N. "Study of Cyclic Variability in Diesel-Hydrogen Dual Fuel Engine Combustion." *International Journal of Mechanical & Mechatronics Engineering*, 12:52–6.

Selim, M. Y. E. (2004). "Sensitivity of dual fuel engine combustion and knocking limits to gaseous fuel composition." *Energy Conversion and Management*, 45, 411–425.

Senthilkumar, K., and Vivekanandan, S., (2016). "Investigating the Biogas as secondaryfuel for CI engine." *International Journal of Applied Environmental Sciences,* 11 (1), 155–163.

Solarte-Toro, J. C., Chacón-Pérez, Y., & Cardona-Alzate, C. A. (2018). Evaluation of biogas and syngas as energy vectors for heat and power generation using lignocellulosic biomass as raw material. *Electronic Journal of Biotechnology*, 33, 52–62.

Subramanian, K. A., Mathad, V. C., Vijay, V. K., and Subbarao, P. M. V. (2013). "Comparative evaluation of emission and fuel economy of an automotive spark-ignition vehicle fuelled with methane-enriched biogas and CNG using chassis dynamometer." *Applied Energy*, 105, 17–29.

Sudheesh, K.,and Mallikarjuna, J.M. (2010). "Diethyl ether as an ignition improver for biogas homogeneous charge compression ignition (HCCI) operation - An experimental investigation." *Energy*, 35, 3614-3622.

Surendra, K. C., Takara, D., Hashimoto, A. G., & Khanal, S. K. (2014). Biogas as a sustainable energy source for developing countries: Opportunities and challenges. *Renewable and Sustainable Energy Reviews*, 31, 846–859.

Teh, J. S., Teoh, Y. H., How, H. G., Le, T. D., Jun, Y., and Jason, J. (2021). "The Potential of Sustainable Biomass Producer Gas as a Waste-to-Energy Alternative in Malaysia." *Sustainability*, 13, 3877 1–31.

Tesfa, B., Mishra, R., Gu, F., and Ball, A. D. (2012). "Water injection effects on the performance and emission characteristics of a CI engine operating with biodiesel." *Renewable Energy*, 37(1), 333–344.

Tippayawong, N., Promwungkwa, A., and Rerkkriangkrai, P. (2007). "Long-term operation of a small biogas/diesel dual-fuel engine for on-farm electricity generation." *Biosyst. Eng.*, 98(1), 26–32.

Verma, S., Das, L. M., and Kaushik, S. C., (2017). "Effects of varying composition of biogas on performance and emission characteristics of compression ignition engine using exergy analysis." *Energy Conversion and Management*, 138, 346–359.

Venkadesan, G and Mohandoss, N. M., (2019). "Environmental Effects Combustion , performance and emission analysis of dual fuel engine using tsrb biogas." *Energy Sources, Part A: Recovery, Utilization, and Environmental Effects*, 41, 2171–83.

Wang, Y., Xiao, F., Zhao, Y., Li, D., and Lei, X. (2015). "Study on cycle-by-cycle variations in a diesel engine with dimethyl ether as port premixing fuel." *Applied Energy*, 143, 58–70.

Wang, Q., Wang, B., Yao, C., Liu, M., Wu, T., Wei, H., and Dou, Z. (2016). "Study on cyclic variability of dual fuel combustion in a methanol fumigated diesel engine." *Fuel*, 164, 99–109.

Wei, L., and Geng, P., (2016). "A review on natural gas/diesel dual fuel combustion,

emissions and performance." *Fuel Processing Technology*, 142, 264–278.

Wierzbicki, S. (2012). "Biogas as a fuel for diesel engines." *Journal of kones*, 19, 477-482.

Wu, H. W., Fan, C. M., He, J. Y., and Hsu, T. T. (2017). "Optimal factors estimation for diesel/methanol engines changing methanol injection timing and inlet air temperature." *Energy*, 141, 1819–1828.

Xu, F., Li, Y., Ge, X., Yang, L., & Li, Y. (2018). Anaerobic digestion of food waste Challenges and opportunities. *Bioresource Technology*, 247, 1047–1058.

Yaqoob, H., Teoh, Y. H., Sher, F., Farooq, M. U., and Jamil, M. A. (2021). "Potential of Waste Cooking Oil Biodiesel as Renewable Fuel in Combustion Engines: A Review." *Energies*, 14, 2565.

APPENDIX-I

Specifications of the diesel engine test rig used for research work

Engine	Make Kirloskar, Model TV1, Type Single cylinder, 4 stroke Diesel, water cooled, power 5.2 kW (7 BHP) at 1500 rpm, stroke 110 mm, bore 87.5 mm. compression ratio 17.5:1, capacity 661 cc.
Dynamometer	Make Saj test plant Pvt. Ltd., Model AG10, Type Eddy current.
Dynamometer Loading unit	Make Apex, Model AX-155. Type constant speed, Supply 230V AC.
Propeller shaft	Make Hindustan Hardy Spicer, Model 1260, Type A
Manometer	Make Apex, Model MX-104, Range 100-0-100 mm, Type U tube, Conn. 1/4`` BSP hose back side, Mounting panel
Fuel measuring unit	Make Apex, Glass, Model:FF0.012
Piezo sensor	Make: PCB Piezotronics, Model: HSM111A22, Range:5000 psi, Diaphragm stainless steel type & hermetic sealed
White coaxial teflon cable	Make PCB piezotronics, Model 002C20, Length 20 ft, Connections one end BNC plug and other end 10-32 micro
Crank angle sensor	Make Kubler-Germany Model 8.3700.1321.0360 Dia: 37mm Shaft Size: Size 6mmxLength 12.5mm, Supply Voltage 5-30V DC, Output Push Pull (AA,BB,OO), PPR: 360, Outlet cable type axial with flange 37 mm to 58 mm
Data acquisition device	NI USB-6210 Bus Powered M Series
Piezo powering unit	Make-Cuadra, Model AX-409
Temperature sensor	Make Radix Type K, Ungrounded, Sheath Dia.6mmX110mmL, SS316, Connection 1/4"BSP (M) adjustable compression fitting
Temperature sensor	Make Radix, Type Pt100, Sheath Dia.6mmX110mmL, SS316,

	Connection 1/4"BSP(M) adjustable compression fitting
Temperature transmitter	Make Wika, model T19.10.3K0-4NK-Z, Input Thermocouple (type K), output 4-20mA, supply 24VDC, Calibration: 0-1200 °C.
Temperature transmitter	Make Wika, Model T19.10.1PO-1 Input RTD(Pt100), output 4-20 mA, supply 24VDC, Calibration: 0-100 °C
Load sensor	Make Sensotronics Sanmar Ltd., Model 60001,Type S beam, Universal, Capacity 0-50 kg
Load indicator	Make Selectron, model PIC 152–B2, 85 to 270VAC, retransmission output 4-20 mA
Power supply	Make Meanwell, model S-15-24, O/P 24 V, 0.7 A
Digital voltmeter	Make Meco, 3.1/2 digit LED display, range 0-20 VDC, supply 230VAC, model SMP35
Fuel flow transmitter	Make Yokogawa, Model EJA110-EMS-5A-92NN, Calibration range 0-500 mm H_2O, Output linear
Air flow transmitter	Make Wika, Range (-) 250 mm WC
Rotameter	Make Eureka Model PG 5, Range 25-250 lph, Connection 3/4" BSP vertical, screwed, Packing neoprene
Rotameter	Make Eureka Model PG 6, Range 40-400 lph, Connection ¾" BSP vertical, screwed, Packing neoprene
Pump	Make Kirloskar, Model Mini 18SM, HP 0.5, Size 1" x 1", Single ph 230 V AC
Air Box	M S fabricated with orifice meter and manometer
Fuel tank	Capacity 15 lit with glass fuel metering column
Calorimeter	Type: Pipe in pipe
Software	IC Engine software V 9.0 - Engine performance analysis software

APPENDIX-II

Specification of shell and tube heat exchanger

Shell diameter	0.06 m
Length of heat exchanger (shell)	0.45 m
Thickness of the shell wall	0.002 m
Diameter of the tube (copper)	0.006 m
Length of the copper tube	2.9 m
Tube thickness	0.6 mm
Shell material	GI
Number of baffle plates	6
Thermal conductivity of tube material	386 W/m-k
Critical radius of insulation	0.0525 m

APPENDIX-III

Specifications of the five gas exhaust analyzer

Make: AVL

Measured values	Measurement range	Resolution
CO	0 ... 10 % Vol	0.01 % Vol.
HC	0 ... 20,000 ppm	10 ppm
CO_2	0 ... 20 % Vol.	0.1 % Vol.
O_2	0 ... 22 % Vol.	0.01 % Vol.
NO	0 ... 5,000 ppm	1 ppm
Lambda	0…9.999 calculated	0.001

BIO-DATA

Name: Jagadish. C

Father's Name: Chandrashekara. S

Date of Birth: 18-10-1988

Nationality: Indian

Marital Status: Single

Address:

Permanent Address

No.3, A block, 8ft road, siddaramaiah
vrutha, University layout,
Mysore- 570034

Present Address

Research Scholar,
Department of Mechanical Engineering
National Institute of Technology Karnataka.
Surathkal, Mangalore-575025

Mobile Number: +91-9945426973

E-mail id: jagadish.sharath18@gmail.com

Educational Qualification:

Course	Institution	University	Batch
Ph. D. (Mechanical Engineering)	National Institute of Technology Karnataka. Surathkal.	NITK	2022
M.Tech. (Thermal Engineering)	National Institute of Technology Karnataka. Surathkal.	NITK	2012
B.E. (Industrial & Production Engineering)	Sri Jayachamarajendra college of Engineering, Mysore.	VTU	2010